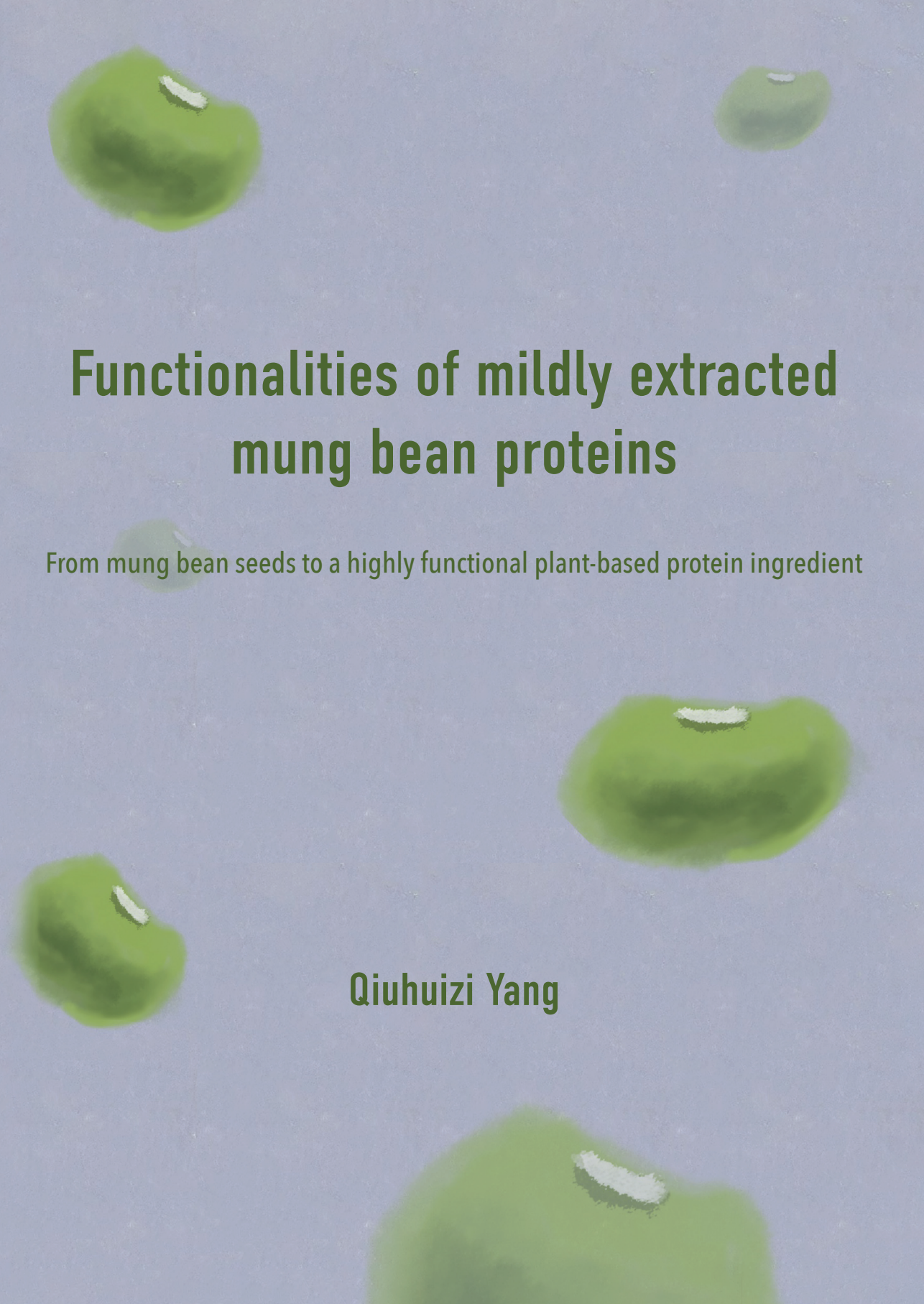

Functionalities of mildly extracted mung bean proteins

From mung bean seeds to a highly functional plant-based protein ingredient

Qiuhuizi Yang

Propositions

1. Customising extraction of mung bean proteins is more promising to functionalisation than applying extraction from an alternative source.
   (this thesis)

2. Gelation behaviour of mung bean proteins is determined by their processing history.
   (this thesis)

3. The role of investment in fundamental research is underestimated in the article by Herrero *et al*.
   (Herrero, M., Thornton, P. K., Mason-D'Croz, D., Palmer, J., Benton, T. G., Bodirsky, B. L., . . . West, P. C. (2020). Innovation can accelerate the transition towards a sustainable food system. *Nature Food*, *1*(5), 266-272.)

4. The definition of ultra-processed food in the article of Leung *et al.* is too ill-defined.
   (Leung, C. W., Fulay, A. P., Parnarouskis, L., Martinez-Steele, E., Gearhardt, A. N., & Wolfson, J. A. (2022). Food insecurity and ultra-processed food consumption: the modifying role of participation in the Supplemental Nutrition Assistance Program (SNAP). *Am J Clin Nutr*, *116*(1), 197-205.)

5. Accepting the fact that something has to be carried out while not necessarily being enjoyable, makes life easier.

6. Individualism and collaboration are both necessary personal trades to fulfil a PhD journey.

Propositions belonging to the thesis, entitled

Functionalities of mildly extracted mung bean proteins: From mung bean seeds to a highly functional plant-based protein ingredient

Qiuhuizi Yang

Wageningen, 31 March 2023

Functionalities of mildly extracted mung bean proteins

From mung bean seeds to a highly functional plant-based protein ingredient

Qiuhuizi Yang

Thesis committee

Promotors

Prof. Dr Erik van der Linden
Professor of Physics and Physical Chemistry of Foods
Wageningen University & Research

Dr Renko de Vries
Associate professor of Physical Chemistry and Soft Matter
Wageningen University & Research

Co-promotors

Dr Paul Venema
Assistant professor, Physics and Physical Chemistry of Foods
Wageningen University & Research

Other members

Prof. Dr Atze Jan van der Goot, Wageningen University & Research

Dr Hans Tromp, Utrecht University

Prof. Dr Lilia Ahrné, University of Copenhagen, Denmark

Dr Laurice Pouvreau, Wageningen Food & Biobased Research

This research was conducted under the auspices of VLAG Graduate School
(Biobased, Biomolecular, Chemical, Food and Nutrition Sciences).

Functionalities of mildly extracted mung bean proteins

From mung bean seeds to a highly functional plant-based protein ingredient

Qiuhuizi Yang

Thesis

submitted in fulfilment of the requirements for the degree of doctor
at Wageningen University
by the authority of the Rector Magnificus,
Prof. Dr A.P.J. Mol,
in the presence of the
Thesis Committee appointed by the Academic Board
to be defended in public
on Friday 31 March 2023
at 1.30 p.m. in the Omnia Auditorium.

Qiuhuizi Yang

Functionalities of mildly extracted mung bean proteins: From mung bean seeds to a highly functional plant-based protein ingredient
218 Pages

PhD thesis, Wageningen University, Wageningen, the Netherlands (2023)
With references, with summary in English

ISBN: 978-94-6447-559-3
DOI: 10.18174/585531

Table of Contents

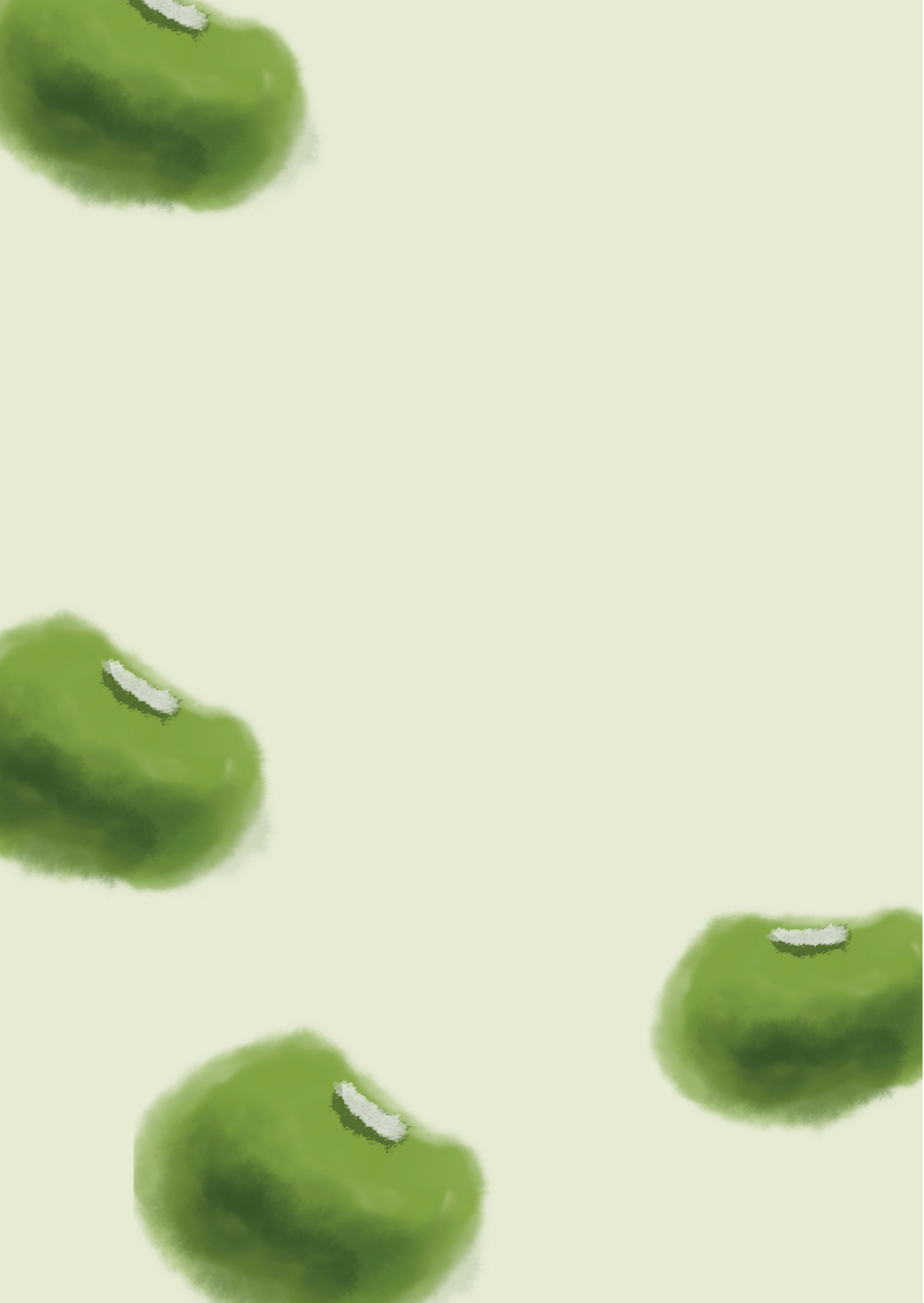

1

General introduction

1.1 Introduction

Proteins are important biopolymers naturally present in foods. They are a major class of essential nutrients. Over the last decade, the food industry is accelerating the launch of plant-based products and the plant-based protein market increasing dramatically (MordorIntelligence, 2022). This could be explained by concerns of consumers about health, allergenicity and by an increase of vegetarianism (Aydemir & Yemenicioğlu, 2013; Carbonaro et al., 2015). On the other hand, the environmental impact of food production, or more broadly sustainability, is also increasingly a concern, such that it is thought to be necessary for the food industry to make production, processing, storage, distribution etc. more sustainable (Godfray et al., 2010). These factors lead the food industry to seek to replace animal-based proteins by plant-based proteins in many of their products.

Mung bean, *Vigna radiata* (L.) is traditionally consumed in Asian countries but recently also gained more attention in Europe and Northern America. One reason is that it contains 20-25% of protein which is well-balanced in terms of amino acids (Coffmann & Garciaj, 1977; Kudre et al., 2013). Additionally, in terms of sustainability, mung bean requires less water than many other sources, and can be grown without fertilizers. This makes mung bean a promising plant-based protein source. But functional properties of mung bean proteins and its various fractions (such as foaming, emulsification and gelation) have not been extensively studied yet, as compared to other plant-based protein sources.

As a sustainable alternative to animal-derived proteins, plant-based proteins in general have gained much attention recently in terms of functionalities, such as solubility, emulsification, foaming and gelation. Recent scientific studies, plus the recent availability of more plant-derived protein ingredients have allowed food formulators to create plant-based food products of better quality. For example, less “beany” or even non- “beany” and non-bitter soybean protein ingredients have

been developed for products with proper textural and sensorial attributes, which are able to fulfil consumer demands. Nevertheless, poor solubility and high sedimentation rates in dispersions of plant protein ingredients still restrict the scope of textures and functionalities that can be obtained.

As to extraction and purification methods, it is especially the traditional isoelectric precipitation method that is widely used for plant proteins in the food industry. This process requests large amounts of chemicals, water and a high energy input to obtain the final isolates, with relatively high protein content (>70%). However, this high protein purity is achieved at the cost of denaturing the proteins during iso-electric precipitation and subsequent spray drying. As a result, functionality of these proteins is often limited.

Milder processing approaches have the potential to be more sustainable, as well as to better preserve protein structure. Indeed, by applying mild aqueous fractionation (avoiding extreme pH and heating conditions) or dry fractionation methods, the use of chemicals, water, and energy is reduced and native structures of proteins are better preserved, also leading to higher protein functionality (Pelgrom et al., 2013). It should be noted that this enhanced functionality is typically comes at the cost of sacrificing protein purity: purity of mildly fractionated fractions can be for example only 30%, such that in some cases it may be necessary to still further concentrate or purify such fractions to increase the protein content.

In the present thesis, we use sustainable dry fractionation followed by a number of mild wet processing routes (such as sedimentation-based layer separation and liquid-liquid phase separation) to obtain mildly extracted Mung Bean protein fractions, instead of the traditional wet process of isoelectric precipitation (see Figure 1). We investigate the functionalities of these mildly fractionated mung bean proteins, and their potential as future plant-based protein ingredients.

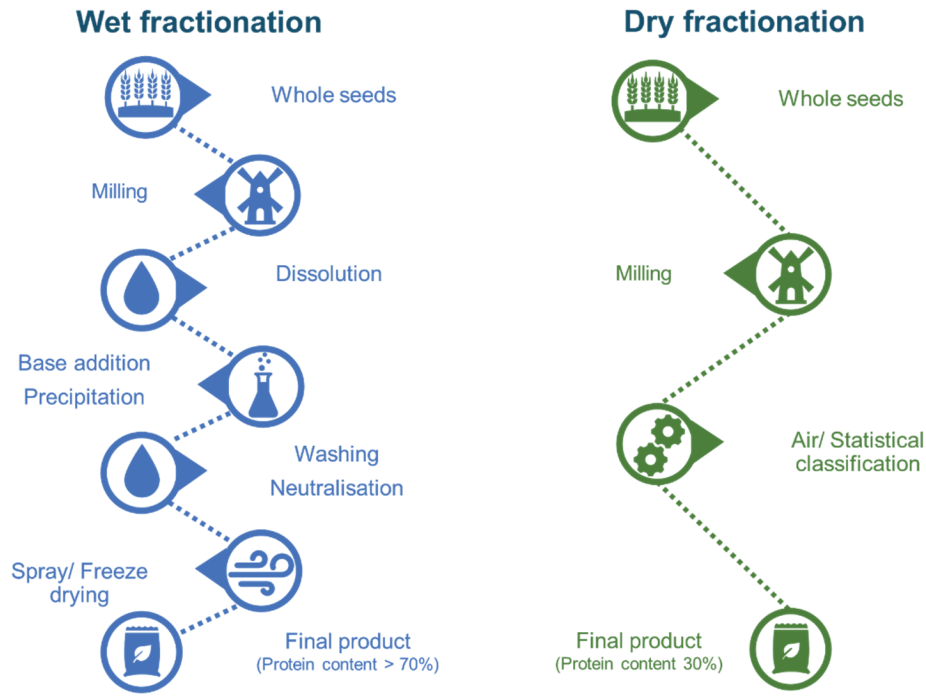

Figure 1.1 *Overview of dry fractionation and traditional wet (isoelectric precipitation) fractionation methods to obtain plant-based proteins.*

1.2 Plant protein fractionations

Replacing animal-based protein sources for plant-based protein sources is of much interest due to its potential to increase the sustainability of our food supply (Aiking, 2011). Meat production poses a severe burden on land, water, and fossil fuels, and it is though that with the present level of consumption of animal-based protein, it is impossible to sustainably ensure food security for the future world population (Aiking, 2011; Godfray et al., 2010). The present market for plant-based proteins is dominated by proteins from just a few plant species, especially soybean and yellow pea (*Pisum sativum L.*). These vegetal protein sources are specifically of interest as they are pulses rich in proteins and are cultivated throughout the whole world (Kudre et al., 2013). Next to these sources however, Mung bean proteins also have a well-balanced amino acid composition, bland taste and are known for their

possible health benefits (Adebiyi & Aluko, 2011; Du et al., 2018; Kudre et al., 2013; Taherian et al., 2011). These may be a promising additional source, which is important for example because some soybean proteins are known allergens (Beran et al., 2018; Boye et al., 2010) , because they have a strong beany flavour, *etc*. Table 1.1 shows the overall composition of these three legumes on dry matter base.

Table 1.1 *Average nutritional composition of raw soybean, mung bean and yellow pea crops based on dry matter.*

Legume	Protein (%)	Carbohydrates (%)	Lipids (%)	Ash (%)
Soybean [a]	32.5-36.5	30.2-31.3	14.9-19.9	4.8-4.9
Mung bean [b]	24.6-26.3	62-68.9	1.3	3.7
Yellow pea [c]	21.6-23.1	61.2-68.4	0.9-2.4	2.8-3.7

Data source: [a] (Amonsou et al., 2011; USDA, 2019), [b] (Boye et al., 2010; Coffmann & Garciaj, 1977; USDA, 2019), [c] (Khattab et al., 2009; Ma et al., 2011)

Proteins of most pulses in storage cells are found in so-called protein bodies surrounded by a membrane (Schmidt, 2013; Tombs, 1967). The size of protein bodies is between 2 to 20 µm, shapes are either irregular (soybeans) (Tombs, 1967) or spherical (other legumes) (Kornet et al., 2020; Zhu et al., 2018). Protein bodies have been found suspended in seeds together with starch granules and oil bodies. It is required to fractionate plant proteins from seeds to remove some of the undesired components before using them in food products. Here we do this using mild fractionation methods that leave the protein structure largely intact.

1.2.1 Dry fractionation

Dry fractionation is a mild and sustainable approach to produce protein concentrates from cereals and legumes, although generally protein purities obtained are relatively low compared to isoelectric precipitation method (Pelgrom, Boom, et al., 2015b). Impurities present can be e.g., carbohydrates, salts, phenols, and oil. However, the overall functionality may be equal or even better than a highly purified protein isolate (Kornet et al., 2020; Q. Yang et al., 2022).

Dry fractionation typically consists of two steps. The first is milling of the seeds to release the protein bodies and starch granules from the matrix. This is followed by a step of dry separation of the flour, into various fractions with different particle sizes using air classification. Eventually, a fraction enriched in protein, the so-called fine fraction (FF) and other one mostly containing starch and cell wall material, the so-called coarse fraction (CF) is obtained. The protein content of the FF can vary a lot depending on protein source: between 17 to 56 g protein/ 100 g dry matter according to previous research on soybean, pea, lupin, corn, and quinoa (Assatory et al., 2019; Opazo-Navarrete et al., 2018; Pelgrom et al., 2014; Pelgrom et al., 2013). It should be noted that legumes which are high in lipids or moisture are not the ideal materials to be processed by dry fractionation (Pelgrom, Boom, et al., 2015b; Pelgrom, Wang, et al., 2015; Schutyser & van der Goot, 2011). These would necessitate pre-treatments such as defatting to obtain higher yields.

The dissociation of the seed components is critical to enable efficient separation. This is largely dependent the structures in the seeds and on the milling conditions. Pelgrom, Boom, et al. (2015b) studied optimal separation conditions for pea, bean, lentil, and chickpea and found that the protein content of fine fraction is determined by differences in particle density, seed hardness and starch granule size at the same mill conditions. The seed hardness and starch granule size (Delcour & Hoseney, 2010) have been found to be, respectively, negatively and positively correlated with the efficiency of protein separation from starch during milling. Various milling options such as impact mill, pin milling and jet milling *etc.* are available to further tune fractionation. In the present thesis, we restrict ourselves to the impact milling technique.

Several factors have been demonstrated to influence the separation efficiency during air classification. A well-chosen milling speed can result in a higher protein content, but excessive milling can damage the starch granules. Also, a flour that is

too fine may adhere to the walls of the mill (Pelgrom et al., 2014), resulting in more starch fragments ending up in the FF. The speed of the air classification is another important factor to be considered. By increasing the air classification speed, reduced particle sizes and increased protein content were found in the lupine FF. Additives may also help. For example, by adding potato starches, the attractive forces between particles can be decreased and the inter-particle distance can be increased, leading to a higher protein separation efficiency.

Finally, next to air classification, one can also use another mode of dry separation: electrostatic separation. This exploits differences in the dielectric properties of flour particles instead of difference in size and density. In order to charge up feed particles, tribo-electrification is used (Wang et al., 2015). Due to the many ionizable groups of proteins, protein-rich particles can be charged up much more than starch particles and dietary fibres. Consequently, protein-rich and starch-rich fractions can be separated by an electric field (Wang et al., 2016). However, the tribo-charging of protein bodies is highly plant-species dependent. For example, protein-rich particles in wheat bran adopt a positive charge (Wang et al., 2015), whereas , rice protein particles have been observed to be negatively charged (Pelgrom, Boom, et al., 2015b). Likewise, particle size and milling speed affect the separation efficiency of electrostatic separation. In particular, smaller particles were found to charge up stronger than larger particles (J. Wang et al., 2014) and a high milling speed was observed to make the particles agglomerate during tribo-charging (Wang et al., 2016).

In summary, dry fractionation is an attractive process to extract proteins from plant seeds in a sustainable and solvent-free way. The dry separation methods air classification and electrostatic separation are techniques which can avoid the usage of chemical reagents, and fully maintain the functionalities of the native proteins. The main disadvantage of dry fractionation is the relatively low protein of the FF as

compared to the protein content of traditional plant protein isolates. Further research on mild processes that can enrich protein content of FF is therefore much needed.

1.2.2 Mild wet processing

Next to dry fractionation, another trend is the use of mild wet fractionation methods to obtain protein-rich fractionations. In this case, fractionation conditions such as pH, ionic strength and temperature *etc.* are chosen carefully to avoid damage to the structure of the plant proteins. Some of these processes may also be more sustainable as compared to the traditional iso-electric precipitation process.

Sedimentation-based separation

A first process that can be used after dry fractionation to generate protein-enriched fractions with higher protein concentration is sedimentation-based separation also referred as aqueous phase separation in literature (Avila Ruiz et al., 2016; Pelgrom, Boom, et al., 2015a). For this process, FF can be further milled and suspended, or directly suspended in aqueous solvents. Next low-speed centrifugation is used for a set time, and this yields distinct layers, where separation is based on the Stokes friction that determines the sedimentation speed of the particles. The number of layers is plant-species specific. For instance, pea flour (Pelgrom, Boom, et al., 2015a) and mung bean FF (Q. Yang et al., 2022) were found to give 4 distinct layers while quinoa flour only yielded 3 layers (Avila Ruiz et al., 2016). The composition of the layer is quite predictable, with starches, proteins, and cell wall materials usually being enriched in different layers, the top layers being protein-rich and the bottom layers being starch-rich (Pelgrom, Boom, et al., 2015a). Protein content of top layers was reported around 67 g/ 100 g dry matter with a protein yield of 63% for pea FF (Pelgrom, Boom, et al., 2015a) and 60 g/ 100 g dry matter with a protein yield of 62% for quinoa flour (Avila Ruiz et al., 2016), respectively, after concentrated by

ultrafiltration. Protein purity values are up to 80 w/w % for this method. Water usage and energy input can both be reduced by around 80% for this method, as compared to traditional procedures (Pelgrom, Boom, et al., 2015a).

The sedimentation efficiencies of the different particles are affected by various solution conditions. For example, for NaCl concentration ranging from 0 M to 0.5 M, and for quinoa suspensions, Avila Ruiz et al. (2016) found that higher salt concentration resulted in an increased dry matter content of the top layer, but significant increases in protein yield and purity were not observed. We find similar results for Mung Bean in this thesis (**Chapter 2**), but also find that instead, pH has a considerable effect on the protein content of the top layers. The functionality of dry fractionated proteins that have additionally undergone mild wet processing may be equal or even better than traditional highly purified protein isolates (Kornet et al., 2020). Therefore, dry separation plus sedimentation-based fractionation is a promising, economical, and sustainable process which in the future should allow the industry to obtain plant-based protein ingredients with good functionality.

Liquid-Liquid phase separation

Another mild wet process to increase protein content is protein liquid-liquid phase separation, also known as coacervation. While for pure proteins, liquid-liquid phase separation eventually leads to macroscopic phase separation, in impure systems (or when not waiting long enough for macroscopic phase separation to occur) one can typically observe the formation of dense protein-rich droplets in a protein-poor continuous phase.

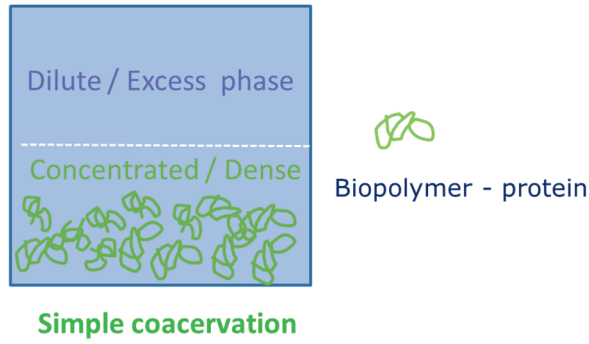

Figure 1.2 *Simplified schematic of liquid-liquid phase separation (simple coacervation).*

Figure 1.2 illustrates macroscopic liquid-liquid biopolymer phase separation or coacervation. Note that typically, when only one biopolymer component is involved, the phase separation is referred to as "simple coacervation" (Lazko et al., 2004). In contrast, when coacervation is due to complex formation of two different (often oppositely charged) biopolymers, it is referred to as "complex coacervation". Biopolymer coacervation can occur due to several weak attractive interactions such as hydrogen bonding, hydrophobic, electrostatic and van der Waals forces etc. (Pathak et al., 2017). For complex coacervation, it has been shown that compact coacervate structures form especially when the strongest interactions between polymers are induced by electrostatic interactions. As a result, the overall system is electroneutral in this case (Cochereau et al., 2019; de Kruif et al., 2004; Li & de Vries, 2018; Liu et al., 2017).

Since, coacervation may be an attractive method to produce protein-rich colloidal particles or microgels, in this thesis, we let Mung bean protein liquid-liquid phase separation take place such that micron- or submicron sized protein droplets are formed, and then to heat-set such droplets to form solid Mung bean protein colloids.

1.3 Mung bean protein fractionation and functionalities

Below we present some more specific information on Mung bean proteins, their fractionation and their functionalities. As in other seeds, Mung bean proteins are mainly storage proteins (Zhu et al., 2018), present in protein bodies bounded by a single membrane (see in Figure 3). The isoelectric point (pI) of Mung bean protein is between 4 and 5 (Boye et al., 2010). For the mature mung bean seeds specifically, the protein composition is approximately 15% albumins and 60% globulins (including 11S glycinin and legumin, 7S β-conglycinin and 8S vicilin) present in mung beans (Zhu et al., 2018), and the 8S globulin is predominant. In turn, vicilin is mainly composed of four polypeptides with molecular weights of about 60, 48, 32 and 26 kDa (Tang & Sun, 2010; Zhu et al., 2018). The 8S globulins have a molecular weight of about 150 kDa and are heterotrimers of about 49 kDa (Itoh et al., 2006).

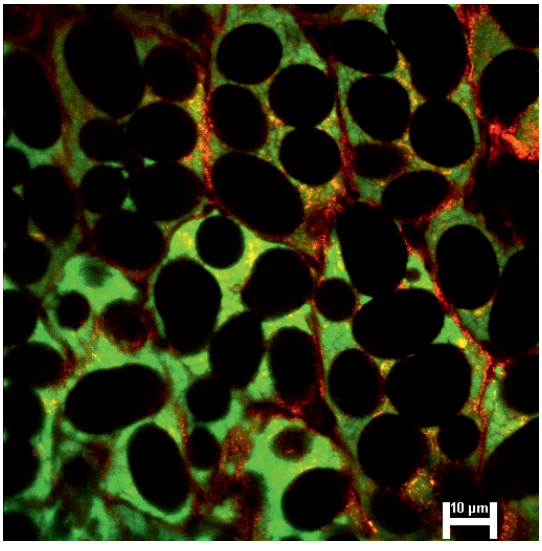

Figure 1.3 *Autofluorescence image of mung bean seed obtained by Confocal laser scanning microscope. Scale bar: 10 µm.*

1.3.1 Mung bean proteins fractionation

Typically, plant seed storage proteins are much less hydrophilic than e.g. milk- and egg proteins. At least in part due to this property, it is difficult to efficiently extract

them from the seeds in their native state (Li & de Vries, 2018). Currently, relatively harsh conditions such as alkaline extraction, acid precipitation and spray drying are used in the industry for the purification of proteins from seeds. For Mung Bean, little work has been done yet on milder purification methods. As for other sources, for Mung Bean the traditional alkaline extraction followed acid precipitation and spray drying leads to Mung Bean protein isolates with proteins that are largely denatured and hence limited food functionality (Kudre et al., 2013; Wang et al., 2022; M. Yang et al., 2021).

In recent years, dry fractionation has drawn much attention as a mild and sustainable protein extraction technology. Even though the purities obtained are lower than obtained from traditional processes (Pelgrom, Boom, et al., 2015b), the functionalities are comparable or better, since even though purity is less, the proteins retain more of their original functionality. However, studies on such mild extraction methods are still largely limited to widely investigated legumes such as soybean, yellow pea, lentil, and quinoa. Data on mild extraction processes for Mung Bean protein is still lacking.

1.3.2 Mung bean protein properties and functionalities

Proteins not only provide nutrition and energy but also play a role in determining food structure and hence sensory attributes. Structuring properties of proteins, or "functionality" include for example protein gelation, emulsification, and the ability to generate stable foams. Such properties are significantly influenced by the protein fractionation processing. For example, denaturation caused by spray dying or isoelectric precipitation can lead to a reduced solubility, strongly affecting functionalities such as emulsification and foaming.

For Mung Bean protein isolates, the highest solubility was reported to be around 81% at pH 10, and lowest solubility values were found around pH 4.6. As for other proteins, solubility of mung bean proteins also depends on ionic strength. Kudre et

al. (2013) found, for Mung Bean protein isolates, that addition of NaCl up to 0.45 M increases solubility of mung bean proteins, but that at higher NaCl concentrations, solubility decreases. The drying process also significantly affects the solubility of the resulting powders, for example a higher solubility was found for freeze dried mung bean protein isolates than spray dried isolates (Brishti et al., 2020).

Protein gelation (induced by e.g. heat, or by a drop in pH) is a crucial functionality, that is often desired, but which sometimes also is to be avoided (e.g. in drinks). Many food products require pasteurization or sterilization, and in these processes control over protein gelation is also crucial. For Mung bean proteins, both acid-induced and heat-induced gelation have been studied to some extent. For example, the minimum concentration of Mung Bean protein required to induce gelation was studied for Mung Bean protein extracted and dried in different ways (Brishti et al., 2020). Also, acid induced gelation, with applications in plant-based dairy analogues, was compared for Mung Bean protein and Pea protein (M. Yang et al., 2021). Emulsification and foaming using Mung Bean proteins have also been investigated by a number of authors, but not in great detail. Again, functionality is found to be highly dependent on the way the Mung Bean proteins are extracted and processed (Brishti et al., 2020; Du et al., 2018). Processing can also mean, e.g., an enzymatic treatment. This was shown for example to lead to a higher emulsification ability, emulsion stability and foam capacity for Mung Bean protein isolates, although it was also found that foam stability was reduced (Liu et al., 2022).

In summary, there is only limited research on mung bean protein functionality. Particularly lacking are investigations on more mildly purified Mung bean protein fractions, for which we may expect more functionality than for the Mung Bean protein isolates that are currently on the market.

1.4 Objective and thesis outline

In the present thesis, we study mung beans as a starting material for obtaining highly functional plant proteins via mild fractionation. In all cases we start by milling of the Mung Beans, followed by dry fractionation and then apply mild wet processing steps.

In **Chapter 2**, as a mild wet processing step, we use sedimentation-based fractionation. We study the efficiency of protein extraction, and the functionalities of the protein fractions resulting from this process, in particular viscosity and gelation. In **Chapter 3,** as a mild wet processing step, we use liquid-liquid phase separation of Mung Bean proteins. By reducing pH to moderately acidic values, we find that submicron droplets high in Mung Bean protein are formed that we can heat set and dry to form a new "Mung Bean protein ingredient" we will refer to throughout the thesis as Mung Bean protein colloids mixture (MPCM). We study the internal protein content and bulk behaviour of the Mung Bean protein colloids, finding in particular that the colloidal formulation leads to a relatively low viscosity, suitable for beverage formulations. In **Chapter 4** and **5**, the air-water interface of mung bean protein colloids stabilised foam was studied. **Chapter 4** demonstrates excellent foam capacity and foam stability for the mung bean protein colloids, as compared to other types of Mung Bean protein fractions (albumin, globulin, dry fractionated mung bean flour). To understand why the colloidal formulation leads to such excellent foams, in **Chapter** 5 we analyse the composition and foaming ability of the mung bean protein colloid mixtures in more detail. We fractionate the Mung Bean protein colloid mixtures into a supernatant fraction and pellets fraction by centrifugation, and further separate the supernatant using ultrafiltration. Next we studies the interfacial and foaming properties of all fractions thus obtained and find that it is the synergistic action of components of different sizes that leads to the excellent foaming of the Mung Bean protein colloid mixtures. Finally, **Chapter**

6 provides an overview of the main findings in the present thesis and places them in the broader context of the current literature.

References

Adebiyi, A. P., & Aluko, R. E. (2011). Functional properties of protein fractions obtained from commercial yellow field pea (Pisum sativum L.) seed protein isolate. *Food Chemistry*, *128*(4), 902-908.

Aiking, H. (2011). Future protein supply. *Trends in Food Science & Technology*, *22*(2-3), 112-120.

Amonsou, E., Taylor, J., & Minnaar, A. (2011). Microstructure of protein bodies in marama bean species. *LWT - Food Science and Technology*, *44*(1), 42-47.

Assatory, A., Vitelli, M., Rajabzadeh, A. R., & Legge, R. L. (2019). Dry fractionation methods for plant protein, starch and fiber enrichment: A review. *Trends in Food Science & Technology*, *86*, 340-351.

Avila Ruiz, G., Arts, A., Minor, M., & Schutyser, M. (2016). A Hybrid Dry and Aqueous Fractionation Method to Obtain Protein-Rich Fractions from Quinoa (Chenopodium quinoa Willd). *Food and Bioprocess Technology*, *9*(9), 1502-1510.

Aydemir, L. Y., & Yemenicioğlu, A. (2013). Potential of Turkish Kabuli type chickpea and green and red lentil cultivars as source of soy and animal origin functional protein alternatives. *LWT - Food Science and Technology*, *50*(2), 686-694.

Beran, M., Drahorad, J., Vltavsky, O., Urban, M., Laknerova, I., Fronek, M., . . . Formankova, S. (2018). Pilot-Scale Production and Application of Microparticulated Plant Proteins. *Journal of Nutrition & Food Sciences*, *08*(01).

Boye, J., Zare, F., & Pletch, A. (2010). Pulse proteins: Processing, characterization, functional properties and applications in food and feed. *Food Research International*, *43*(2), 414-431.

Brishti, F. H., Chay, S. Y., Muhammad, K., Ismail-Fitry, M. R., Zarei, M., Karthikeyan, S., & Saari, N. (2020). Effects of drying techniques on the physicochemical, functional, thermal, structural and rheological properties of mung bean (Vigna radiata) protein isolate powder. *Food Res Int*, *138*(Pt B), 109783.

Carbonaro, M., Maselli, P., & Nucara, A. (2015). Structural aspects of legume proteins and nutraceutical properties. *Food Research International*, *76*, 19-30.

Cochereau, R., Nicolai, T., Chassenieux, C., & Silva, J. V. C. (2019). Mechanism of the spontaneous formation of plant protein microcapsules in aqueous solution. *Colloids and Surfaces A: Physicochemical and Engineering Aspects*, *562*, 213-219.

Coffmann, C. W., & Garciaj, V. V. (1977). Functional properties and amino acid content of a protein isolate from mung bean flour*. *International Journal of Food Science & Technology*, *12*(5), 473-484.

de Kruif, C. G., Weinbreck, F., & de Vries, R. (2004). Complex coacervation of proteins and anionic polysaccharides. *Current Opinion in Colloid & Interface Science*, *9*(5), 340-349.

Delcour, J., & Hoseney, R. C. (2010). Principles of cereal science and technology authors provide insight into the current state of cereal processing. *Cereal Foods World*, *55*(1), 21-22.

Du, M., Xie, J., Gong, B., Xu, X., Tang, W., Li, X., . . . Xie, M. (2018). Extraction, physicochemical characteristics and functional properties of Mung bean protein. *Food Hydrocolloids*, *76*, 131-140.

Godfray, H. C., Crute, I. R., Haddad, L., Lawrence, D., Muir, J. F., Nisbett, N., . . . Whiteley, R. (2010). The future of the global food system. *Philos Trans R Soc Lond B Biol Sci*, *365*(1554), 2769-2777.

Itoh, T., Garcia, R. N., Adachi, M., Maruyama, Y., Tecson-Mendoza, E. M., Mikami, B., & Utsumi, S. (2006). Structure of 8Salpha globulin, the major seed storage protein of mung bean. *Acta Crystallogr D Biol Crystallogr*, *62*(Pt 7), 824-832.

Khattab, R. Y., Arntfield, S. D., & Nyachoti, C. M. (2009). Nutritional quality of legume seeds as affected by some physical treatments, Part 1: Protein quality evaluation. *LWT - Food Science and Technology*, *42*(6), 1107-1112.

Kornet, C., Venema, P., Nijsse, J., van der Linden, E., van der Goot, A. J., & Meinders, M. (2020). Yellow pea aqueous fractionation increases the specific volume fraction and viscosity of its dispersions. *Food Hydrocolloids*, *99*.

Kudre, T. G., Benjakul, S., & Kishimura, H. (2013). Comparative study on chemical compositions and properties of protein isolates from mung bean, black bean and bambara groundnut. *J Sci Food Agric*, *93*(10), 2429-2436.

Lazko, J., Popineau, Y., & Legrand, J. (2004). Soy glycinin microcapsules by simple coacervation method. *Colloids and Surfaces B: Biointerfaces*, *37*(1), 1-8.

Li, X., & de Vries, R. (2018). Interfacial stabilization using complexes of plant proteins and polysaccharides. *Current Opinion in Food Science*, *21*, 51-56.

Liu, F. F., Li, Y. Q., Wang, C. Y., Liang, Y., Zhao, X. Z., He, J. X., & Mo, H. Z. (2022). Physicochemical, functional and antioxidant properties of mung bean protein enzymatic hydrolysates. *Food Chem*, *393*, 133397.

Liu, J., Shim, Y. Y., Shen, J., Wang, Y., & Reaney, M. J. T. (2017). Whey protein isolate and flaxseed (Linum usitatissimum L.) gum electrostatic coacervates: Turbidity and rheology. *Food Hydrocolloids*, *64*, 18-27.

Ma, Z., Boye, J. I., Simpson, B. K., Prasher, S. O., Monpetit, D., & Malcolmson, L. (2011). Thermal processing effects on the functional properties and microstructure of lentil, chickpea, and pea flours. *Food Research International*, *44*(8), 2534-2544.

MordorIntelligence. (2022). *Protein ingredients market size, share, trends: 2022 - 27*. Mordor Intelligence. Retrieved 23 November from https://www.mordorintelligence.com/industry-reports/protein-ingredients-market?gclid=CjwKCAiApvebBhAvEiwAe7mHSCGuLLg--J9ytWjcSyx8MJ_t60x-RwynZu62Sz5UmOdjJNGk_et-EBoCfCkQAvD_BwE

Opazo-Navarrete, M., Freire, D. T., Boom, R. M., Janssen, A. E. M., & Schutyser, M. A. I. (2018). Dry fractionation of quinoa sweet varieties Atlas and Riobamba for sustainable production of protein and starch fractions. *Journal of Food Composition and Analysis*, *74*, 95-101.

Pathak, J., Priyadarshini, E., Rawat, K., & Bohidar, H. B. (2017). Complex coacervation in charge complementary biopolymers: Electrostatic versus surface patch binding. *Advances in Colloid and Interface Science*, *250*, 40-53.

Pelgrom, P. J. M., Berghout, J. A. M., van der Goot, A. J., Boom, R. M., & Schutyser, M. A. I. (2014). Preparation of functional lupine protein fractions by dry separation. *LWT - Food Science and Technology*, *59*(2), 680-688.

Pelgrom, P. J. M., Boom, R. M., & Schutyser, M. A. I. (2015a). Functional analysis of mildly refined fractions from yellow pea. *Food Hydrocolloids*, *44*, 12-22.

Pelgrom, P. J. M., Boom, R. M., & Schutyser, M. A. I. (2015b). Method Development to Increase Protein Enrichment During Dry Fractionation of Starch-Rich Legumes. *Food and Bioprocess Technology*, *8*(7), 1495-1502.

Pelgrom, P. J. M., Vissers, A. M., Boom, R. M., & Schutyser, M. A. I. (2013). Dry fractionation for production of functional pea protein concentrates. *Food Research International*, *53*(1), 232-239.

Pelgrom, P. J. M., Wang, J., Boom, R. M., & Schutyser, M. A. I. (2015). Pre- and post-treatment enhance the protein enrichment from milling and air classification of legumes. *Journal of Food Engineering*, *155*, 53-61.

Schmidt, S. R. (2013). Protein bodies in nature and biotechnology. *Mol Biotechnol*, *54*(2), 257-268.

Schutyser, M. A. I., & van der Goot, A. J. (2011). The potential of dry fractionation processes for sustainable plant protein production. *Trends in Food Science & Technology*, *22*(4), 154-164.

Taherian, A. R., Mondor, M., Labranche, J., Drolet, H., Ippersiel, D., & Lamarche, F. (2011). Comparative study of functional properties of commercial and membrane processed yellow pea protein isolates. *Food Research International*, *44*(8), 2505-2514.

Tang, C. H., & Sun, X. (2010). Physicochemical and structural properties of 8S and/or 11S globulins from mungbean [Vigna radiata (L.) Wilczek] with various polypeptide constituents. *J Agric Food Chem*, *58*(10), 6395-6402.

Tombs, M. P. (1967). Protein bodies of the soybean. *Plant Physiol*, *42*(6), 797-813.

USDA. (2019). *FoodData Central*. Retrieved July 20 from https://fdc.nal.usda.gov/

Wang, J., de Wit, M., Schutyser, M. A. I., & Boom, R. M. (2014). Analysis of electrostatic powder charging for fractionation of foods. *Innovative Food Science & Emerging Technologies*, *26*, 360-365.

Wang, J., Smits, E., Boom, R. M., & Schutyser, M. A. I. (2015). Arabinoxylans concentrates from wheat bran by electrostatic separation. *Journal of Food Engineering*, *155*, 29-36.

Wang, J., Zhao, J., de Wit, M., Boom, R. M., & Schutyser, M. A. I. (2016). Lupine protein enrichment by milling and electrostatic separation. *Innovative Food Science & Emerging Technologies*, *33*, 596-602.

Wang, Y., Zhao, J., Zhang, S., Zhao, X., Liu, Y., Jiang, J., & Xiong, Y. L. (2022). Structural and rheological properties of mung bean protein emulsion as a liquid egg substitute: The effect of pH shifting and calcium. *Food Hydrocolloids*, *126*.

Yang, M., Li, N., Tong, L., Fan, B., Wang, L., Wang, F., & Liu, L. (2021). Comparison of physicochemical properties and volatile flavor compounds of pea protein and mung bean protein-based yogurt. *Lwt*, *152*.

Yang, Q., Eikelboom, E., van der Linden, E., de Vries, R., & Venema, P. (2022). A mild hybrid liquid separation to obtain functional mungbean protein. *Lwt*, *154*.

Zhu, Y., Sun, S., & FitzGerald, R. (2018). Mung bean proteins and peptides: nutritional, functional and bioactive properties. *Food Nutr Res*, *62*.

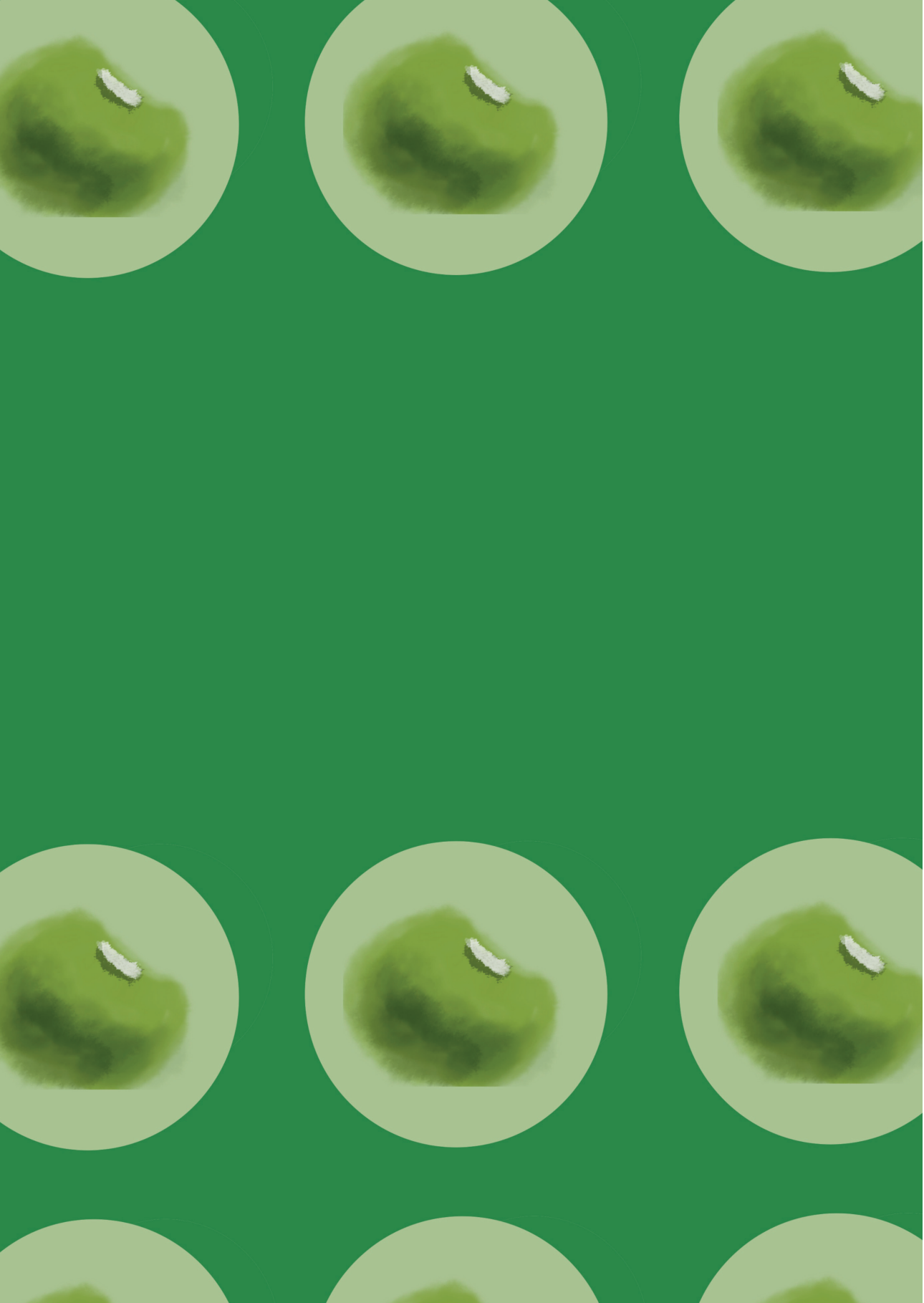

2

A mild hybrid liquid separation to obtain functional Mung bean protein

This chapter is published as:
Yang, Q., Eikelboom, E., van der Linden, E., de Vries, R., & Venema, P. (2022). A mild hybrid liquid separation to obtain functional mung bean protein. Lwt, 154.

Abstract

A dry fractionation combine with an aqueous phase separation approach is developed as a mild and sustainable Mung bean protein extraction process. Mung bean seeds were dehulled or intactly milled and air classified to produce fine fractions which are enriched in proteins. Subsequently, aqueous phase separation was employed to yield a 4 layers separation system to increase the protein content. The protein content of different layers distributed depend on varied conditions, the pH condition was proved to be the parameter which influences the protein yield strongly, the highest protein yield for Layer 1 was 80.9% at pH 8. Air classification speed, stirring time, and salt addition did not show the ability to increase protein yield significantly. Finally, shear viscosity and oscillatory measurements were performed to investigate the rheological behaviour of the Mung bean proteins obtained by our hybrid method. The viscosity of the mild extracted Mung bean proteins was found lower than commercial Mung bean protein concentrates at a comparable protein concentration, whereas the mild process did not have a significant influence on heat-set gelation.

2.1 Introduction

Plant proteins are drawing increasing interest as food ingredients. The global plant protein market is expected to increase from 10.3 billion dollars in 2020 to 15.6 billion dollars by 2026 (MarketsandMarkets, 2021). This increase is a consequence of the continuous growth of the world population and the shift of people's dietary pattern, towards a more sustainable, healthy and balanced diet. Therefore, plant proteins have been studied as a potential replacer for the typical animal-derived protein-rich products, such as cheese, milk, and meat (Mattice & Marangoni, 2020; Rinaldoni *et al.*, 2014; Waschatko *et al.*, 2012; Wang *et al.*, 2019; Kumar *et al.*, 2016).

At this moment, the protein-rich fraction is extracted from plants by so-called wet fractionation. This yields relatively pure protein isolates, but requires large amounts of water and often leads to a loss of the native structure of the proteins (Pelgrom *et al.*, 2015a; Schutyser & van der Goot, 2011). In turn, this leads to poor solubility, relatively high viscosity and compromised functionalities for emulsification, gelation etc.

For applications such as plant-based beverages, presenting a pleasant viscosity while possessing a desired protein concentration is especially problematic. For example, a challenge is the relatively high protein concentration of minimal 6 (v/v) % that is demanded. This often results in a drink with a high viscosity, which is usually undesirable for high protein drinks (de Kort *et al.*, 2011). Additionally, the preferred viscosity depends on the consumer group. For instance, Štreimikytė *et al.* (2013) reported that the geriatric consumers with swallowing difficulties probably prefer to products with 'honey' – level (350 - 1750 mPa.s) viscosity. Therefore, plant protein ingredients that have a good solubility with low viscosity would be favoured for plant-based beverages.

Except for high protein content, the undesired high viscosity can also be generated by thermal preservation processes due to protein structure alteration even

denaturation. Several approaches such as vacuum packing, freeze drying, irradiation, etc. have been carried out to eliminate this disagreeable influence. Moreover, milder fractionation procedures help to preserve the native structure of plant proteins, leading to lower viscosities than at comparable protein concentration, when compared with proteins obtained via other fractionation procedures (Purwanti *et al.*, 2011). An example is dry fractionation, which is both more sustainable and leaves protein structures intact. In this procedure, milling is followed by air classification to separate components based on the difference in density or size. Eventually, this gives a fine fraction rich in native proteins and a coarse fraction rich in starch.

Previous research has shown that peas, lupine, and beans can all be processed using dry fractionation (Pelgrom *et al.*, 2013; Schutyser & van der Goot, 2011; Pelgrom *et al.*, 2015b; Simons *et al.*, 2017; Wu & Nichols, 2005). Schutyser *et al.* (2015) reported that after air classification protein concentration can be increased from 23.8 to 58.8 g/100g dry matter for yellow pea, 40.4 to 59.4g /100g dry matter for lupine. The method has also been applied for soybean. Xing *et al.* (2018) found that for this case, protein can be enriched from 37 g/100g dry matter to 45 g/100g dry matter (for defatted soybean).

So far, the crucial relation between plant protein functionality and the type of processes used, has only been addressed for the (currently) most common commercial crops such as soybeans and yellow pea. For other potentially important crops, this relation has not yet been investigated. Here we focus on an attractive proteinaceous material, viz. Mung bean (*Vigna radiata (L.)*), which possesses a well-balanced amino acid composition and is cultured diffusely all over the world. Its high protein- and low lipid content make it suitable for dry fractionation. Additionally, Mung bean is known for its possible health benefits such as lowering of plasma cholesterol, prevention of diabetes (Du *et al.*, 2018; Kudre *et al.*, 2013).

Commercial Mung bean proteins are mostly extracted by wet fractionation, which causes protein denaturation during both the protein precipitation and drying steps, typically leading to loss of proteins native structure. Thus, research on native Mung bean protein would be interesting and promising. However, research on the functionality of mildly extracted Mung bean proteins is still lacking.

Here we consider a mild Mung bean purification using milling and air-classification to obtain a protein enriched fine fraction (MBFF) and a dehulled protein enriched fine fraction (DMBFF), followed by dissolution and centrifugation (at 2500 g) to increase protein content. Different types of particles swell to different extents in the dispersions after (low-speed) centrifugation, typically obtains a number of distinct layers which are separated based on Stokes law dictated by the $\Delta\rho * a^2$ for particles which Pe >> 1, the Peclet number (Pe) indicating that the system is dominated by convection. The total number of layers depends on the protein source used. For instance, pea flour was reported to form 4 distinct layers (Pelgrom *et al.*, 2015a), while quinoa flour exhibited 3 layers (Ruiz *et al.*, 2016). Starches, proteins, and cell wall materials typically separate into different layers, with the top layers being protein-rich and the bottom layer being starch-rich (Pelgrom *et al.*, 2015a). In earlier work, this hybrid extraction method was shown to be promising for extracting native pea protein: protein yields were found to be 66.9 g /100 g dry matter in the top phases. The hybrid separation used considerably less water and energy as compared to conventional separation methods (Pelgrom *et al.*, 2015a; Schutyser, 2015).

For the hybrid Mung bean protein purification described above we study the influence of basic process parameters such as milling wheel speed, classification rotation speed, dehulling, stirring time, pH, and salt addition on the protein extraction and resulting functionality of the proteins. In particular, we focus on measuring and understanding differences in the viscosity between the mildly

purified Mung bean proteins and commercial Mung bean protein concentrates at comparable protein concentrations.

2.2 Materials and Methods

2.2.1 Materials

Dried Mung bean (*Vigna radiata)* used for the experiments was purchased from a local Asian store. The specification for the dried Mung bean with 6.4% moisture content was protein 24 g/100 g, fat 2 g/100 g, carbohydrate 60 g/100 g (all based on dry weight). All beans still contained their hulls and had not been heated. As the reference, a commercial Mung bean protein concentrates M65 was obtained from Barentz B.V. (Hoofddorp, Netherlands). The characteristics of M65 were protein 67.5g/100g, fat 0.10g/100g, carbohydrate 20.98g/100g and moisture content 6.88 g/100g. All other chemicals (Analytical grade) were obtained from Sigma Aldrich (St. Louis, Missouri, United States).

2.2.2 Dehulling

Since polyphenols may interact with proteins both reversibly and irreversibly, we removed the seed coat before milling to produce dehulled Mung bean fine fraction (DMBFF) and dehulled Mung bean coarse fraction (DMBCF). The schematic overview of the Mung bean hybrid separation method is shown in Fig. 2.1. Dehulling was carried out by soaking the seeds in excess water for 8 hours at room temperature. Afterward, the seed coat was removed by manual abrasion. After dehulling, beans were dried using a Venticell Laboratory Oven LSISB2V/ VC111 (MMM Medcenter Einrichtungen GmbH, Planegg, Germany). The final moisture content was lower than 9% as required to perform the subsequent dry fractionation step at 50 °C without denaturing the proteins.

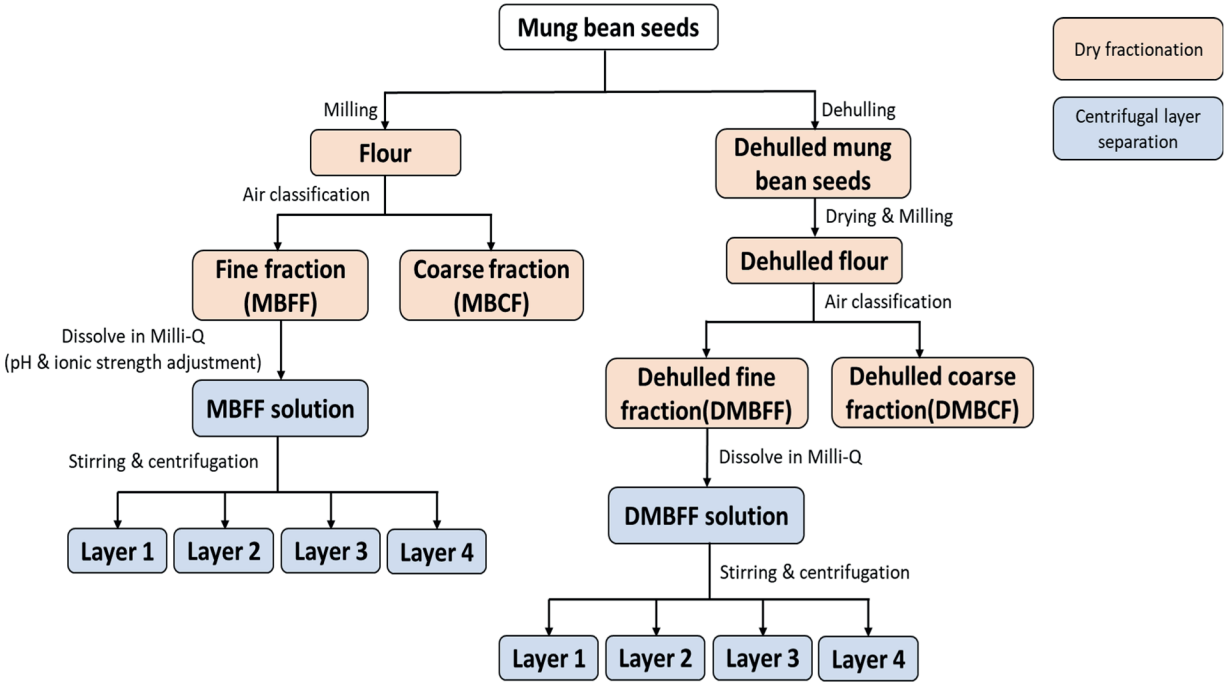

Figure 2.1 *Overview of dry fractionation to obtain mung bean fractions (left) and dehulled mung bean fractions (right) and mildly hybrid liquid separation process to produce mung bean proteins. Mung bean seeds were dehulled (for dehulled fine fraction) then milled or directly milled (for fine fraction) to liberate proteins from the seeds. Subsequently, fine fractions were dissolved in ultrapure water and stirred at different conditions to extract proteins. The fine fraction solution was centrifuged at 2500 RCF to separate proteins in Layer 1 from other components.*

2.2.3 Dry fractionation

For both Mung bean fine fraction (MBFF) and DMBFF, beans were milled using a Multimill Hosokawa System (Hosokawa Micron B.V., Doetinchem, the Netherlands) equipped with a ZPS50 (Hosokawa Micron B.V., Ausburg, Germany) impact mill. Wheel speed was set to 8000 rpm and 4000 rpm for MBFF and DMBFF, respectively. Mill feeding was carried out by a screw feeder at a rate 20 rpm and a batch size was used of 400 g at the airflow 52 m^3/h. After milling, the Multimill Hosokawa was equipped with an ATP50 (Hosokawa Micron B.V., Ausburg, Germany) air classifier. Subsequently, the impact milled flour was further air classified at different classifier wheel speeds (1000 rpm, 2500 rpm and 4000 rpm for MBFF, 8000 rpm for DMBFF), as indicated, at constant feed rate (20 rpm) and airflow (52 m^3/h). The final protein-rich Mung bean fine fractions (MBFF) and starch-rich coarse fractions were obtained, the MBFF was used for experiments.

2.2.4 Scanning electron microscope

MBFF produced at different classification speeds were fixed on sample holders with Carbon adhesive discs, the excess of flour was removed using an air gun. Afterward, the samples were sputter coated with 2nm Tungsten (MED 020, Leica, Vienna, Austria) and investigated with a field emission scanning electron microscope (Magellan 400, FEI, Eindhoven, the Netherlands). All images were recorded at a working distance of 5 mm with SE detection mode at 2kV at room temperature.

2.2.5 Layer Formation in centrifugal field

For layer formation in the centrifugal field, 20 grams of MBFF was dissolved in 80 grams Milli-Q water (PURELAB Ultra, United Kingdom) at room temperature. Stirring times were 10, 30, and 120 minutes, as indicated. After stirring, the samples were transferred into 50mL blue cap centrifuge tubes and centrifuged at 2500 g for

30 minutes by a Hermle Z-383K centrifuge (HERMLE Labortechnik GmbH, Wehingen, Germany), resulting in layer formation.

Layer formation experiments were also performed at different ionic strengths and pH values (as indicated, respectively). For these experiments, MBFF was first dissolved in Mili-Q water. Next, the pH was set by the addition of small amounts of 1M HCl or NaOH solutions, and the ionic strength was adjusted by the addition of solid NaCl.

Layers are numbered from the top of the tube, with the centrifugal field pointing downwards. The top layer (Layer 1) was collected and prepared as a concentrated stock solution (referred to as stock) by Amicon Stirred Cells Ultrafiltration system (Merck KGaA, Darmstadt, Germany) using a 10kDa filter membrane. The stirred cell was pressurized to 3.8 atm until the desired protein concentration (approximately 20%) was reached. The protein content of the stock solution was determined by Dumas (Nitrogen analyser, Flash EA 1112 series, Thermo Scientific, Breda, the Netherlands) with a nitrogen conversion factor of 6.25 (Mariotti *et al.*, 2008). Before measurements, stock solutions were stored in the fridge at 4 °C for no longer than 5 days.

2.2.6 Particle size distribution

Particle size distribution of the MBFF powders were analysed using a laser diffraction Mastersizer 3000 equipped with an Aero S dry dispersion unit (Malvern Instruments Ltd., United Kingdom), the pressure was set at 200 kPa. For the layers obtained after centrifugation, the particle size distribution measurements were conducted by a laser diffraction particle size analyser Mastersizer 2000 (Malvern Instruments Ltd., United Kingdom), the particle refractive index was set at 1.48 for all samples.

2.2.7 SDS-PAGE

Non-reducing SDS-PAGE were conducted to analyse the protein composition. An Invitrogen 4-12% gradient Bis-Tris gel and 20x MES SDS running buffer (Thermo fisher scientific Inc., Waltham, Massachusetts, United States) were used. Samples were taken from the different layers obtained (1-4) after centrifugation of dissolved MBFF. Subsequently, samples were diluted with deionized water to reach a protein concentration range suitable for SDS-PAGE analysis. The gel electrophoresis was performed for 30 min at a constant voltage (200 V) using an XCell Surelock Mini-Cell electrophoresis system (Thermo fisher scientific Inc., Waltham, Massachusetts, United States). Afterward, the gels were stained using Simply Blue Safe Stain and imaged using a Biorad GS900 gel scanner (Bio-Rad, Hercules, California, United States).

2.2.8 Protein content

Dry matter content (g/g) of the different samples were determined by drying the samples overnight in an Venticell Laboratory oven at 105 °C. To determine the protein content, the Dumas analysis was used with a nitrogen conversion factor of 6.25 as introduced in section 2.2.4. Protein content of layers and MBFF was calculated by Eq. 2.1

$$Protein\ content\ (dm\ \%) = \frac{protein\ from\ Dumas\ [g]}{total\ mass\ [g]} \times\ 100\% \qquad (2.1)$$

Protein yield was calculated for each layer by Eq. 2.2

$$Protein\ yield\ (\%) = \frac{protein\ in\ layer\ from\ Dumas\ (g)}{total\ protein\ in\ sample\ from\ Dumas\ (g)} \times 100\% \qquad (2.2)$$

2.2.9 Mineral content analysis

The mineral composition was determined using inductively coupled plasma atomic emission spectroscopy (ICP-OES) (iCAP 6300, Thermo Fisher Scientific Inc., Waltham, Massachusetts, United States).

2.2.10 Rheology

Flow curves before heat treatment

A stock solution with a protein concentration 22% was prepared by concentrating MBFF Layer 1 obtained at pH 8 (the maximum protein yield pH condition for the aqueous phase separation) using ultrafiltration. This stock solution was used to make a concentration series (5.3% -16.5%) by diluting with Milli-Q water. M65 reference samples were made similarly with concentrations 5%-11%, where the upper limit was chosen in view of the observed M65 solubility of 11.0 wt%. The shear viscosity was measured over a shear rate range from 1 s^{-1} to 1000 s^{-1} using an MCR 502 rheometer (Anton Paar, Graz, Austria), which was equipped with a sand-blasted concentric cylinder (CC17) geometry (Anton Paar, Graz, Austria). Data were analysed using the Power-law model to acquire the flow index (n) and consistency index (K). A volume of 4.7 ml of each sample was loaded in the cup of the geometry and a solvent trap was used to prevent solvent evaporation. The flow curves were measured in duplicate.

Small-strain dynamic rheology during heat treatment

After the flow curve measurements, small-strain dynamical rheological measurements were performed during heat treatment. The temperature was increased from 23 °C to 90 °C at a constant rate of 3 °C / min, kept at 90 °C for 30 min and finally decreased again at a rate of 3 °C / min. During the heat treatment, values for the storage modulus (G') and loss modulus (G'') were recorded at a strain of 1% and a frequency of 1Hz. The loss tangent (tan δ = G''/G') at the end of the heat treatment was also calculated. These measurements were conducted in duplicate.

2.2.11 Statistical analysis

All measurements were performed at least in triplicate except for indicated otherwise. The results are presented as the mean ± standard deviation of replicates.

Statistic analysis was conducted by IBM SPSS Statistics 25 (IBM SPSS Inc., Chicago, USA) with a one way ANOVA using the post-hoc method Tukey at $P < 0.05$ level.

2.3 Results and discussion

2.3.1 Dry fractionation

The particle size distributions of the fine fractions of the Mung bean flours (MBFF) after air classification at different speeds were analysed using static light scattering. The resulting particle size distributions are shown in Fig. 2.2A. For all three speeds used (1000 rpm, 2500 rpm, 4000 rpm classifier wheel speed) there are two main peaks, a smaller one at around 20 µm and a larger one at around 150 µm. There is little difference between the particle size distributions at these different air classification speeds. Next, the protein contents were determined for the MBFF. Results are shown in Fig. 2.2B. There is little variation in protein content, all powders have a protein content in the range of 23-24 g/100 g.

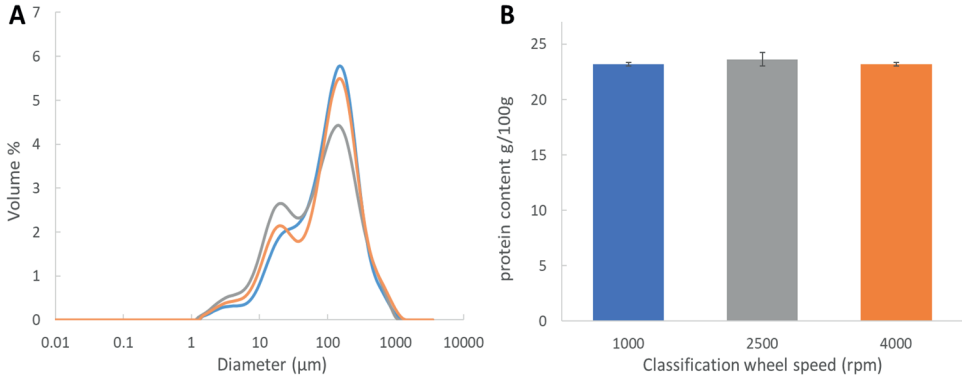

Figure 2.2 *The relative volume as a function of particle diameter distribution* ***A)*** *and protein content* ***B)*** *of mung bean powder produced at 1000, 2500 and 4000 rpm classifier wheel speed. All measurements were carried out in triplicate.*

To determine the nature of the two particle populations in the powders, we turn to scanning electron microscopy. A number of typical images are shown in Fig. 2.3 Despite the similarity in particle size distribution obtained from light scattering, a comparison of Fig. 2.3A-2.3C seems to indicate that at 1000 rpm air classification is

insufficient and large fragments still exist in the fine fraction. In general, after dry fractionation, for fractured mung bean seed cells, a considerable amount of oval starch granules with a typical size of 20 µm and several protein bodies with a much smaller size than starch granules can be seen to be liberated. The protein bodies are much smaller in size, they can be better recognized in the image taken at a higher magnification shown in Fig. 2.3D. Only dry fractionation does not separate all protein bodies from all starch granules: many protein bodies are associated with (fragments of) starch granules. Hence, if higher concentrations of native Mung bean proteins are required, a further purification step will be necessary, for which we here use (layer-based) centrifugal separation of (rather concentrated) aqueous dispersions of MBFF.

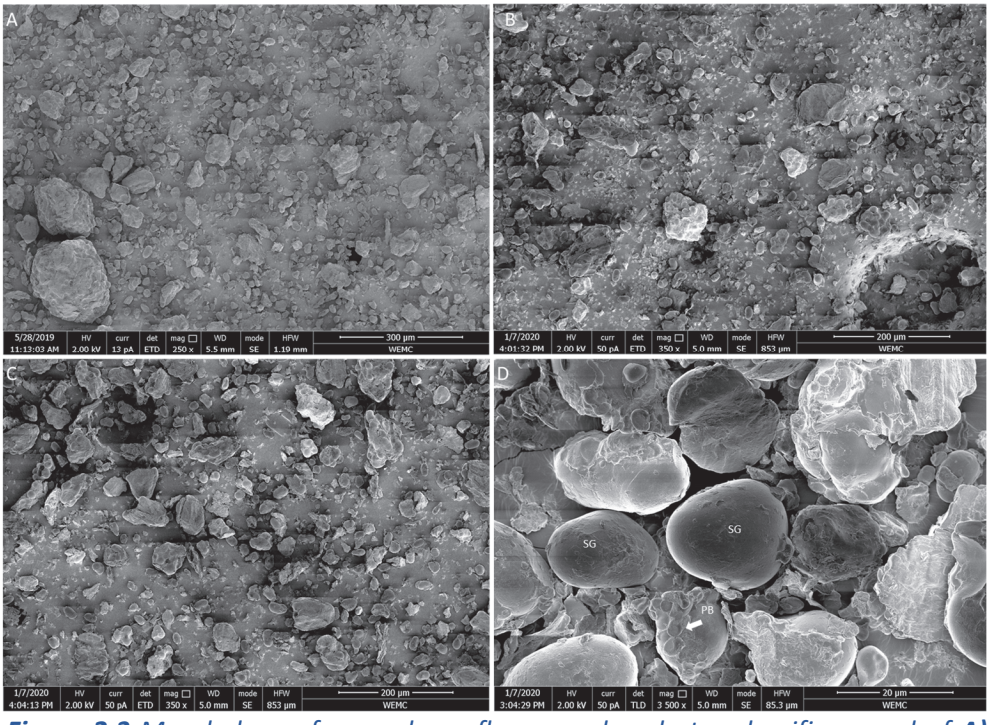

Figure 2.3 *Morphology of mung bean flours produced at a classifier speed of* ***A)*** *1000,* ***B)*** *2500,* ***C)*** *4000,* ***D)*** *2500 rpm, showing unground fragments and individual starch granules associated with protein bodies. PB: protein body, SG: starch granule. Scale bars correspond to 200 µm (A, B, C), and 20 µm (D).*

2.3.2 Layer formation after centrifugation

After dispersing the MBFF in ultrapure water, and after centrifugation, the MBFF has separated into 4 clearly distinguishable layers, as shown in Fig. 2.4A. Layers are numbered from top to bottom, with the centrifugal field pointing downwards. The compositional analysis of the layers will be discussed later, we start by noting some general features. For these layer-based separations of plant proteins, it is found that the top layers contain most of the protein, whereas the bottom layers contain most of the carbohydrates (Pelgrom *et al.*, 2015a). In our case, the volume of Layer 1 was by far the largest. Layer 1 was a low viscosity liquid. Layer 2 had a soft gel-like consistency, whereas Layer 3 and 4 had a solid-like consistency, with Layer 4 being the hardest. From here on, we mostly focus on Layers 1 and 2, which contain most of the Mung bean protein.

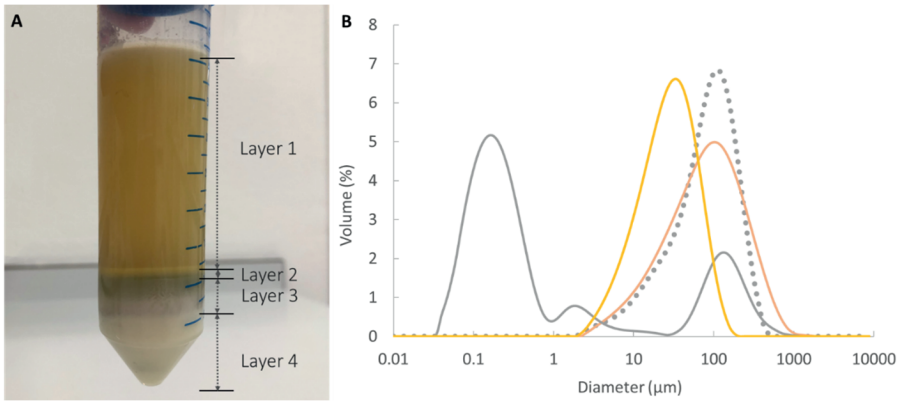

Figure 2.4 *Aqueous phase separation mung bean A) after 120 minutes of stirring and 30 min centrifugation at 4500 g; B) particle size distribution of Layer 1 (grey solid line), Layer 2 (yellow solid line), concentrated stock solution (dark yellow solid line) and commercial product M65 (grey dashed line). All measurements were carried out in triplicate.*

First, for Layers 1 and 2, a stock solution and a commercial Mung bean protein sample (denoted by M65) we analyzed the size distribution of the particles in the dispersions, using static light scattering. Results are shown in Fig. 2.4B. Layer 1 showed a highly polydisperse distribution with a peak at 0.2 µm and aggregates size around 100 µm, Layer 1 concentrate, Layer 2 and M65 presented a peak around

100 µm, 35 µm and 120 µm, respectively. Since Layer 1 was a low viscosity liquid layer, it was believed to mostly contain free protein particles. And Layer 2 could be considered as more dense protein particles separated by the centrifugal force. Although a similar particle size was confirmed for Layer 1 concentrate and M65 at the same protein concentration, rheological behaviour such as viscosity of these two samples were found different. The rheological properties will be investigated and discussed in detail later.

Next an SDS-PAGE analysis under nonreducing condition was carried out on Layers 1 and 2, to determine whether some Mung bean proteins preferentially partition in one of the layers or not. Results are shown in Fig. 2.5. Major bands are similar in (relative) intensity for Layers 1 and 2: bands around 66 KDa, 50 KDa, 31 KDa, and 26KDa can be attributed to the most abundant 8S globulins (Vicilin) in Mung beans. Bands around 40KDa and 20KDa can be considered as 11S globulins (Legumin) (Tang & Sun, 2010). Except for some bands related to smaller proteins present in phase 2, SDS-PAGE shows no noticeable difference between the protein compositions of Layers 1 and 2. Layer 2 does show more protein material that has not migrated into the gel, signifying that it contains more protein in an aggregated state, as was also found using light scattering. In short, the conclusion is that with respect to protein composition, SDS-PAGE does not show much difference between the layers, the only difference is in the total concentration and the aggregation state of the proteins.

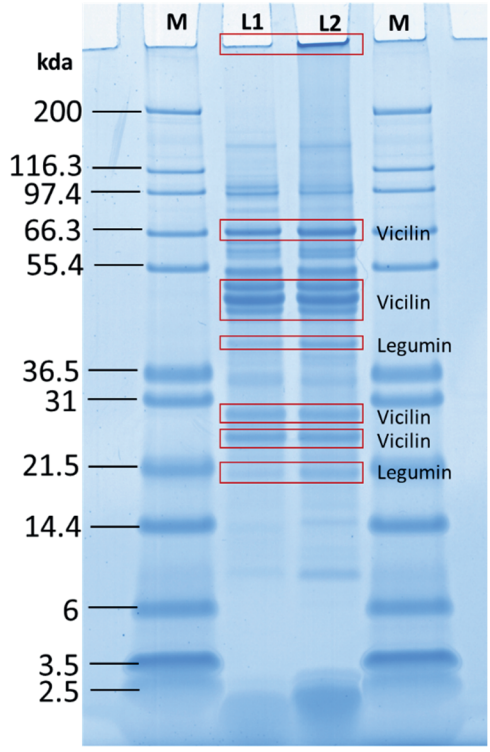

Figure 2.5 *The non-reducing SDS-PAGE pattern of Layer 1 and Layer 2 of MBFF generated by aqueous phase separation at pH 8 without salt addition. M, L1, and L2 represent Marker 12, Layer 1, and Layer 2, respectively.*

2.3.3 Protein content and yield

Subsequently, we analysed the protein content on a dry matter basis (g/g dm) and as a yield for each of the 4 layers, for several variations of the fractionation and purification process parameters. Parameters that were varied were: the wheel speed for the air-classification, stirring time, pH and concentration of added NaCl for the solvent to disperse the MBFF. Results are shown in Table 2.1. First, irrespective of process parameters, and as expected, we find that protein yield decreases with layer number. By far, most of the protein ends up in Layer 1. The protein concentration of the Layer 2 is higher, but since its volume is much smaller, the protein weight is lower than Layer 1 (3.188 g and 0.352 g for Layer 1 and Layer 2, respectively), leading to the protein yield of Layer 2 is lower. When optimizing

the fractionation and purification process, we focus on the combined protein yield for Layers 1 and 2, to which we simply refer as 'protein yield'. Likewise, when investigating the functionality of the isolated Mung bean proteins, we will do so for the combined Layers 1 and 2.

We find that many of the varied processing parameters do not strongly affect the protein yield of layer. First, consider the speed used for air-classification. When increasing the wheel speed from 1000 rpm to 4000 rpm (keeping the stirring time for the resulting MBFF at 10 min), we find the protein yield increases moderately from 78.9% to 84.4% (See Appendix Figure S2.1). The difference between the yields for 2500 rpm and 4000 rpm was not large, thus, 2500 rpm was used for the remainder of the work. The effect of stir time when dispersing the MBFF, was even less pronounced (See Appendix Figure S2.2), and we use the shortest stirring time (10 min) for the remainder of the work. Likewise, we find that added NaCl only has a minor influence on the protein yield of the layer (See Appendix Figure S2.3), hence for the remainder of the work no NaCl was added.

The only process parameter we investigated that significantly affects the protein yield is the pH of the MBFF dispersion used for the centrifugal layer separation. Results for the protein contents of the layers, and the protein yield as a function of pH (taken from Table 2.1), are shown in Fig. 2.6. When dispersed in Milli-Q water, the pH of the MBFF dispersions was around 6.5. Acid and base were added to the dispersions to bring the pH to values of pH 6 and pH 8 respectively. We find that adding acid strongly reduces protein yield, whereas adding base, leads to a small increase of the yield. The highest yield, obtained for air classification at 2500 rpm and 10 min stirring at pH 8, with no added salt, is 85.1%. While in practice it may not be worthwhile to perform the additional pH adjustment, for investigating the functionality of the Mung bean proteins, we here continue with the Layer 1 proteins obtained at the highest yield proteins, we here continue with the Layer 1 proteins

obtained at the highest yield conditions (air classification at 2500 rpm, 10 min stirring at pH 8, no added salt).

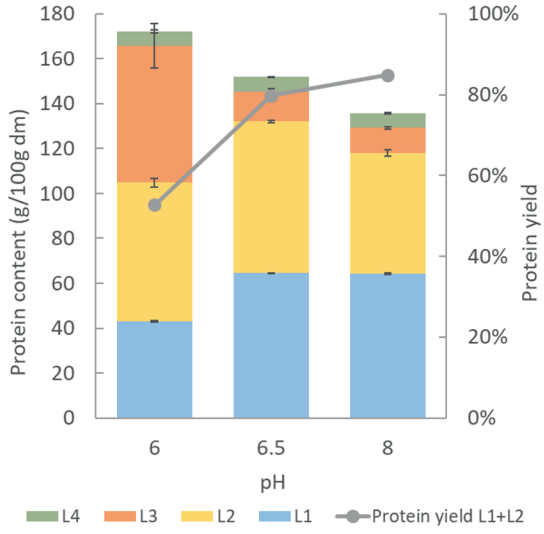

Figure 2.6 *Protein content and yield of 2500 rpm mung bean fine fraction at pH 6, pH 6.5 (neutral) and pH 8 aqueous phase separation with 10 min stirring. All measurements were carried out in triplicate.*

Finally, we also investigated the effect of dehulling on protein yield (data not in Table 2.1). Dehulled Mung bean seeds were milled at 4000 rpm, and subsequently air-classified at a wheel speed of 8000 rpm, resulting in Dehulled Mung bean fine fractions (DMBFF). We find that DMBFF has a much higher protein content (49 g/ 100g dm, at 4000 rpm wheel speed) than MBFF (highest value is 24g/100g dry matter, at 8000 rpm wheel speed). This result is not unexpected, since dehulling leads to a significant reduction of non-protein material. Afterward, we continued by performing centrifugal layer separation on the DMBFF. Surprisingly, here we find that the dehulling reduces the overall protein yield (Appendix Figure S2.4A), the total protein yield of DMBFF Layer 1 and Layer 2 was 72.8% whereas the total yield of MBFF was 79.8% (neutral pH, no salt added). It is believed that the aqueous system applied during centrifugal separation has a limited protein dissolve capacity. Since DMBFF brings more proteins than MBFF into the system and a part of the excessive proteins cannot be dissolved in the aqueous system, unable to be

maintained in Layer 1 or Layer 2 after centrifugation. The extra proteins added but cannot be dissolved could lower the protein yield. Wheel speed and air classification speed employed to produce DMBFF could also influence the separation efficiency. The setting we applied in the present study (mill speed 4000 rpm, classification speed 8000 rpm) probably break the seeds insufficiently, therefore, it cannot liberate maximum protein bodies from seeds. However, further research should be performed to determine the optimum settings for DMBFF dry fractionation.

Table 2.1 *Protein content and protein yield of aqueous phase separation systems under different conditions.*

				L1			L2			L3			L4		
Rotation speed (Classification) RPM	**Stirring time (min)**	**pH**	**Salt addition (M)**	**Protein yield (%)**	**protein content (g)**	**dry matter (g)**	**Protein yield (%)**	**protein content (g)**	**dry matter (g)**	**Protein yield (%)**	**protein content (g)**	**dry matter (g)**	**Protein yield (%)**	**protein content (g)**	**dry matter (g)**
1000	**10**	**6.5**	**0**	69.94	3.11	5.52	7.75	0.34	0.56	10.64	0.47	3.02	13.31	0.59	7.82
2500		**6**		28.83	1.28	3.27	23.85	1.06	1.88	24.66	1.10	1.97	13.40	0.60	10.49
		6.5		71.81	3.19	5.42	7.92	0.35	0.57	15.61	0.69	5.74	7.51	0.33	5.59
			0.25	76.94	3.42	6.85	7.65	0.34	0.55	6.47	0.29	1.52	14.88	0.66	8.91
			0.5	75.62	3.36	7.76	4.66	0.21	0.33	11.01	0.49	4.03	9.15	0.41	7.28
		8	**0**	80.90	3.59	6.17	3.92	0.17	0.65	7.83	0.35	3.43	8.46	0.38	6.37
	30	**6.5**		74.02	3.29	5.64	8.36	0.37	0.57	10.64	0.47	1.95	15.45	0.69	7.81
	120			75.62	3.36	5.72	6.71	0.30	0.42	12.25	0.54	2.88	13.48	0.60	7.46
4000	**10**			76.06	3.38	5.80	8.09	0.36	0.54	8.88	0.40	2.23	14.15	0.63	7.69

2.3.4 Mineral analysis

Mineral content is a key attribute of food ingredients that may (partly) depend on fractionation and purification processes. Therefore, we have analysed the mineral content for the MBFF and the MBCF, as obtained from the air-classification. Similarly, we analysed the mineral content of the Layers 1-4 obtained of the MBFF dispersions, a stock solution obtained by ultrafiltration of Layer 1, and a reference commercial Mung bean protein powder (labelled M65). Except for powder samples, other liquid or semi-solid samples are freeze dried before analysis. Results are shown in Table 2.2.

Results were obtained using a flow injection analyser for Cl and ICP-OES for all other elements. The coarse and fine flour fractions MBCF and MBFF present comparable mineral contents except for Ca^{2+}. This is probably caused by the higher fraction of Calcium-enriched hull (Lombardi-Boccia *et al.*, 1998) in the coarse fraction. In general, the total mineral content of the stock is 36.99 g/kg which is higher than M65 (24.51 g/kg), the difference between these samples is largely contributed by K content which came from the raw material. Whereas mung bean protein samples possess higher total amount of ions than commercial whey proteins. The Ca content of Layer 1 and stock (0.9 g/kg) is 10-fold higher than whey proteins (0.09 g/kg) (Cornacchia, Fortelle & Venema, 2014). This property makes the stock a promising protein ingredient that can be employed in calcium fortification protein drinks.

For the layers, we find that Ca, Fe, Mg, Mn, P, Zn ions are enriched in Layer 2, presumably because they are more strongly associated with proteins. This result is partly aligning with the previous research. According to Posch et. al (1995) and Wiiliams & Silva (2000), Mn and Zn as transition metal ions, interacting strongly with proteins via electrostatic forces. The presence of Mg- and Ca-ions probably can be explained by previous observation for soybean seed (Sussulini *et al.,* 2006). The content of Ca and Mg depends on applied extraction approaches since they

were found to possess moderate interactions with proteins. Due to mildly extraction method employed in the present study, Ca and Mg were allowed to maintain their coordination with proteins, therefore, these ions were preserved.

Table 2.2 *Elements distribution upon different fractions and treatments.*

Elements	Unit	MBCF	MBFF	Layer 1	Layer 2	Layer 3	Layer 4	STOCK	M65
Ca		1.92	0.51	0.83	2.55	0.57	n/a*	0.88	4.10
Cu		0.010	0.011	0.028	0.021	0.009	0.002	0.037	0.016
Fe		0.104	0.102	0.124	0.164	0.101	n/a	0.133	0.180
K		12.3	12.8	30.0	20.5	12.7	2.7	15.8	3.7
Mg		1.97	1.54	3.36	7.32	1.25	0.24	2.60	1.13
Mn	g/kg	0.014	0.014	0.027	0.093	0.013	n/a	0.031	0.034
Na		n/a	n/a	4.970	2.973	2.051	0.395	2.610	4.334
P		4.14	4.83	11.20	18.7	4.0	0.88	9.53	7.44
S		1.92	2.21	5.22	4.01	2.07	0.37	4.26	3.24
Zn		0.028	0.031	n/a	0.074	0.025	n/a	0.084	0.057
Cl		0.40	0.55	1.67	n/a	0.36	0.08	1.04	0.29

**n/a represents results lower than the detection limit. The detection limit for Ca: 0.15g/kg; Fe: 60 mg/kg; Mn: 0.05 g/kg; Na: 15 mg/kg; Zn: 5 mg/kg.*

On the other hand, for Cu, K, Na, S, and Cl the amounts correspond to water content in all layers, more amount of elements were detected in the layer which has higher water content. It is suggesting that they are mostly not associated with proteins or polysaccharides. While K, as a monovalent ion, tended to be lost during processing since it binds to protein weakly (Sussulini *et al.*, 2006). This can also explain the considerable reduction in Na and K content that we observe after ultrafiltration to obtain the stock solution from Layer 1 (from 4.970 to 2.610 g/kg and 30.0 to 15.8 g/kg, respectively). Amounts of Sodium in Layer 1 are similar to those in the M65 and lower than M65 after ultrafiltration. Unfortunately, this value is still significantly higher than commercial whey proteins, it is undesirable when considering the low sodium diet recommendation. A further filtration process can be applied to remove the extra sodium from the stock solution to qualify it as a

commercial plant protein ingredient if necessary. Note that no significant amounts of sodium were present in the dry fractions. This implies that the high Sodium content is due to additions during processing, in particular during pH adjustment.

2.3.5 Rheology

First, we consider the viscosity of the mildly purified Mung bean proteins before thermal treatment. Results for the flow curves of the MBFF Layer 1 protein and the M65 protein isolate at different concentrations are shown in Fig. 2.7.

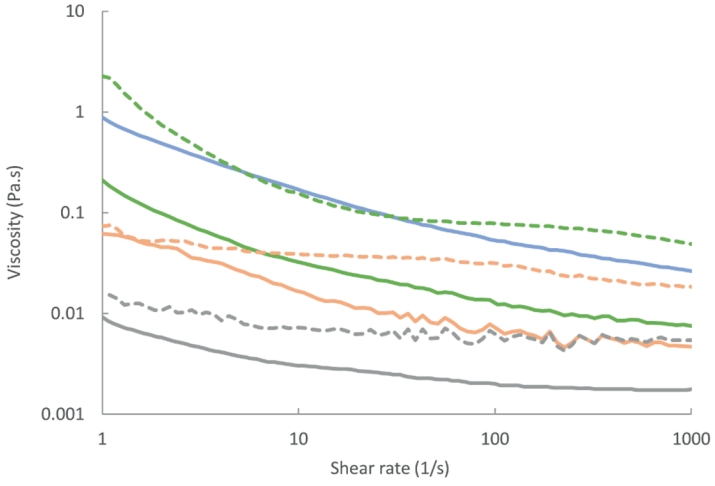

Figure 2.7 *Viscosities of MBFF aqueous phase separation samples (solid lines) at protein concentrations 5.3% (grey), 8.3% (orange), 11.0% (green), 16.5% (blue) and commercial mung bean protein concentrates M65 (dashed lines) at 5.3% (grey), 8.3% (orange) and 11.0% (green). MBFF samples were prepared by diluting the 22.0% concentred protein stock solution. All measurements were carried out in duplicate.*

All samples showed shear-thinning behaviour. At comparable protein concentration, M65 was found to have significantly higher viscosities than the MBFF Layer 1 samples. The highest viscosities were found for M65 at a concentration of 11%, while at a concentration of 16.5%, the MBFF Layer 1 proteins still exhibit a viscosity appreciably less than the M65 proteins at 11%. The Powder – law model was applied to characterise the rheological behaviour of protein solutions since it fitted the shear stress and shear rate data well. Table 2.3 showed

that all samples are typical pseudoplastic fluids with n < 1. Protein solutions exhibited significant decreases ($P < 0.05$) in flow index n with the increase in protein concentration (indicating increased pseudoplasticity), whereas consistency index K increased upon the increasing protein concentration. Hence, more expressed viscous and shear thinning behaviours were observed with increasing protein concentration (Dissanayake *et al.*, 2013). Remarkably, K increased sharply (from 0.06 to 0.69) for M65 when protein concentration increased from 8.3% to 11.0% while MBFF only increased from 0.05 to 0.11. This finding correlated with the research of Bains & Pal (2019), who showed a similar K increase trend of emulsions. The difference in K increase could be illustrated by the water-binding capacity of the protein. Štreimikytė *et al.* (2020) reported that the protein which possesses good water-binding capacity contributed to a more pronounced shear-thinning behaviour in solutions.

Table 2.3 *Rheological characteristics of M65 and MBFF protein solutions.*

Sample	Protein concentration	Flow index n	Consistency index K (Pa.s^n)	Determination coefficient R^2
M65	5.3%	0.88±0.01^a	0.01±0.00*^{b}	0.99±0.00*
	8.3%	0.83±0.01^{ab}	0.06±0.01^b	1.00±0.00*
	11.0%	0.55±0.02^c	0.69±0.00*^{a}	0.97±0.01
MBFF	5.3%	0.79±0.02^{ab}	0.01±0.00*^{b}	0.99±0.00*
	8.3%	0.63±0.09^{bc}	0.05±0.03^b	0.97±0.02
	11.0%	0.56±0.01^c	0.11±0.00*^{b}	0.97±0.01
	16.5%	0.52±0.06^c	0.60±0.23^a	0.98±0.01

**Represents the standard deviation is lower than 1%.*

Values are presented as mean ± standard deviation. Letters indicate significant difference between protein samples at $P < 0.05$.

We also consider structure formation during heat treatment at higher protein concentrations (>5%). Small deformation rheology is used to monitor protein gelation during the thermal treatment, which consists of a heating ramp (23 °C - 90 °C at 3°C /min), followed by 30 min at 90 °C, and a cooling ramp (90 °C -23 °C, at 3 °C /min). The results are shown in Fig. 2.8. The minimal gelling concentration is around 10% for both the MBFF Layer 1 protein and the commercial M65 concentrates (Fig. 2.8C). As shown in Fig. 2.9, the final gel moduli (after the gels having been cooled down back to the room temperature) increase rapidly with increasing protein concentration, once above the critical concentration of around 10%, with not much difference between the MBFF Layer 1 proteins and the M65 protein isolate.

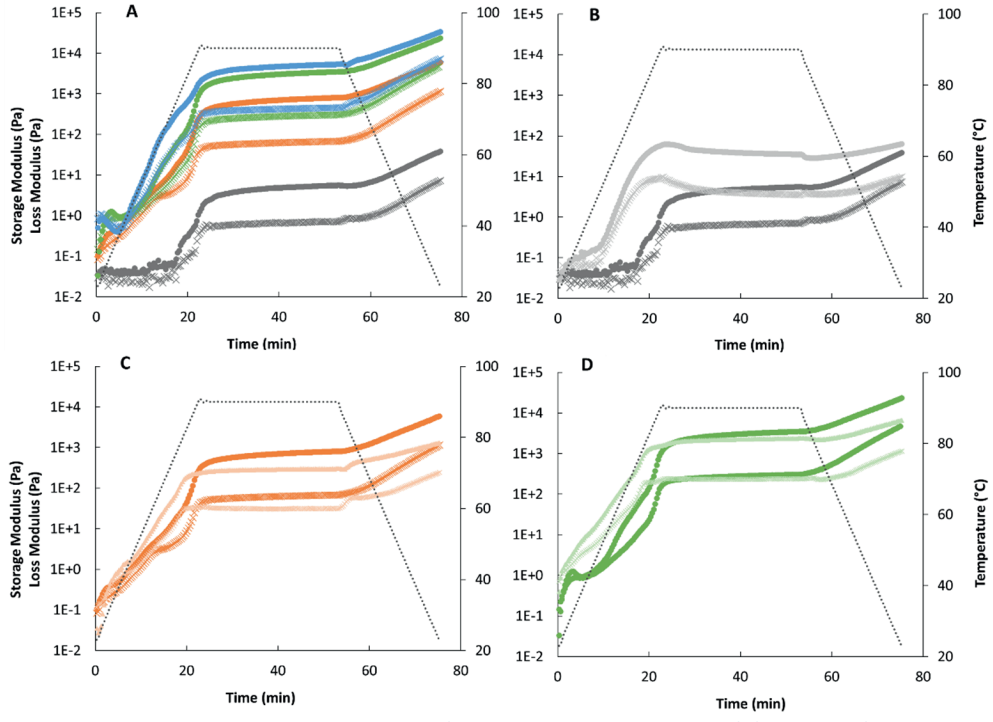

Figure 2.8 *The temporal evolution of the storage modulus G' (triangles) and loss modulus G''(crosses) of* ***A)*** *MBFF protein dilutions with 5.3% (grey), 8.3% (orange), 11.0% (green) and 16.5% (blue) protein concentration;* ***B)*** *MBFF protein dilution (grey) and M65 solution (light grey) with a total protein concentration of 5.3%;* ***C)*** *MBFF protein dilution (orange) and M65 solution (light orange) with a total protein*

concentration of 8.3%; ***D)*** *MBFF protein solution (green) and M65 solution (light green) with a total protein concentration of 11.0%. The thermal treatment is shown by the dashed line. All measurements were conducted at a constant frequency of 1Hz and a constant strain of 1%. All measurements were carried out in duplicate.*

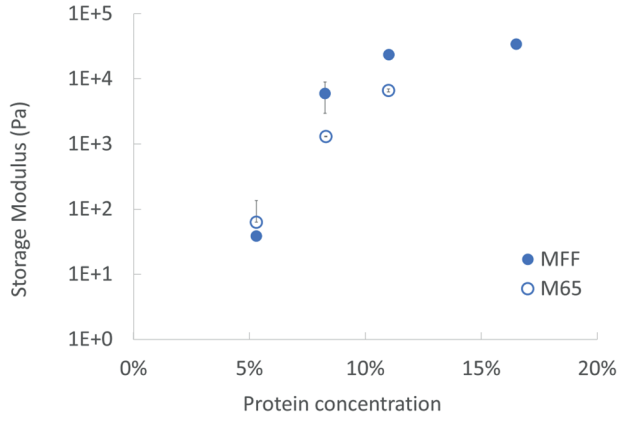

Figure 2.9. *Gel properties of MBFF (solid symbols) and M65 (open symbols) heated at 90 ˚C as a function of protein concentration. All measurements were carried out in duplicate.*

2.4 Conclusion

We have shown how air-classification and centrifugal layer separation can be combined to mildly purify Mung bean proteins, minimizing the level of denaturation. In particular, we found that after performing centrifugal layer separation on the MBFF at either its natural pH of 6.5 or at pH 8, both the yield (71.61% and 80.92%, respectively) and protein content (64.57% and 64.22%, respectively) of the Layer 1 fraction are very high.

In general, one expects protein denaturation and aggregation during ingredients preparation to have a deleterious effect on the resulting ingredient functionality (Schutyser & van der Goot, 2011). For example, for beverages, one requires high solubility and low viscosity. Indeed, we find that solubility is lower, and viscosity is higher for the reference commercial M65 Mung bean protein concentrates, as compared to the MBFF Layer 1 proteins.

Both differences can probably be attributed to the formation of protein aggregates during ingredient preparation in the case of the commercial isolate M65. Indeed, from light scattering we found (Fig. 4B) that the average particle diameters in dispersions of MBFF Layer 1, concentrated MBFF Layer 1 and M65 were, respectively, 0.2, 100, and 120 µm.

Our results are consistent with what has been reported for other sources, such as for pea. Kornet *et al.* (2020) found that for more mildly processed pea protein fractions, the viscosity increased less rapidly with increasing protein concentrations than pea protein fractions that had experienced more extreme pH and temperature values. It should be noted that except for conditions applied to produce protein ingredients, sterilisation approaches such as Pasteurisation could have an influence on the viscosity of final products as well. Remarkably, we find that at least for this case, the purification process and the associated degree of protein denaturation and aggregation, does not seem to have a strong impact on heat-set gelation.

A crucial final step will be to develop a drying process for the MBFF Layer 1 dispersions that likewise maintains the native state of the proteins, such that these mildly purified Mung bean proteins can be applied in, for example, plant protein beverages.

References

Avila Ruiz, G., Arts, A., Minor, M., & Schutyser, M. (2016). A Hybrid Dry and Aqueous Fractionation Method to Obtain Protein-Rich Fractions from Quinoa (Chenopodium quinoa Willd). *Food and Bioprocess Technology*, *9*(9), 1502–1510.

Bains, U., & Pal, R. (2019). In-Situ Continuous Monitoring of the Viscosity of Surfactant-Stabilized and Nanoparticles-Stabilized Pickering Emulsions. *Applied Sciences, 9*(19), 4044.

Cornacchia, L., Forquenot de la Fortelle, C., & Venema, P. (2014). Heat-induced aggregation of whey proteins in aqueous solutions below their isoelectric point. *Journal of Agricultural and Food Chemistry*, *62*(3), 733–741.

de Kort, E., Minor, M., Snoeren, T., van Hooijdonk, T., & van der Linden, E. (2011). Effect of calcium chelators on physical changes in casein micelles in concentrated micellar casein solutions. *International Dairy Journal*, *21*(12), 907–913.

Dissanayake, M., Ramchandran, L., & Vasiljevic, T. (2013). Influence of pH and protein concentration on rheological properties of whey protein dispersions. *International Food Research Journal, 20*(5), 2167.

Du, M., Xie, J., Gong, B., Xu, X., Tang, W., Li, X., … Xie, M. (2018). Extraction, physicochemical characteristics and functional properties of Mung bean protein. *Food Hydrocolloids*, *76*, 131–140.

Kornet, C., Venema, P., Nijsse, J., van der Linden, E., van der Goot, A. J., & Meinders, M. (2020). Yellow pea aqueous fractionation increases the specific volume fraction and viscosity of its dispersions. *Food Hydrocolloids*, *99*, 105332.

Kudre, T. G., Benjakul, S., & Kishimura, H. (2013). Comparative study on chemical compositions and properties of protein isolates from Mung bean, black bean and bambara groundnut. *Journal of the Science of Food and Agriculture*, *93*(10), 2429–2436.

Kumar, P., Chatli, M. K., Mehta, N., Singh, P., Malav, O. P., & Verma, A. K. (2016). Meat analogues: Health promising sustainable meat substitutes. *Critical Reviews in Food Science and Nutrition*, *57*(5), 923–932.

Lombardi-Boccia, G., Lucarini, M., Di Lullo, G., Del Puppo, E., Ferrari, A., & Carnovale, E. (1998). Dialysable, soluble and fermentable calcium from beans (Phaseolus vulgaris L.) as model for in vitro assessment of the potential calcium availability. *Food Chemistry*, *61*(1-2), 167–171.

Mariotti, F., Tomé, D., & Mirand, P. P. (2008). Converting Nitrogen into Protein—Beyond 6.25 and Jones' Factors. *Critical Reviews in Food Science and Nutrition*, *48*(2), 177–184.

MarketsandMarkets. (2021). *Plant-based Protein Market worth $15.6 billion by 2026*. Retrieved from https://www.marketsandmarkets.com/PressReleases/plant-based-protein.asp. Accessed April 8, 2021

Mattice, K. D., & Marangoni, A. G. (2020). Physical properties of plant-based cheese products produced with zein. *Food Hydrocolloids*, *105*, 105746.

Pelgrom, P. J. M., Boom, R. M., & Schutyser, M. A. I. (2015a). Functional analysis of mildly refined fractions from yellow pea. *Food Hydrocolloids*, *44*, 12–22.

Pelgrom, P. J. M., Vissers, A. M., Boom, R. M., & Schutyser, M. A. I. (2013). Dry fractionation for production of functional pea protein concentrates. *Food Research International*, *53*(1), 232–239.

Pelgrom, P. J. M., Wang, J., Boom, R. M., & Schutyser, M. A. I. (2015b). Pre- and post-treatment enhance the protein enrichment from milling and air classification of legumes. *Journal of Food Engineering*, *155*, 53–61.

Purwanti, N., Smiddy, M., Jan van der Goot, A., de Vries, R., Alting, A., & Boom, R. (2011). Modulation of rheological properties by heat-induced aggregation of whey protein solution. *Food Hydrocolloids*, *25*(6), 1482–1489.

Renkema, J. M. S., Knabben, J. H. M., & van Vliet, T. (2001). Gel formation by β-conglycinin and glycinin and their mixtures. *Food Hydrocolloids*, *15*(4-6), 407–414.

Rinaldoni, A. N., Palatnik, D. R., Zaritzky, N., & Campderrós, M. E. (2014). Soft cheese-like product development enriched with soy protein concentrates. *LWT - Food Science and Technology*, *55*(1), 139–147.

Schutyser, M. A. I., & van der Goot, A. J. (2011). The potential of dry fractionation processes for sustainable plant protein production. *Trends in Food Science & Technology*, *22*(4), 154–164.

Schutyser, M. A. I., Pelgrom, P. J. M., van der Goot, A. J., & Boom, R. M. (2015). Dry fractionation for sustainable production of functional legume protein concentrates. *Trends in Food Science & Technology*, *45*(2), 327–335.

Simons, C., Hall, C., & Biswas, A. (2017). Characterization of pinto bean high-starch fraction after air classification and extrusion. *Journal of Food Processing and Preservation*, *41*(6).

Štreimikytė, P., Keršienė, M., Eisinaitė, V., Jasutienė, I., Lesauskaitė, V., Damulevičienė, G., Knašienė, J., & Leskauskaitė, D. (2020). Formulating protein-based beverages for the dysphagia diets of the elderly: viscosity, protein quality, in vitro digestion, and consumers acceptability. *Journal of the Science of Food and Agriculture, 100*(10), 3895–3901.

Sussulini, A., Garcia, J. S., Mesko, M. F., Moraes, D. P., Flores, É. M., Pérez, C. A., & Arruda, M. A. (2006). Evaluation of soybean seed protein extraction focusing on metalloprotein analysis. *Microchimica Acta*, *158*(1-2), 173–180.

Tang, C.-H., & Sun, X. (2010). Physicochemical and Structural Properties of 8S and/or 11S Globulins from Mung bean [Vigna radiata(L.) Wilczek] with Various Polypeptide Constituents. *Journal of Agricultural and Food Chemistry*, *58*(10), 6395–6402.

Wang, J., Zhao, J., de Wit, M., Boom, R. M., & Schutyser, M. A. I. (2016). Lupine protein enrichment by milling and electrostatic separation. *Innovative Food Science & Emerging Technologies*, *33*, 596–602.

Wang, R., Jin, X., Su, S., Lu, Y., & Guo, S. (2019). Soymilk gelation: The determinant roles of incubation time and gelation rate. *Food Hydrocolloids*, *97*, 105230.

Waschatko, G., Junghans, A., & Vilgis, T. A. (2012). Soy milk oleosome behaviour at the air–water interface. *Faraday Discussions*, *158*, 157.

Wu, Y. V., & Nichols, N. N. (2005). Fine grinding and air classification of field pea. *Cereal Chemistry Journal*, *82*(3), 341–344.

Xing, Q., de Wit, M., Kyriakopoulou, K., Boom, R. M., & Schutyser, M. A. I. (2018). Protein enrichment of defatted soybean flour by fine milling and electrostatic separation. *Innovative Food Science & Emerging Technologies*, *50*, 42–49.

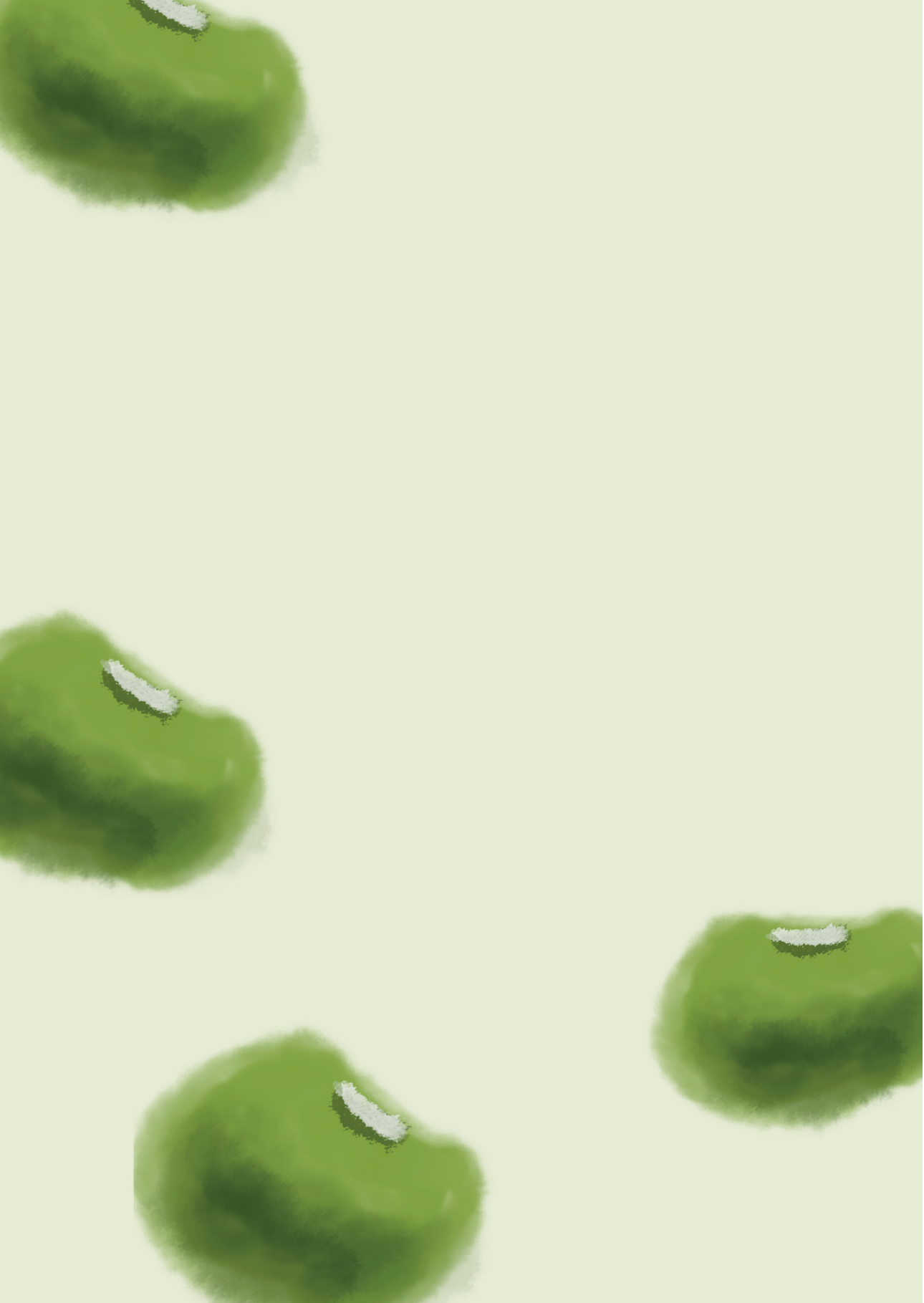

3

Soluble protein particles produced directly from mung bean flour by simple coacervation

This chapter is published as:

Yang, Q., Venema, P., van der Linden, E., & de Vries, R. (2023). Soluble protein particles produced directly from mung bean flour by simple coacervation. Food Hydrocolloids, 108541.

Abstract

Poor solubility is a common characteristic of many plant protein ingredients which often hampers product formulation. We exploit simple coacervation, or liquid-liquid phase separation, of plant proteins in flours, to formulate plant proteins as powders of submicron colloids with good solubility and dispersibility. We consider the specific case of mung bean flour, but the approach is more general. First, we study the influence of pH on the formation of submicron protein droplets ("coacervates") after alkaline protein extraction from Mung bean flour. Next, the proteins in droplets were heat-set into colloidal protein microgels, and the morphology of the colloids was assessed by scanning electron microscopy. The mung bean protein colloids have an intrinsic viscosity much lower than typical food thickeners, indicating the dense nature of the particles. After spray-drying, they maintain good solubility even close to the isoelectric point. Heat-induced gelation of redispersed protein particles resulted in gels with moduli much less than those of commercial mung bean protein concentrates at equivalent protein concentration. Hence, the main impact of the pre-treatment is on solubility, dispersibility and heat stability, with relevance to formulations such as plant-protein based beverages.

3.1 Introduction

Concerns over sustainability of animal proteins in our diet have led to a shift in consumer preferences towards diets richer in plant proteins (Aydemir & Yemenicioğlu, 2013; Carbonaro et al., 2015). This is accompanied by an intense interest in the food technology of processing plant proteins for novel food formulations (Aiking, 2011). It is generally acknowledged that many plant protein ingredients currently on the market suffer from problems with low solubility and low functionality, which is disadvantageous in formulating new food products with these ingredients. This behaviour is probably caused by intrinsic properties of plant proteins and by processing steps used to isolate the proteins (Wouters et al., 2016). Various approaches have been studied to remedy the deficiencies of current plant protein ingredients. For example, dry fractionation (Assatory et al., 2019; Pelgrom et al., 2013) can be used to obtain powders that retain the native structure of the plant proteins, improve their functionality.

In applications such as beverages, it is often the solubility of plant proteins which is limiting formulations. Earlier, researchers have shown for whey proteins that a colloidal formulation is highly advantageous for formulating thermally stable dispersions high in protein (Sağlam et al., 2013; Saglam et al., 2012). We here propose to investigate simple coacervation of plant proteins from flours as a mean to obtain dense, colloidally sized plant protein micro and nano gels, in order to formulate plant protein powders with high solubility and dispersibility.

It is well known that upon acidification, before becoming insoluble close to their iso-electric points, many plant storage proteins exhibit liquid-liquid phase separation, sometimes also called simple coacervation (Lazko et al., 2004). Liquid-liquid phase separation of plant storage proteins has also been observed upon acidifying soybean fraction isolates (Chen et al., 2020) or yellow pea flours (Lui et al., 2007) initially dispersed at alkaline pH. For the case of flours (as opposed to the

case of purified native plant storage proteins) macroscopic phase separation often does not occur, but rather micro phase separation is observed, in the form of the formation of small liquid, protein rich droplets which are typically of micron scale (Cochereau et al., 2019; Kornet, Roozalipour, et al., 2022; Li et al., 2020; Lui et al., 2007).

For relatively pure plant storage proteins, a number of recent studies have highlighted that simple coacervation in combination with heat induced gelation can be used to create a wide variety of microstructures including thin-walled capsules (Chen et al., 2017; Chen et al., 2020; Teng et al., 2012; Zhao et al., 2020). Microgels of plant storage proteins obtained directly from flours have not yet been studied extensively with respect to their functionality, as far as we are aware of.

For the specific case of mung bean flour, our aim is therefore to identify conditions of simple coacervation, to obtain microgels by heat set gelation of the protein microdroplets, and to test whether these droplets can be spray dried or freeze dried while retaining their functional properties. We used dry fractionation to start off with ingredients that are somewhat higher in native proteins than whole mung bean flour.

As we will show, mung bean protein coacervates (MBPC) obtained from dry fractionated mung bean flour are much smaller (submicron) than the droplets previously found upon acidifying (defatted) soybean flour (Lui et al., 2007). We find the heat-gelled (sub)micron mung bean protein droplets can be spray dried and resuspended without affecting the colloidal nature of the particles, and we characterize the properties of the re-dispersed proteins using various physical-chemical approaches.

3.2 Materials and methods

3.2.1 Materials

Dried mung beans (*Vigna radiata)* were obtained from a local store. According to the supplier the composition of the dried mung beans was protein 24%, fat 2%, carbohydrate 60% g. All beans still contained their hull and were unheated. Commercial mung bean protein concentrate (M65) containing 67.5 g/100 g protein, 0.10 g/100 g fat, and 20.98 g/100 g total carbohydrate was obtained from Barentz B.V. (Hoofddorp, The Netherlands). All other chemicals and reagents were analytical grade and purchased from Sigma Aldrich (Schnelldorf, Germany).

3.2.2 Dry fractionation

Mung bean seeds were milled at a wheel speed of 8000 rpm using an Alpine Multi-processing System (Hosokawa Micron B.V., Doetinchem, the Netherlands) equipped with a ZPS50 impact mill (Hosokawa Micron B·V., Ausburg, Germany). After the milling step, the Alpine Multi-processing system was equipped with an ATP50 air classifier to obtain a mung bean fine fraction (MBFF) at 2500 rpm classification speed. For both milling and air classification, the feed rate was set to 20 rpm, a batch size was used of 400 g, and the airflow was set to 52 m^3/h, continuously.

3.2.3 Protein colloid production and characterization

Protein colloid production

Sodium metabisulfite was dissolved in MilliQ water to obtain a 15mM salt solution. Next, 20% wt MBFF was suspended in the salt solution and stirred for 5 min. For alkaline protein extraction, the pH was adjusted to 8.5 using 1M NaOH and the solution was stirred for 1 hour at room temperature. This solution was subsequently centrifuged (Hermle Z-383K centrifuge, HERMLE Labortechnik GmbH, Wehingen, Germany) at 10,000 g for 30 min to remove insoluble fractions, and the

supernatant was filtered using a grade 1 filter paper (Whatman, Massachusetts, United States). Lastly, the pH of the supernatant was adjusted to pH 7 using 1M HCl. This protein solution was stored at 4 °C until further use.

For protein colloid production, the protein solution was first allowed to re-equilibrate to room temperature. Next, the pH was slowly decreased by the dropwise addition of 1M HCl. Samples were prepared with final pH values in the range of pH 5.8 to pH 6.8. Acidified mung bean protein samples for which micro-phase separation was established are referred to as “mung bean protein simple coacervate” (MBPSC) samples. The micro-phase separation was examined under an Axioskop 50 Microscope (Zeiss, Vienna, Austria). MBPSC samples were heated at 80°C for 20min to gel the submicron protein droplets, resulting microgels are referred to as “mung bean protein colloids” (MBPC).

Scanning electron microscope (SEM)

MBPC samples were critical point dried (CPD) and investigated with a field emission scanning electron microscope (Magellan 400, FEI, Eindhoven, the Netherlands). To prepare the CPD sample, a drop of 10% MBPC solution was transferred to a poly-L-lysine Cellware 12mm round Glass coverslip (BioCoat, Discovery Labware Inc., USA) and fixed for 30 min. Afterwards, the coverslip was gently rinsed in Milli-Q and dehydrated in a series of 30%, 50%, 70% and 100% (twice) acetone solutions for 10 min each. The sample was subsequently dried by critical point dryer (CPD300, Leica, Germany) using carbon dioxide. To make the sample conductive for SEM analysis, samples were sputter coated (SCD 500, Leica, Germany) with 2 nm Tungsten. All images were recorded at a working distance of 5 mm with SE detection mode at 2kV at room temperature.

3.2.4 Drying techniques

Freeze drying

Mung bean Protein Colloids (MBPC) were freeze-dried using a Freeze dryer Alpha 2-4 LD plus (Martin Christ Gefriertrocknungsanlagen GmbH, Osterode am Harz, Germany) to obtain freeze-dried mung bean protein colloids (FDMBPC).

Spray drying

Spray-dried mung bean protein colloid powder (SDMBPC) was obtained by drying MBPC samples (heat treated as described above) using a Buchi Mini spray dryer B-290 (BUCHI Corporation, New Castle, USA). The inlet and outlet temperature were 150 °C and 60°C, respectively. The aspirator was set to 95% of its maximum aspirator rate, the pump speed was set to 15% of its maximum pump rate. Gas flow was set to 50 kg/h, and the nozzle cleaner was set on level 3 to prevent sample clogging.

3.2.5 Protein content

Dumas

The dry matter content of (possibly hydrated) MBFF was determined by precisely determining the weight before and after drying of approximately 100 milligrams MBFF. Samples were dried in an evaporation dish overnight in an oven at 105 °C. To determine the protein content, Dumas analysis (Flash EA 1112 series, Thermo Scientific, Breda, the Netherlands) was used, assuming a nitrogen conversion factor of 6.25 (Mariotti et al., 2008).

Internal protein concentration

The protein concentration inside the (heat-set) protein droplets in the FDMBPC samples was inferred from the intrinsic viscosity of FDMBPC samples. The continuous phase surrounding the protein droplets in the MBPC samples contains dissolved protein that interferes with viscosimetry, since that proceeds via the

analysis of a dilution series, “washed” MBPC samples of known total dry matter were prepared for viscosimetry with 20 mM sodium phosphate buffer (pH 7.0) as the continuous phase. Washing was achieved by centrifuging 10% wt samples at 30,000g for 30 min and removing supernatant from the tube, and then same amount of buffer was added to dissolve the pellet. 7 times and 10 times diluted pellet suspensions were used to make further series of dilutions, the final internal protein content was obtained by averaging results of 7 times and 10 times. Viscosities η of a dilution series of washed FDMBPC were determined using a capillary viscometer (Ubbelohde) placed in a water bath at 25 °C. For each dilution the viscosity η was measured in triplicate. The intrinsic viscosity ([η]) was obtained from the intercept of the Huggins plot (the specific viscosity η_{sp} / dry matter concentration versus dry matter per unit of volume). Specific viscosities (η_{sp}) were obtained from the sample viscosities η using

$$\eta_{sp} = \frac{\eta - \eta_0}{\eta_0} \tag{3.1}$$

where η_0 is the viscosity of the continuous phase. An estimate for the specific volume v_{sp} (ml/ dry mass in g) of the protein colloids can be obtained assuming the colloids are spherical, from the Einstein relation

$$v_{sp} = \frac{2}{5}\,[\eta] \tag{3.2}$$

Finally, the inverse of the specific volume provides the estimate for the internal protein concentration of the FDMBPC

$$C_{w,internal} = \frac{1}{v_{sp}} \tag{3.3}$$

3.2.6 Colloidal stability

To investigate the colloidal stability of MBPSC, samples of 20 ml were loaded in a glass test tubes with a stirrer bar inside. Samples were heated at 80 °C in a water bath for 5, 10, 15 and 20 minutes. Immediately after the heat treatment, samples

were placed in an ice bath to prevent further aggregation. They were kept at 4 °C, together with an unheated reference sample, until further measurements. For all samples, particle size distributions were measured using static light scattering (Mastersizer 2000, Malvern instruments, Malvern, United Kingdom), setting the particle refractive index to 1.48.

3.2.7 Re-dispersibility and particle dissolution for dried protein particle powders

To assay re-dispersibility after drying, SDMBPC or FDMBPC powders were dispersed in water at the same concentration as before drying. Particle size distributions after re-dispersion were determined using a Mastersizer 2000 (Malvern instruments, Malvern, United Kingdom).

Next, to investigate whether the protein colloids in the SDMBPC or FDMBPC powders would dissolve when dispersed in buffers of varying pH, 1% w/w FDMPC and SDMBPC dispersions were prepared at pH 4, 5, 6.75 (natural), 9 and 11 at 0.1 M of added salt (NaCl) to eliminate the influence of ionic strength changes on the fraction of proteins dissolved. Dispersions were first stirred for 30 min at room temperature before pH values were carefully adjusted by the dropwise addition of 1M NaOH or 1M HCl. Next, samples were stirred for 1 h and centrifuged (Hermle Z-383K centrifuge, HERMLE Labortechnik GmbH, Wehingen, Germany) at 17,000g for 30 min. The protein concentration of supernatant was determined by DUMAS with a nitrogen conversion factor of 6.25, and the fraction of protein dissolved, $\Phi_{\text{dissolved}}$, was calculated from

$$\Phi_{dissolved} = \frac{C_{Supernatant}}{C_{Suspension}} \times 100\% \quad (3.4)$$

Where $C_{\text{Supernatant}}$ is the protein concentration of supernatant, and the $C_{\text{Suspension}}$ is the protein concentration of the suspension. To determine the effect of ionic strength on the fraction of proteins dissolved, 1% w/w FDMBPC and SDMBPC

dispersions were prepared at different concentrations of added salt (0 M, 0.1 M and 0.5M NaCl) at fixed pH 6.75 (the natural pH of the dispersions). The same method and calculation were applied as above to determine the fraction of proteins dissolved.

3.2.8 Rheology

Shear viscosity

Shear viscosities of the samples were measured in triplicate, using a double gap cylinder (DG 26.7) geometry over a shear rate range of 1 – 100 s^{-1}. Measurements were conducted using a MCR 502 rheometer (Anton Paar, Graz, Austria). Flow curves were analysed to obtain the flow behaviour index (n) and consistency index (K) using a power-law model

$$\tau = K\dot{\gamma}^n \tag{3.5}$$

Where τ is the shear stress, *K* is the consistency index, $\dot{\gamma}$ is the shear rate, and n is the flow behavior index.

Oscillatory rheology

For oscillatory rheology, an MCR 502 rheometer combined with a sand-blasted concentric cylinder (CC17) geometry was used. Samples were monitored for the linear rheological behaviour during their gelation induced by heating. Storage modulus (G') and the loss modulus (G'') were recorded at a strain of 1% and a frequency of 1Hz, during a heat treatment consisting of an increase in temperature from 23 °C to 90 °C at a constant heating rate of 3 °C / min, a fixed temperature of 90 °C for 30 min, followed by cooling back to 23 °C at a rate of 3 °C / min. Measurements were conducted in duplicate.

3.2.9 Statistical analysis

Unless mentioned otherwise, for all measurements, results are presented as the mean ± standard deviation of replicates. Measurements were performed at least in

duplicate. IBM SPSS Statistics 25 (IBM SPSS Inc., Chicago, USA) was used to conduct one way ANOVA analysis, using the post-hoc method Tukey at the $P < 0.05$ level.

3.3 Results and discussions

3.3.1 Mung Bean Protein Simple Coacervates (MBPSC)

Protein droplet formation upon acidifying flours dispersed in alkaline has been observed for especially soy and yellow pea (Lui, et al., 2007). Here we sought to characterize the same phenomenon for alkaline extracted mung bean flour. To maintain full protein functionality, we first applied an air classification to separate the freshly milled mung beans, giving a mung mean fine fraction (MBFF) powder. A high concentration (20% wt) of MBFF was alkali extracted at pH 8.5. To check for liquid-liquid binary protein phase separation, something accompanied by droplet formation by the newly formed phase, we first performed optical microscopy on different samples obtained by acidifying the supernatant after alkaline extraction to various final pH values.

The results are shown in Figure 1. We find that in the narrow pH window of pH 6.8 to 6.0, there was a progression from spherical, micron-sized droplets that first increased in number and then aggregated and acquired irregular shapes at pH 6. For further studies, we choose pH 6.75, since at this pH a large enough number of droplets appeared to be formed that do not aggregated. This optimum pH is higher than the value of pH 6.2 - 5.7 previously shown to induce liquid-liquid binary phase separation in alkaline extracted soy flour (Lui, et al., 2007).

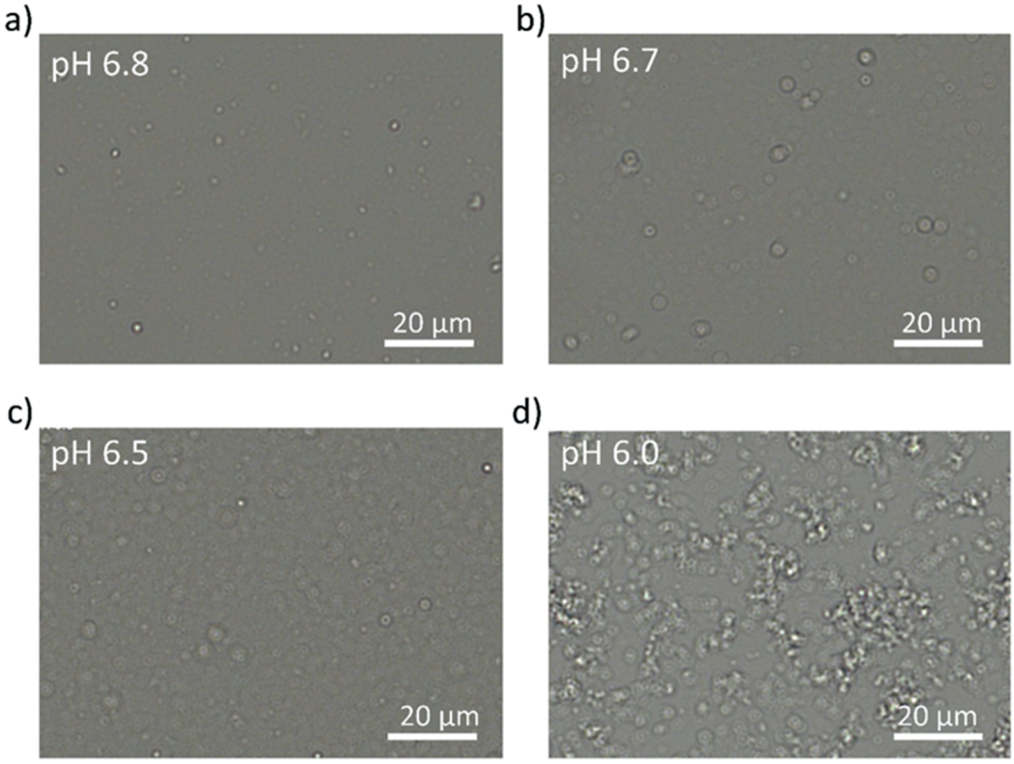

Figure 3.1 *Optical microscopy Images of Mung Bean Protein Simple Coacervates (MBPSC) formed from air classified mung bean flour, by alkaline extraction of 20% (w/w) flour at pH 8.5 followed by acidification to the indicated pH values. Scale bar = 20 µm.*

For a more precise assessment of the size distribution of the Mung bean protein droplets, or MBPSC formed at pH 6.75, we used static light scattering to obtain the particle size distribution (PSD). Results are shown in Figure 3.2a. We find a distinctly bimodal distribution with a large peak in the volume-weighted PSD at around 0.15 µm, and a smaller rather broad peak centred on 10 µm. Additionally, the large peak at 0.15 µm has a distinct shoulder at around 1 µm. This implies the droplets observed with the optical microscopy represented only a small fraction of the total particles that are presented in the sample, and that most particles were in fact below the resolution of light microscopy.

Therefore, we also sought to use electron microscopy to visualize the many smaller particles present in the MBSPC samples. Results of SEM imaging on the MBSPC samples is shown in Figure 3.2b. This figure appears to be at least consistent with the PSD obtained from light scattering in that it shows a few larger particles (indicated by a blue arrow), and many much smaller particles (indicated by yellow arrows), stuck to each other and to the larger particles.

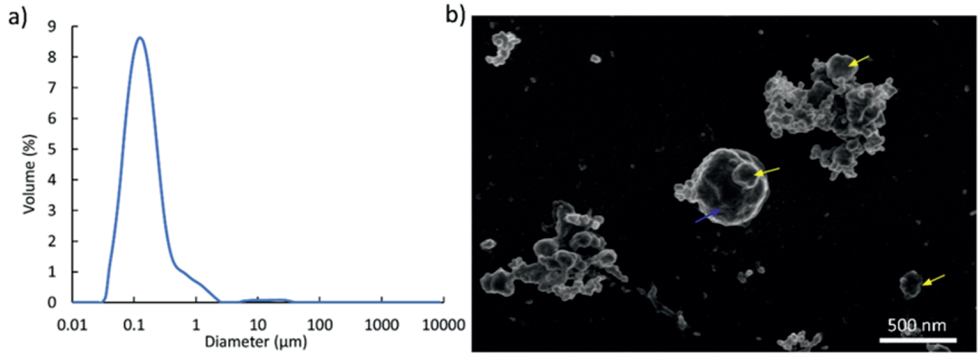

Figure 3.2 A) *Particle size distributions of Mung bean protein simple coacervates, prepared by acidifying 20% wt of alkaline extracted (pH 8.5) air classified Mung Bean Flour to pH 6.75 as determined using static light scattering* ***B)*** *Scanning electron micrographs (SEM) of Mung bean protein colloids (critical point dried and Tungsten coated). Scale bar=500 nm.*

None of the methods used above can distinguish protein-containing from non-protein containing particles. Therefore, we next used Confocal Laser Scanning Microscopy (CLSM). Freshly prepared MBSPC dispersions acidified down to pH 6.75 were stained with Rhodamine B and imaged using CLSM. Representative results are shown in Fig 3.3. The CLSM-optical microscopy overlayed images clearly show that not all of the particles in the dispersions obtained from the mung bean flour were rich in protein: some could be small air bubbles, whereas others may be starch fragments not removed by the centrifugation step following the alkaline extraction. On the other hand, it is very clear that other particles do correspond to regions of high fluorescence and hence high protein concentration. Unfortunately, with CLSM we can only image the few very large particles that existed in the overall (volume

weighted) distribution, which was dominated by the much smaller particles with a characteristic size of around 150 nm.

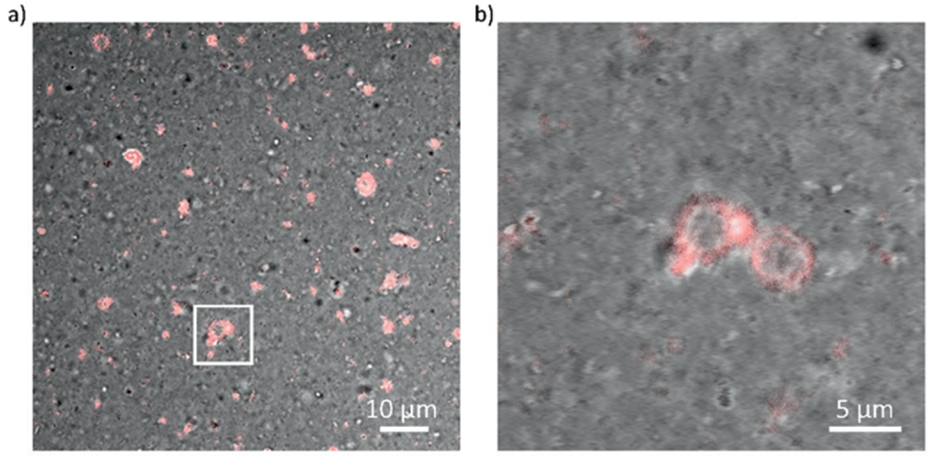

Figure 3.3 *Confocal laser scanning microscopy (CLSM) images of* ***A)*** *MBPSC prepared by acidifying 20% wt of alkaline extracted (pH 8.5) air classified Mung Bean Flour to pH 6.75, labelled with Rhodamine b. Scale bar = 10 µm.* ***B)*** *detail view of region indicated by the white square in Figure 3.3a. Scale bar = 5 µm, respectively.*

For the microscopically visible particles we can therefore conclude that they are oftentimes spherical and contain a high concentration of protein. The presence of these particles indicates that also in Mung Bean Flour, there is micro-phase separation into a continuous phase and liquid droplets high in protein, as was earlier observed for soy flour. However, a characteristic difference appears to be that at least for the MBFF that we use here, these droplets for the majority, did not grow out to achieve sizes of many microns, as they did for soy flour, but instead, remained small, having submicron sizes.

3.3.2 Mung Bean Protein Colloids (MBPC)

Since simple coacervates are reversible structures formed by liquid-liquid phase separation, they may disappear, for example if the pH changes (Popello et al., 1992). A heating step is necessary to convert the Mung Bean Protein Simple Coacervate

(MBPSC) droplets into solid Mung Bean Protein Colloids (MBPC) by gelling the protein coacervate droplets.

To investigate the stability of MBPC formed by heating MBPSC droplets, we first studied changes to macroscopic and microscopic visual appearance caused by heating. Results are shown in Figure 3.4.

As is clear from Figures 3.4 a and b, at the macroscopic level, the heat treatment resulted in the dispersions becoming much opaquer, possibly indicating that denser, more strongly scattering particles generated upon heating. Consistently, optical microscopy, shown in Figure 3.4c (MBPSC droplets, unheated) and Figure 3.4d (MBPC, heated) suggests a higher optical contrast for the heated particles.

Even though in optical microscopy there were no indications of aggregation being caused by heating, this does not tell the whole story since the majority of the particles have submicron sizes and cannot be seen in optical microscopy. Therefore, particle size distributions before and after heating were obtained from static light scattering.

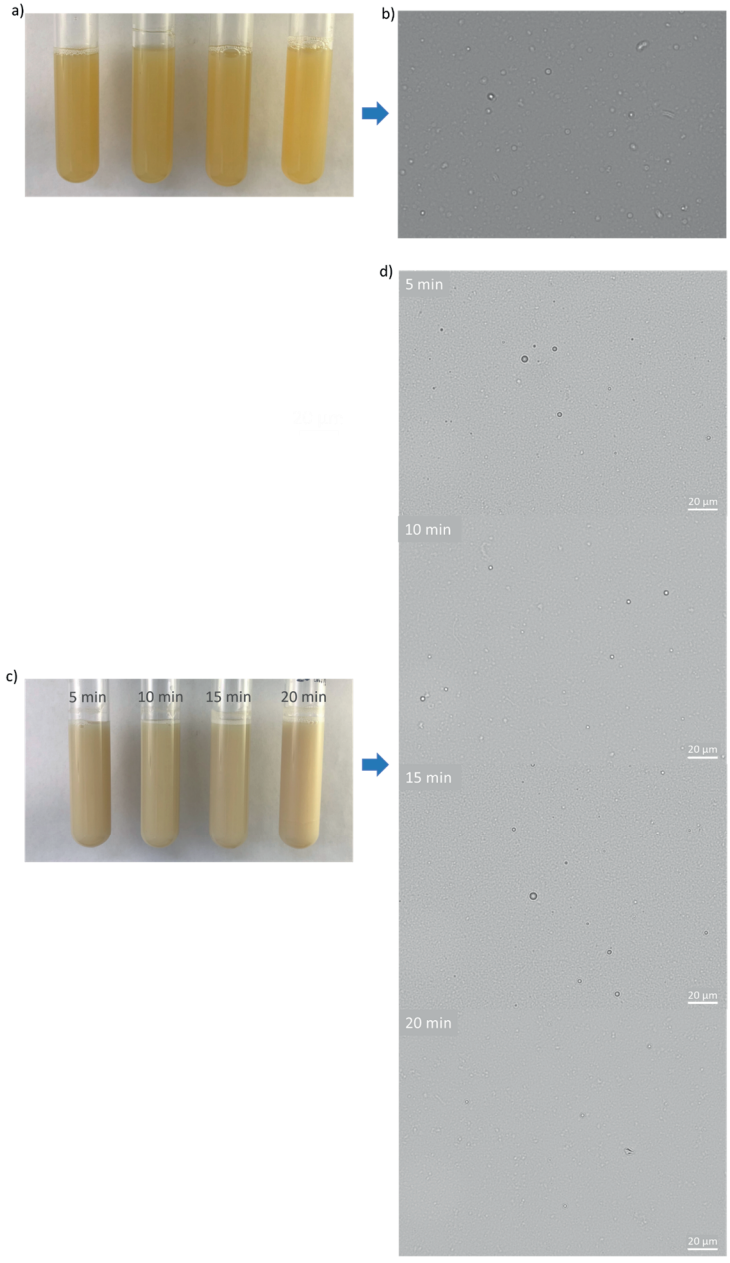

Figure 3.4 *Changes to macroscopic and microscopic visual appearance caused by heating MBPSC droplets, to form MBPC. Samples prepared by acidifying 20% wt of alkaline extracted (pH 8.5) air classified Mung Bean Flour to pH 6.75* ***A)*** *Macroscopic appearance before heating (MBPSC) and* ***B)*** *after heating (MBPC).* ***C)*** *optical microscope images of MBPSC (unheated) and* ***D)*** *MBPC (heated for 5 min, 10 min, 15 min, and 20 min at 80 °C, respectively). Scale bar= 20µm.*

Results in Figure 3.5a confirm that heating hardly influences particle size distribution: no large aggregates were formed after heating. Diameters of unheated (MBPSC droplets), 5 min, 10 min, 15 min, and 20 min heated MBPC were centred around 0.15 µm, within the error of the measurement. Note that Fig. 5b shows volume averaged results, such that there were only a small number larger particles, with diameters between 1 µm to 10 µm, and most particles in the MBPC samples were submicron.

Achieving near complete preservation of the original size distributions upon heating is desired, but nontrivial. In the case of pea (Cochereau, et al., 2019), structural changes were observed upon heating for simple protein coacervate droplets, and others including soy (Zhao, et al., 2020), were changed into hollow microcapsules. Presumably, the fact that we use much less purified proteins and rapid heating may also have contributed to observed preservation of size distributions.

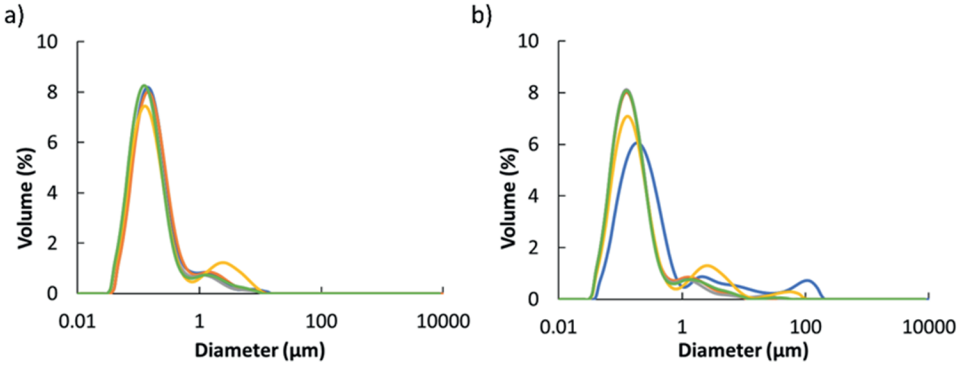

Figure 3.5 *Particle size distributions of unheated (—) and 5 min (—), 10 min (—), 15 min (—), 20 min (—) heated MBPC, prepared by acidifying 20% wt of alkaline extracted (pH 8.5) air classified Mung Bean Flour to pH 6.75, on* ***A)*** *Day 0 and* ***B)*** *Day 5.*

As a side note, we observed the (unheated) MBPSC droplets undergo reversible self-association upon cooling to 4°C. Even though at room temperature, the MBPSC dispersions were stable against sedimentation even at 10,000 g (for 30 min, Appendix Figure S3.1), storing them at 4 ˚C overnight led to the formation of a dense

and a dilute layer (see Appendix Figure S3.2). Mild agitation at room temperature dispersed the droplets again. In contrast, the heated MBPC dispersions did not show this behaviour.

3.3.3 Drying and redispersing MBPC

The MBPC can only be useful as a plant protein ingredient if we can actually dry them without loss of their functional properties and without loss of solubility. In particular drying methods can negatively affect the dispersibility of plant proteins (Pelgrom et al., 2013; Shen et al., 2021). Both freeze-drying and spray drying of MBPC dispersions were used to obtain, respectively FDMBPC and SDMBPC powders. These were dispersed at different pH and ionic strengths and their solubility/dispersibility were assayed using a centrifugation test. Results are shown in Figure 3.6.

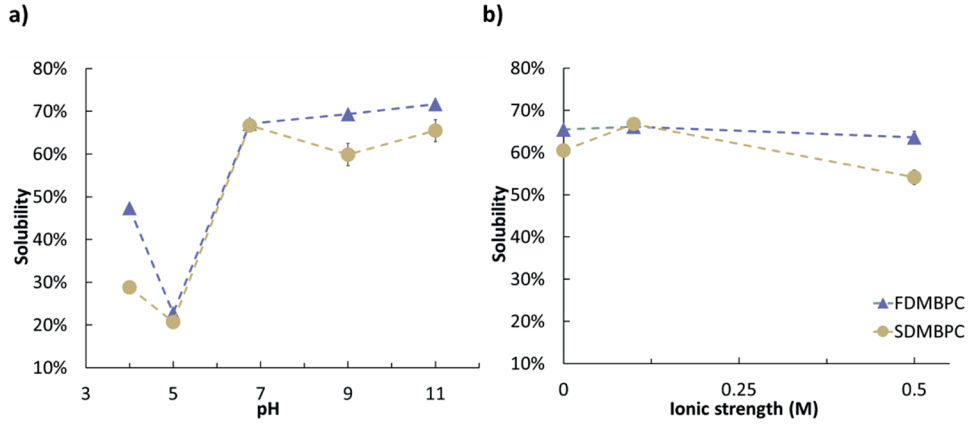

Figure 3.6 *Solubility curves (w/w) of freeze-dried MBPC (FDMBPC, triangles) and spray dried MBPC (SDMBPC, circles) as a function of* ***A)*** *pH (left) and* ***B)*** *ionic strengths (right). MBPC were prepared by acidifying 20% wt of alkaline extracted (pH 8.5) air classified Mung Bean Flour to pH 6.75.*

As shown in Figure 3.6a, the FDMBPC and SDMBP were both more soluble at alkaline conditions than at acidic conditions. A minimum solubility was found around pH 5 as expected, since this was close to the isoelectric point of mung bean proteins (pH 4.6) (Du et al., 2018). Comparing with mung bean protein isolate, the

FDMBPC had a much higher solubility even at the isoelectric point (approximately 20%). At pH 4, the FDMBPC and SDMBPC still showed remarkably high solubilities of around 47% and 30% respectively, while mung bean protein isolates typically have solubilities lower than 10% at this pH (Du et al., 2018; Kudre et al., 2013). We attribute this good solubility close to the mild methods used during the MBPC production. Indeed, it is widely agreed that extensive purification can lead to protein denaturation and lower protein solubility (Du et al., 2018; Kudre et al., 2013; Pelgrom et al., 2013). Finally, the salt dependence of the FDMBPC and SDMBPC powders is shown in Figure 3.6b. We found salt hardly affects the solubility of the FDMBPC and SDMBPC powders.

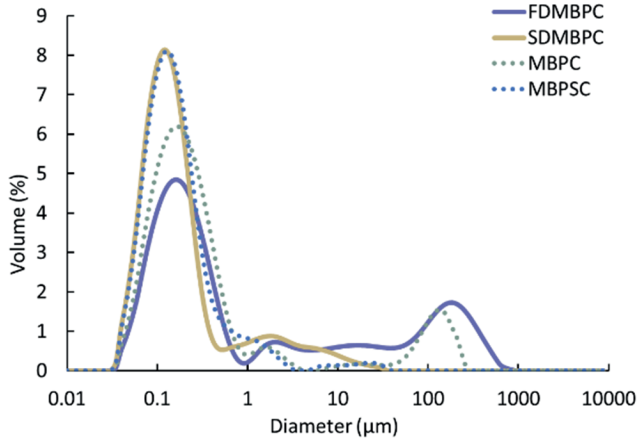

Figure 3.7 *Particle size distributions of unheated mung bean protein simple coacervates (MBPSC) dispersions (blue dash line), 20 min heated mung bean protein colloids (MBPC) dispersions (green dash line), re-dispersed freeze-dried mung bean protein colloids (FDMBPC) powder (purple line) and re-dispersed spray-dried mung bean protein colloids (SDMBPC) powder (yellow line). MBPSC were prepared by acidifying 20% wt of alkaline extracted (pH 8.5) air classified mung bean flour to pH 6.75.*

Next to knowing that the FDMBPC and SDMBPC powders have good re-dispersibility, we were interested in finding out whether particle sizes after redispersion will be very much affected by drying. Results are shown in Figure 3.7. FDMBPC and SDMBPC powders were dispersed in water at a protein concentration (4%), identical to the protein concentration of the MBPC dispersions before drying.

After re-dispersion, particle size distributions were determined, and compared to those of the original (unheated) MBPSC dispersions and (heated) MBPC dispersions. We found that both freeze drying and spray drying allow for the redispersion of the protein particles with sizes very close to those before drying. Unavoidably, there was a somewhat larger fraction of larger particles after drying, but this fraction remains small.

3.3.4 Viscosity and thermal stability of FDMBPC

We proceed with evaluating functional properties of the FDMBC powders for application in beverages. Desired functionalities are low viscosity and good thermal stability. A low viscosity arises if the MBPC are compact and non-swelling, or in other words, have a high internal concentration.

By using centrifugation to pellet pea protein coacervate dispersions, Kornet, et al. (2022) estimated an internal protein content of the coacervate droplets around 45% wt via mass balance. Instead of that, we followed a more precise method of Saricay, Wierenga, and de Vries (2016) based on specific viscosity measurements (cf. section 2.2.4), and estimated the internal concentration for redispersed freeze-dried mung bean proteins colloids (FDMBPC). Assuming the mung bean protein colloids are roughly spherical we can estimate their specific volume from their intrinsic viscosity and the Einstein relation for the viscosity of hard spheres. Next, we can take the inverse of the specific volume as our estimate for the weight concentration (based on dry mass) inside the individual mung bean protein colloids.

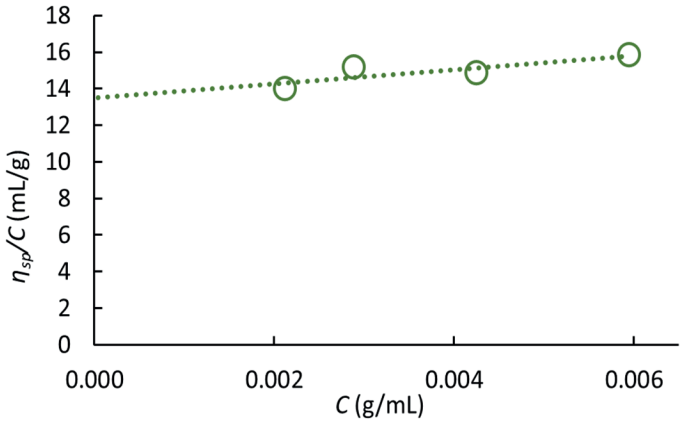

Figure 3.8 *Huggins plot for washed FDMBPC powder. η_{sp} is the specific viscosity measured using capillary viscosimetry. C is the weight concentration of washed FDMBPC, based on dry mass. The FDMBPC was prepared by acidifying 20% wt of alkaline extracted (pH 8.5) air classified Mung Bean Flour to pH 6.75 (MBPSC), heating for 20 minutes to form MBPC, and subsequent freeze drying to obtain the FDMBPC powder. The FDMBPC powder was washed once by preparing a 10% wt FDMBPC dispersion in PO_4 spinning down the protein colloids using an ultracentrifuge and resuspending the pellet to the desired concentration.*

A washing step was employed to ensure that dilution did not affect the viscosity of the continuous phase. Figure 3.8 shows a Huggins plot for the specific viscosity (obtained using capillary viscosimetry) from which we can deduce the intrinsic viscosity by extrapolating to concentration zero. Results of the analysis of the Huggins plot are given in Table 3.1.

Table 3.1 *Results of analysis of Huggins plot (Figure 3.8) for washed FDMBPC powder.*

Intrinsic viscosity (mL/g)	15±1
Specific volume (mL/g)	6±1
Internal concentration (g/mL)	0.17±0.02

** All measurements were conducted at least in triplicate. Values are presented as mean ± standard deviation*.

The average intrinsic viscosity for FDMBPC is 15 ± 1 mL/g. This is significantly lower than typical food thickeners, which have intrinsic viscosities in the range of 30-150 mL/g (Saricay et al., 2016). Reported intrinsic viscosities for denatured whey protein isolates and concentrates (Daubert et al., 2006; Eissa et al., 2013) are also a factor two larger than those we found here. On the other hand, the internal concentration was on the lower end (approaching 20% wt) of the values of 20-45% wt reported previously for other simple legume protein coacervate droplets (Kornet, Roozalipour, et al., 2022; Li et al., 2020; Lui et al., 2007). This may be related to the fact that we have additionally heated, dried and redispersed the protein colloids, and with the fact that the simple protein coacervates for mung bean flour appear to behave different from those in pea- and soy flour, where typical coacervate droplets sizes can be many microns, much larger than in the case of mung bean flour.

As mentioned, in the context of plant proteins for beverage applications we are looking for high solubility, low viscosity and basically no, or only very weak heat-induced gelation. While the fact that the intrinsic viscosity of FDMBPC was low, is encouraging, we also would like to check the (shear-rate dependent) viscosity of redispersed FDMBPC powders at higher concentrations more representative of applications. This was performed for two representative pH values, pH 6.75 and pH 3.5. Results are shown in Fig. 3.9. Furthermore, we also investigated the recovery process of samples and there was no time dependency found for FDMBPC. The flow curves could be well represented by a power law model. Fit parameters (consistency indices *K* and flow indices *n*) are given in Table 3.2.

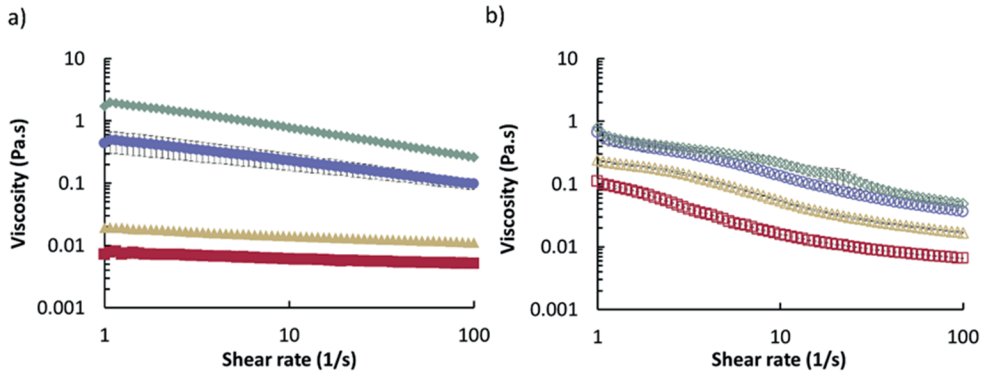

Figure 3.9 *Viscosity of FDMBPC as a function of shear rate, for various concentrations, at both neutral and acidic pH* ***A)*** *pH 6.75, protein concentrations: 6% (■),8% (▲),10% (●), and 12% (◆)* ***B)*** *pH 3.5, protein concentrations: 6% (□),8% (△),10% (○), and 12% (◇). FDMBPC was prepared by acidifying 20% wt of alkaline extracted (pH 8.5) air classified Mung Bean Flour to pH 6.75, heating and freeze drying. Error bars represent standard deviation of triplicate experiments.*

Table 3.2 *Fit parameters (consistency index K and flow index n) and for flow curves shown in Figure 3.9.*

Sample	Protein concentration	Flow index *n*	Consistency index *K* (Pa.s^n)	Determination coefficient R^2
pH 6.75	6%	0.91±0.01^{d}	0.01±0.00^{a}	1.00±0.00*
	8%	0.88±0.00^{d}	0.02±0.00^{a}	1.00±0.00*
	10%	0.66±0.05^{c}	0.52±0.21^{ab}	1.00±0.00*
	12%	0.55±0.01^{bc}	2.13±0.20^{c}	1.00±0.00*
pH 3.5	6%	0.37±0.01^{a}	0.09±0.00^{a}	0.89±0.01
	8%	0.36±0.00^{a}	0.26±0.01^{ab}	0.96±0.00*
	10%	0.37±0.04^{a}	0.58±0.05^{ab}	0.96±0.01
	12%	0.42±0.06^{ab}	0.71±0.06^{b}	0.96±0.02

** Represents standard deviation is lower than 1%.*

All measurements were conducted at least in duplicate. Values are presented as mean ± standard deviation. Letters indicate significant difference at P < 0.05.

For pH 6.75, we found a Nearly Newtonian behaviour for concentrations of 6% and 8%. At higher concentrations, FDMBPC dispersions started exhibiting shear-thinning behaviour as expected for concentrated dispersions of protein microgels (Saricay et al. 2016). For pH 3.5, it appeared that shear thinning already set in at

lower concentrations, possibly indicating an increased swelling of the microgels due to increased electrostatic repulsion inside the microgels at low pH. In all cases the strong shear thinning implies that at the rather high shear rates of oral processing, viscosities of the FDMBPC dispersions will be experienced as low.

Finally, we turned to the rheological behaviour of FDMBPC dispersions when heated. For beverage applications, ideally the plant protein dispersions should not be very sensitive to (re)heating, such as could occur e.g., during pasteurization or sterilization. To characterize changes to the rheology during heating we use oscillatory rheology at a fixed frequency (1Hz) to determine the storage (*G'*) and loss moduli (*G''*) of the FDMBPC dispersions during a heating and cooling ramp (hold time at 90°C of 30 min). We do so for various concentrations and pH values. A commercial mung bean protein isolate (referred to as M65) was used as a benchmark to compare against. A representative measurement, for 12% FDMBPC at pH 6.75, is shown in Figure 3.10. Final storage moduli after cooling down to room temperature for all measurements are given in Table 3.3.

As shown in Table 3.3, final storage moduli (G') seems independent on protein concentrations, while lower pH led significant increases in G' (3-fold and 2-fold increase, respectively). It can be considered as a result of the reduced net charge of the proteins around the isoelectric point (Brückner-Gühmann et al., 2021; Ringgenberg et al., 2013), more intensive aggregation therefore was yielded. As a benchmark, 10% commercial mung bean protein concentrates M65 suspension were prepared and measured at natural pH.

For M65, a much higher G' was observed after cooling, indicating a less thermal stability possesses. Hence, the commercial M65 gels much more readily than our FDMBPC powder, making the latter an attractive ingredient for formulating plant-based beverages.

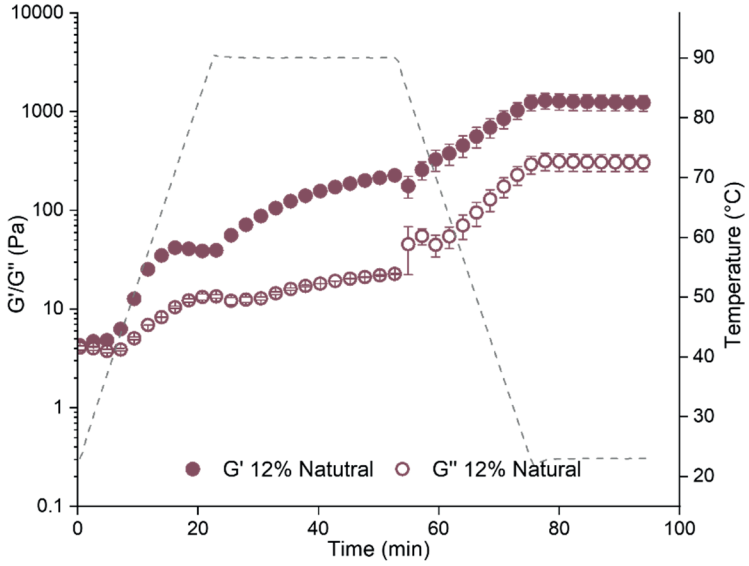

Figure 3.10 *Viscoelastic properties of FDMBC prepared by acidifying 20% wt of alkaline extracted (pH 8.5) air classified Mung Bean Flour to pH 6.75 and freeze drying. Storage modulus (solid symbols) and loss modulus (open symbols) versus time at 12% protein concentration at natural pH. The temperature profiles are indicated by the dashed line. Error bars represent standard deviation of duplicates. Error bars represent standard deviation of duplicates.*

Table 3.3 *Gel properties of FDMBPC heated at 90 °C and cooled to room temperature at Natural pH and pH 3.5. Commercial mung bean protein concentrates M65 were added as reference.*

	Protein concentration	Storage modulus (Pa)	
		Natural pH	pH 3.5
M65	10%	6663.0 ± 254.2^{c}	/
FDMBPC	10%	1006.3 ± 204.1^{a}	2979.4 ± 118.6^{b}
	12%	1231.0 ± 218.1^{a}	2531.8 ± 450.8^{ab}

** All measurements were conducted in duplicate and values are shown as mean ± standard deviation. Letters present significant difference at a P < 0.05.*

3.4 Conclusion

The mung bean protein colloids generated by simple coacervation were proved to be a potential vehicle to deliver proteins in beverage systems. This can be attributed to theirs relatively low intrinsic viscosity, superior re-dispersibility and solubility, and weak gelation behaviour.

By employing a delicate approach to determine the internal protein content of MBPC, we found that the intrinsic viscosity of MBPC is approximately 15 ml/g, which is significantly lower than common protein-based food thickeners (30 ml/g - 150ml/g). In the meanwhile, with an internal protein concentration of 0.17 g/ml. MBPC has good solubilities both at acidic conditions and practical salt levels relevant to industry productions. The drying method did not significantly affect solubilities of MBPC.

In general, the rheological behaviours of a product are inseparably from the consumers acceptance. The viscosity of the FDMBPC was found in the proper range ("honey" level) which is appreciated by consumers. As for gelation behaviours, pH was found have an obvious influence on heat-set gelation of MBPC. The storage moduli of FDMBPC increased significantly after pH was decreased to 3.5. In summary, MBPC showed a much weaker gelation behaviour than benchmark M65 in heat-induced gels, suggesting it can be considered as a promising plant-based ingredient for beverages.

The study shows that MBPC has a high solubility while present an appropriate viscosity and a weaker gelation behaviour, which meet the main requirements of beverage systems. Therefore, plus the remarkable resistance to sedimentation, coalescence, and phase separation of them, MBPC would be an attractive building blocks to plant-based beverages.

References

Aiking, H. (2011). Future protein supply. *Trends in Food Science & Technology*, *22*(2-3), 112-120.

Assatory, A., Vitelli, M., Rajabzadeh, A. R., & Legge, R. L. (2019). Dry fractionation methods for plant protein, starch and fiber enrichment: A review. *Trends in Food Science & Technology*, *86*, 340-351.

Aydemir, L. Y., & Yemenicioğlu, A. (2013). Potential of Turkish Kabuli type chickpea and green and red lentil cultivars as source of soy and animal origin functional protein alternatives. *LWT - Food Science and Technology*, *50*(2), 686-694.

Brückner-Gühmann, M., Kratzsch, A., Sozer, N., & Drusch, S. (2021). Oat protein as plant-derived gelling agent: Properties and potential of modification. *Future Foods*, *4*.

Carbonaro, M., Maselli, P., & Nucara, A. (2015). Structural aspects of legume proteins and nutraceutical properties. *Food Research International*, *76*, 19-30.

Chen, N., Zhao, M., Nicolai, T., & Chassenieux, C. (2017). Exploiting Salt Induced Microphase Separation To Form Soy Protein Microcapsules or Microgels in Aqueous Solution. *Biomacromolecules*, *18*(7), 2064-2072.

Chen, N., Zhao, Z., Wang, Y., & Dimova, R. (2020). Resolving the Mechanisms of Soy Glycinin Self-Coacervation and Hollow-Condensate Formation. *ACS Macro Letters*, *9*(12), 1844-1852.

Cochereau, R., Nicolai, T., Chassenieux, C., & Silva, J. V. C. (2019). Mechanism of the spontaneous formation of plant protein microcapsules in aqueous solution. *Colloids and Surfaces A: Physicochemical and Engineering Aspects*, *562*, 213-219.

Daubert, C. R., Hudson, H. M., Foegeding, E. A., & Prabhasankar, P. (2006). Rheological characterization and electrokinetic phenomena of charged whey protein dispersions of defined sizes. *LWT - Food Science and Technology*, *39*(3), 206-215.

Du, M., Xie, J., Gong, B., Xu, X., Tang, W., Li, X., Li, C., & Xie, M. (2018). Extraction, physicochemical characteristics and functional properties of Mung bean protein. *Food Hydrocolloids*, *76*, 131-140.

Eissa, A. S., Mohamed, D. M., Uoness, K. S., Azab, M. M., Abed, N. S., & El-Aish, D. A. (2013). Characterization of Rheological and Molecular Properties of Whey Protein Thickeners. *International Journal of Food Properties*, *17*(3), 570-586.

Kornet, R., Roozalipour, S. L., Venema, P., van der Goot, A. J., Meinders, M. B. J., & van der Linden, E. (2022). Coacervation in pea protein solutions: The effect of pH, salt, and fractionation processing steps. *Food Hydrocolloids*, *125*.

Kudre, T. G., Benjakul, S., & Kishimura, H. (2013). Comparative study on chemical compositions and properties of protein isolates from mung bean, black bean and bambara groundnut. *J Sci Food Agric*, *93*(10), 2429-2436.

Lazko, J., Popineau, Y., & Legrand, J. (2004). Soy glycinin microcapsules by simple coacervation method. *Colloids and Surfaces B: Biointerfaces*, *37*(1), 1-8.

Li, X., Erni, P., Van Der Gucht, J., & De Vries, R. (2020). Encapsulation Using Plant Proteins: Thermodynamics and Kinetics of Wetting for Simple Zein Coacervates. *ACS Applied Materials & Interfaces*, *12*(13), 15802-15809.

Lui, D. Y. M., Litster, J. D., & White, E. T. (2007). Precipitation of soy proteins: Particle formation and protein separation. *AIChE Journal*, *53*(2), 514-522.

Pelgrom, P. J. M., Vissers, A. M., Boom, R. M., & Schutyser, M. A. I. (2013). Dry fractionation for production of functional pea protein concentrates. *Food Research International*, *53*(1), 232-239.

Popello, I. A., Suchkov, V. V., Grinberg, V. Y., & Tolstoguzov, V. B. (1992). Effects of pH upon the liquid-liquid phase equilibria in solutions of legumins and vicilins from broad beans and peas. *Food Hydrocolloids*, *6*(2), 147-152.

Ringgenberg, E., Alexander, M., & Corredig, M. (2013). Effect of concentration and incubation temperature on the acid induced aggregation of soymilk. *Food Hydrocolloids*, *30*(1), 463-469.

Sağlam, D., Venema, P., de Vries, R., Shi, J., & van der Linden, E. (2013). Concentrated whey protein particle dispersions: Heat stability and rheological properties. *Food Hydrocolloids*, *30*(1), 100-109.

Saglam, D., Venema, P., de Vries, R., van Aelst, A., & van der Linden, E. (2012). Relation between gelation conditions and the physical properties of whey protein particles. *Langmuir*, *28*(16), 6551-6560.

Saricay, Y., Wierenga, P. A., & de Vries, R. (2016). Rheological properties of dispersions of enzymatically cross-linked apo-α-lactalbumin. *Food Hydrocolloids*, *56*, 344-351.

Shen, Y., Tang, X., & Li, Y. (2021). Drying methods affect physicochemical and functional properties of quinoa protein isolate. *Food Chem*, *339*, 127823.

Teng, Z., Luo, Y., & Wang, Q. (2012). Nanoparticles Synthesized from Soy Protein: Preparation, Characterization, and Application for Nutraceutical Encapsulation. *Journal of Agricultural and Food Chemistry*, *60*(10), 2712-2720.

Wouters, A. G. B., Rombouts, I., Fierens, E., Brijs, K., & Delcour, J. A. (2016). Relevance of the Functional Properties of Enzymatic Plant Protein Hydrolysates in Food Systems. *Compr Rev Food Sci Food Saf*, *15*(4), 786-800.

Zhao, H., Guo, M., Ding, T., Ye, X., & Liu, D. (2020). Exploring the mechanism of hollow microcapsule formation by self-assembly of soy 11s protein upon heating. *Food Hydrocolloids*, *108*, 105379.

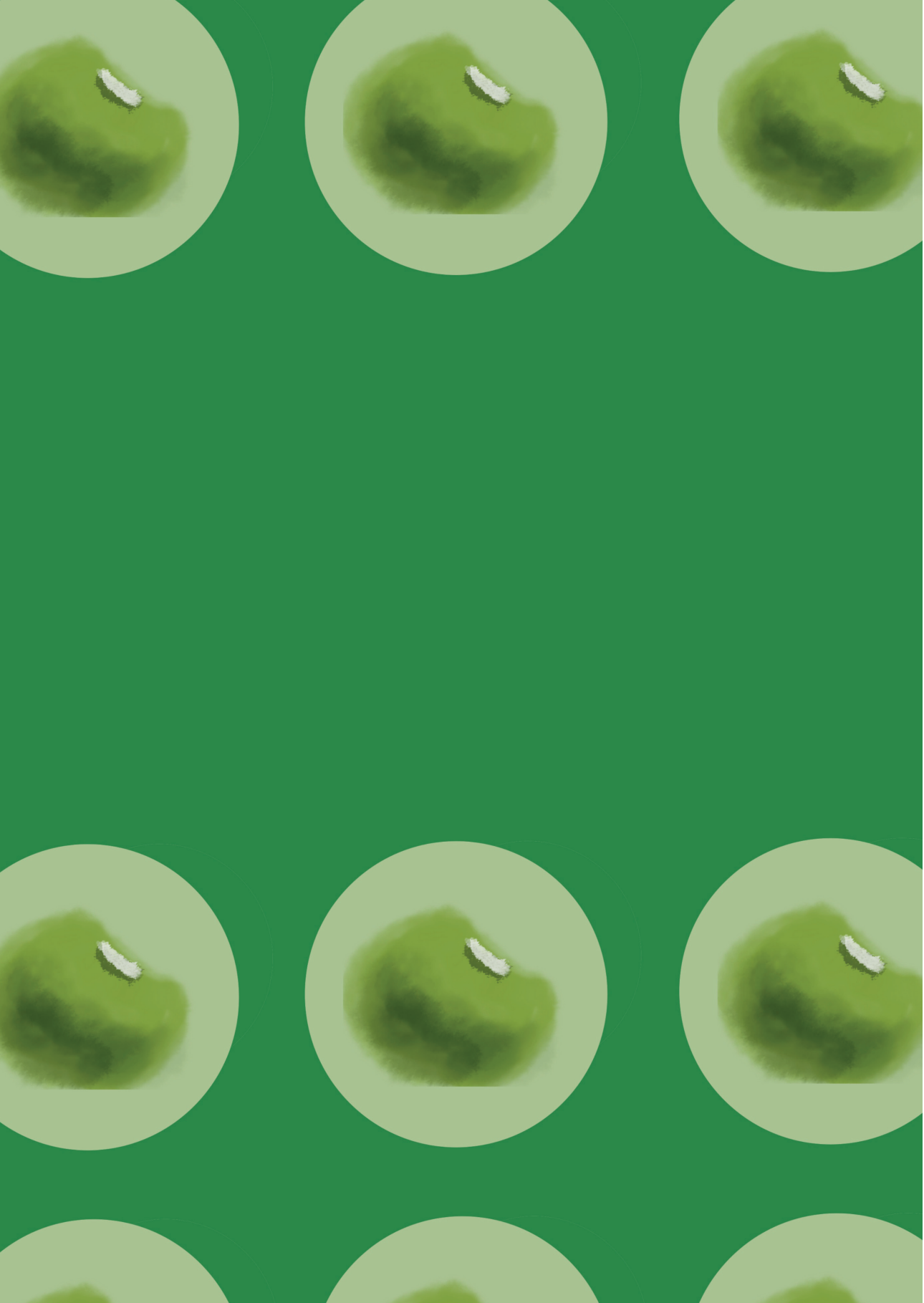

4

Physical, interfacial and foaming properties of different mung bean protein fractions

This chapter has been submitted as:
Yang, J., Yang, Q.*, Waterink, B., Venema, P., de Vries, R., & Sagis, L. M. C., Physical, interfacial and foaming properties of different mung bean protein fractions*

(the authors have contributed equally to this work)*

Abstract

Mung bean is an upcoming source of plant proteins with good foaming properties. The relation between its foaming properties and interfacial properties has not received much attention and was addressed in this work. To this end, five different mung bean protein fractions were produced. First, a protein-rich flour was obtained using dry fractionation, which was further processed into a protein mixture using mild wet fractionation to remove starch granules and other insoluble components. The protein mixture was further treated by isoelectric point precipitation to obtain a globulin- and albumin-rich fraction. Finally, we used the protein nativity of the dry fractionated flour to create protein coacervate droplets via liquid-liquid phase separation of the proteins at slightly acidic pH. The protein-rich coacervate droplets were heated and cross-linked into gelled particles, or "protein colloids". The interfacial and foam-stabilising properties of the flour and protein mixture were dominated by the globulins, producing a foam with a poor stability. Albumins formed substantially stiffer interfaces, leading to foams with a high stability. The highest foam stability was observed for the protein colloids, which we attribute to the formation of stiff interfacial layers and probably also pinning of the lamellae in the foams by the protein colloids. In summary, mung bean albumins were found to possess substantially better foaming properties than the globulins, but especially mung bean protein colloids are a promising candidate for a plant-based foam ingredient.

4.1 Introduction

The interest in plant-based alternatives for animal-based ingredients is rapidly growing. One of these animal-based ingredients to be replaced is egg white, which acts as a widely used foaming agent in a variety of aerated food products, such as meringue, cake and mousse. An upcoming and promising plant-based alternative for egg white is mung bean (MB) (Brishti et al., 2017; Du et al., 2018; Yi-Shen et al., 2018). It is a widely cultivated legume crop in Asia, Southern Europe, and Northern America. MB is high in essential amino acids and bioactive proteins/peptides (Kudre et al., 2013; Yi-Shen et al., 2018). The major component in the seeds are carbohydrates, mostly present as starch granules, which can comprise between 55-65% (w/w) of the seed. The second largest fraction are proteins, which are responsible for 20-33% (w/w) of the seed. Also, MB contains about 1-1.85% (w/w) fat, which is favourable for protein fractionation, as defatting is not required (Anwar et al., 2007; Brishti et al., 2017; Ganesan & Xu, 2018; Mubarak, 2005). MB proteins have been studied for their foaming properties, but an extensive characterisation of their interfacial properties is lacking (Brishti et al., 2017; Du et al., 2018). Therefore, here we aim to perform a detailed study to fully understand the interface and foaming properties of MB proteins, fractionated and processed in various ways.

Plant proteins are commonly used as foaming ingredients. Conventional fractionation involves extensive wet processing. Seeds are milled and dispersed at alkaline pH for optimal protein solubility and yield. (Barać et al., 2015; Du et al., 2018; Kudre et al., 2013; Liu et al., 2015; Tang & Sun, 2010). Next, non-soluble components, such as starch granules and cell wall material, are removed by centrifugation or filtration. The resulting supernatant is high in protein content, but also in other solutes, such as sugars, salts and phenols. These solutes can be removed by precipitating the proteins at their isoelectric point (pI), which is

generally performed between pH 4 – 5 for MB protein (Brishti et al., 2017; Du et al., 2018; Kudre et al., 2013). Finally, the precipitated proteins are obtained and further processed into a protein isolate.

This above wet fractionation method has several disadvantages, as it involves many processing steps, each requiring copious amounts of energy and water (Lie-Piang et al., 2021). Another drawback is a side stream after the second centrifugation step (after iso-electric precipitation) (Chua & Liu, 2019). The major protein fraction in legumes are the storage protein globulins and albumins (Chéreau et al., 2016; Lam et al., 2018), with globulins being defined as being soluble in dilute-saline solutions, and albumins being defined as being soluble in pure water (Osborne, 1924). The globulins often have a pI between pH 4 and 5, while albumins are typically soluble in a wide pH range from 2 – 12 (González-Pérez et al., 2005). This suggests that the precipitate after isoelectric point precipitation mainly contains globulins, while the supernatant mainly contains the albumins. Yi-Shen et al. reported that 60% (w/w) of the protein in the MB seeds comprises of globulins, while 25% (w/w) of the proteins are albumins (Yi-Shen et al., 2018). As a result, up to 25% (w/w) of the MB proteins might be lost after the pI precipitation step. Extensive processing leads to higher proteins purity, but higher purities are often correlated to lower protein yields (Loveday, 2020; Tamayo Tenorio et al., 2018). Avoiding the precipitation step, thus using a milder fractionation process, would significantly increase the protein yield (Tamayo Tenorio et al., 2018). Another major advantage of a milder fractionation process that avoids iso-electric precipitation is that changes in protein structure may be avoided. Such changes do occur with pI precipitation, and are linked to the aggregation of globulins, and to lower protein solubility (Geerts et al., 2017; Pelgrom et al., 2014).

The most energy-consuming step in wet fractionation is final drying step, which is often performed by freeze-drying in scientific studies, or spray-drying or drum-

drying on industrial scales. Avoiding the drying step would significantly increase the sustainability aspect of plant-based protein ingredients (Lie-Piang et al., 2021). An alternative purification method that avoids drying is dry fractionation. Proteins in seeds are stored in so-called protein bodies with typical sizes between 1 and 3 µm (Pernollet, 1978), whereas starch granules have larger sizes in the ranging of 7 to 26 µm for MB (Hoover et al., 1997). By carefully milling MB seeds, protein bodies and starch granules can be detached from each other. Since protein bodies and starch granules differ in size and weight, the two fractions can subsequently be separated by air classification. The results is a flour separated into a coarse fraction rich in starch granules, and a fine fraction (FF) rich in protein bodies. The MB FF is a first MB protein fraction we will study for its interfacial and foaming behaviour. Next to the reducing water and energy usage, dry fractionation fully preserves the native structure of the protein resulting in higher functionality, for example in foaming. Some starch granules may still be present in the fine fraction, and these may affect the foaming properties of MB proteins purified in this way. Therefore, we also use a combination of dry fractionation and wet-processing step to furthermore remove the starch granules (Zhang et al., 2015). This mildly purified protein mixture (MIL) is a second sample we will use to study MB protein foaming. A second and third sample are more extensively purified globulin-rich (GLOB) and the albumin-rich (ALB) fractions, obtained from the MIL fraction.

Finally, we also study heat-processed MB proteins for their foaming properties. We use a process to aggregate MB proteins described in Chapter 3, resulting in MB protein aggregates previously called MB “protein colloids”. Colloidal particles and protein aggregates are known to enhance the stability of protein-stabilised foams by increasing the viscosity of the liquid phase or by blocking the lamellae and/or plateau borders of the foam. Both phenomena can result in slower drainage of the foam, leading to more stable foams (Dhayal et al., 2015; Rullier et al., 2008, 2009). The protein colloids are produced from the MIL fraction by adjusting the pH to

slightly acidic pH values, leading to the formation of protein-rich, submicron droplets (protein coacervates) in a continuous protein-poor phase. These protein droplets are subsequently gelled by a heating step. This is a relatively simple method to create protein colloids. Protein colloids produced in this way can be regarded as nanogels or microgels, and could also be used for other functions, such as fat replacement, encapsulation and targeted delivery in the food industry (Inthavong et al., 2019; Karaca et al., 2009; Sağlam et al., 2013; Sandoval-Castilla et al., 2004; Shewan & Stokes, 2013). This is the last sample (MPCM) for which we will study MB protein interfacial and foaming properties.

In summary, we study the interfacial and foam-stabilising properties of five different MB protein fractions: dry-fractionated fine fraction (FF), mildly purified protein fraction (MIL), globulin-rich fraction (GLOB), albumin-rich fraction (ALB), the protein colloids (MPCM).

For these fractions, a detailed physicochemical characterisation was performed and interfacial properties were evaluated using large amplitude oscillatory dilatation (LAOD) in drop tensiometry. Foam stability for foams obtained from the different MB fractions was studied using whipping and sparging methods. Our comprehensive approach especially aims at establishing a relation between the nature of the different MB protein fractions and their ability to act as a foaming agent.

4.2 Experimental section

4.2.1 Materials

Dried mung bean seeds (GC Mung Bean, Thailand) were obtained from online Asian store MyEUshop (The Netherlands). All chemicals (Sigma-Aldrich, USA) and materials for SDS-PAGE (Invitrogen Nove, Thermo Fisher Scientific, USA) were used

as received. The samples were prepared in water (MilliQ Purelab Ultra, Darmstadt, Germany), unless stated differently.

4.2.2 Sample preparation

4.2.2.1Preparation of dry fractionation fine fraction

Mung beans (MB) were dry fractionated at a batch size of 400 g using a Multimill Hosakawa System (Hosakawa, Germany) equipped with a ZPS50 impact mill. The milling parameters were set at a wheel speed of 8000 rpm, airflow of 52 m^3/hr and feed speed of 20 rpm. The resulting flour was air classified with an ATP50 air classifier at a rotation speed of 2500 rpm, a feed rate of 20 rpm and a 52 m^3/hr airflow. The final result is that the flour separates into a coarse and fine fraction. The fine fraction (FF) was used for further fractionation of the proteins. A schematic overview of the fractionation routes is shown in Figure 4.1.

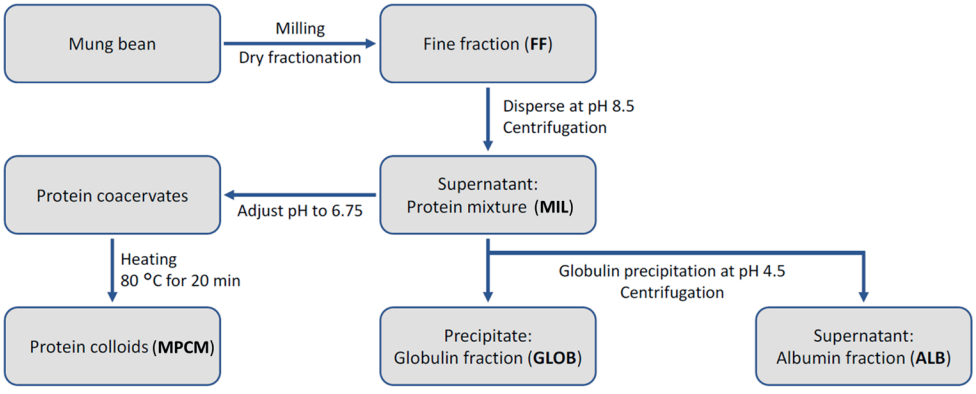

Figure 4.1 *Schematic overview of the protein fractionation routes used to obtain five different protein-enriched fractions.*

4.2.2.2 Preparation of wet fractionated protein fractions

The fine fraction (FF) was dispersed in water in a 1:10 (w/w) FF/water ratio. While stirring for 2 hrs, the pH was adjusted to 8.5 using 1 M NaOH solution. Afterwards, the dispersion was centrifugated at 10000 g for 30 min. The supernatant was separated from the pellet and freeze-dried, which resulted in the mildly purified protein mixture (MIL). The freshly prepared MIL, so not freeze-dried, was further

processed by adjusting the pH to 4.5 using 1M HCl, while stirring for 1 hr, to induce isoelectric point precipitation. The precipitated proteins were separated by centrifugation at 10000 g for 30 min. The pellet was re-dispersed in water and the pH was adjusted to 7.0 using 1 M NaOH. After 1 hr of stirring, this fraction was freeze-dried to obtain the globulin-rich fraction (GLOB). The supernatant from the acid precipitation step was dialysed against water (using a dialysis membrane with a 3.5 kDa cut-off) at 4 °C to remove the small solutes. The dialysate was changed five times, ensuring the conductivity of the water became constant. Afterwards, the dialysed sample was freeze-dried to obtain the albumin-rich fraction (ALB).

4.2.2.3 Preparation of the protein colloids

The protein colloids (MPCM) were prepared using the method from Chapter 3. In brief, FF was dissolved in 15 mM sodium metabisulfite solution in a 1:4 (w/w) FF/solution ratio and stirred for 5 min. Afterwards, the pH was adjusted to 8.5 using 1 M NaOH, followed by 1 hr stirring. The solution was centrifuged at 10000 g for 30 min, and the supernatant was collected through a paper filter. The pH of the supernatant was adjusted to 6.75 to induce liquid-liquid phase separation. The protein coacervates were heated, while slowly stirring with a magnetic stirrer rod at 80 °C for 20 min, to induce cross-linking. Afterwards, the sample was cooled in an ice-water bath and freeze-dried to obtain the protein colloids (MPCM).

4.2.2.4 Determination of protein content

The protein content was analysed using Dumas in a Flash EA 112 NC Analyser (Thermo Fischer Scientific, USA). The nitrogen content was determined and converted into a protein content using a nitrogen conversion factor of 6.25 (Mariotti et al., 2008). All samples were measured in triplicate.

4.2.2.5 Dissolving samples

All samples were dissolved based on protein content (% w/w) in a 20 mM PO_4-buffer, pH 7.0, and stirred for at least 4 hrs at room temperature. Samples were

dissolved in a protein concentration range from 0.1 to 1.0% (w/w), specified in the sections below.

4.2.3 Determination of protein composition by SDS-PAGE

Solutions of 0.1% (w/w) protein were prepared in water. The protein solutions (45 µL) were mixed with NuPAGE LDS sample buffer (7 µL) and 500 mM DDT (6µL). The mixtures were heated for 10 min at 70 °C and loaded on a 4-12% (w/w) BisTris gel. A Mark 12 molecular weight marker in the range of 2.5-200 kDa was also included. Electrophoresis was performed on the gel for 30 min at 200 V. Afterwards, the proteins were stained with SimplyBlue Safestain, and the gel was analysed using a gel scanner and Image Lab v5.2.1. software.

4.2.4 Determination of protein size by SEC

Size exclusion chromatography (SEC) was performed using an ÄKTA pure 25 system (Cytiva, Marlborough, MA, USA) equipped with Superdex® 200 10/300 GL column. First, protein solutions with a 0.1% (w/w) protein content were centrifuged at 15000 g for 10 min. The supernatant (50 µL) was injected into the system, and the eluent was a sodium phosphate buffer (20 mM, pH 7.0) containing 50 mM NaCl. The flow rate was set at 0.5 mL/min. The elution was analysed with UV absorbance at 280 nm.

4.2.5 Determination of zeta-potential and particle size

Except for MPCM, the particle size distribution and zeta-potential were analysed using dynamic light scattering in a Zetasizer Nano ZS (Malvern Instruments Ltd., UK). Solutions with 0.01% (w/w) protein were injected in a DTS1070 Zetasizer cell. The samples were filtered over a 0.45 or 1.2 µm syringe filter (hydrophobic, Whatman) before injection, and the usage of type of filter will be mentioned in the captions. Before analysis, the cell containing the sample was equilibrated for 2 min at 20 °C, followed by a size distribution measurement, where 12 scans were performed in

automatic mode, of which an average was calculated. For MPCM samples, particle size distributions were measured using static light scattering (Mastersizer 2000, Malvern instruments, United Kingdom), setting the particle refractive index to 1.48. The zeta-potential was determined at 40V with at least 25 single measurements. All measurements were at least performed in triplicate at 20 °C.

4.2.6 Determination of protein thermal stability by DSC

The protein denaturation properties were determined by a differential scanning calorimetry (DSC) in a Discovery DSC25 (TA Instruments, USA). Stainless steel high volume pans were filled with about 40 µL of 5% protein (w/w) solutions. An empty stainless-steel high-volume pan was set as a blank reference, and nitrogen was used as a carrier gas. The samples were first equilibrated at 5 °C for 5 min, followed by heating to 140 °C at a rate of 5 °C/min. Subsequently, to investigate potential refolding of the proteins, samples were cooled down from 140 °C to 5 °C at a rate of 10 °C/min, and then reheated to 140°C at a rate of 5 °C/min. All samples were studied in duplicate.

4.2.7 Determination of protein surface hydrophobicity

The protein surface hydrophobicity was determined using 8-anilino-1-napthalenesulfonic acid ammonium salt (ANSA) as a fluorescence agent. Samples were dissolved in buffer based on protein concentration varying from 0.005 – 0.04% (w/w). Double-sided transparent plastic cuvettes of 4 mL were filled with 3 mL protein solution, and 25 µL of an 8 mM ANSA solution was added. The samples were carefully mixed by rotation and incubated for 1 hr in the absence of light to avoid deterioration of the ANSA agent. After incubation, an LS 50B luminescence spectrometer (Perkin Elmer, USA) was used, and the excitation wavelength was 390 nm, and the emission wavelength was set at 470 nm. The buffer solution was also included in the analysis as a blank. The slope of the fluorescence intensity over protein concentration was used as a quantification of the surface hydrophobicity.

The various samples were compared by calculating a relative surface hydrophobicity among the samples. All samples were analysed in triplicate.

4.2.8 Determination of surface tension and surface dilatational properties

The mechanical properties of the air-water interface were studied by performing surface dilatational rheology in a drop tensiometer PAT-1M (Sinterface Technologies, Germany). A 0.1% (w/w) protein solution was used to form a hanging droplet with a surface area of 20 mm^2 at the tip of a hollow needle. The surface tension was calculated by fitting the Young-Laplace equation to the shape of the droplet. Three types of measurements were performed, and prior to the start of each of these analyses, the droplets were equilibrated for 10800 s. Frequency sweeps were performed at a constant amplitude of 3% and a frequency which increased from 0.002 to 0.1 Hz. Amplitude sweeps were performed at a constant frequency of 0.02 Hz and an amplitude which increased from 3 to 30% deformation. In these oscillatory deformations, five cycles were performed for each frequency or amplitude step. The relaxation behaviour of the interface was also studied by performing step-dilations, where the interface was subjected to a 10% rapid compression or extension (2s step time) of the area. All measurements were performed at least in triplicate at 20 °C.

4.2.9 Rheology data analysis

The raw data of the amplitude sweeps were transformed into Lissajous plots by plotting the oscillating surface stress (γ-γ_0) against deformation ((A-A_0)/A_0). Here, γ and A are the surface tension and area of the deformed interface, γ_0 and A_0 are the surface tension and area of the non-deformed interface. The plots were generated using the middle three oscillations.

4.2.10 Determination of foam properties

4.2.10.1. Ability and stability of foams created by whipping

Foams were created by whipping 15 mL of 0.1 – 1.0% protein (w/w) solutions with an overhead stirrer equipped with an aerolatte foam head at 2,000 rpm for 2 min in a plastic container (34 mm diameter). The foamability was determined by marking the bottom and upper level of the foam. The height was measured and recalculated into the maximum foam volume using the radius of the container. The foam overrun was defined by:

$$Foam\ overrun\ (\%) = \frac{Maximum\ foam\ volume\ (mL)}{Initial\ solution\ volume\ (15\ mL)}\ x\ 100\% \quad (4.1)$$

4.2.10.2 Stability of foams created by sparging

Sparged foams were created in a Foam scan foaming device (Teclis IT-concept, France). A glass cylinder (60 mm diameter) was filled with 40 ml of sample, and gas was sparged through a metal frit (27 µm pore size, 100 µm distance between centres of pores, square lattice) at a flow rate of 400 mL/min. The generated foam in the tube was studied by image analysis to obtain a foam volume, and the foams were sparged to a volume of 400 mL. Afterwards, the foam volume was monitored until a 50% decay of volume, which is known as the foam volume half-life time. A second camera recorded a detailed image of the air bubbles, which was analysed using a custom Matlab script with a DIPlip and DIPimage analysis software package (TU Delft, NL) to determine an average bubble size. All experiments were performed at least in triplicate at 20 °C.

4.2.11 Statistical analysis

The results of this study were shown as means with standard deviation. Statistical analysis was conducted using SPSS v25.0 (IIBM SPSS Inc., USA). One-way ANOVA (one-way analysis of variance) with Duncan post-hoc method ($p < 0.05$) was

performed to evaluate the statistical significance of the differences among the means.

4.3 Results and discussion

4.3.1 Protein fractionation process

Dry fractionation of mung bean (MB) resulted in a fine fraction (FF) with 25.2% (w/w) of protein. Next to protein, there are still damaged starch granules in the FF present (shown in microscopy images in Figure S4.1 in the Appendix). This was also found for dry fractionated yellow pea seeds, where starch granules were also damaged upon milling (Möller et al., 2021). The remaining starch granules were removed by dispersing the FF in water followed by centrifugation, which yielded the mildly purified protein mixture (MIL). Removal of starch was reflected in a protein content increase to 58.8% (w/w). A similar fractionation of yellow pea, which is also a pulse, resulted in a protein content of 54.8% (w/w) (R. Kornet et al., 2022). The remaining 41.2% (w/w) of the MIL was previously found to be salts and soluble saccharides for yellow pea (C. Kornet et al., 2020). The MIL was further purified by isoelectric point (pI) precipitation at pH 4.5, which resulted in a nearly zero net protein charge of the globulins, leading to aggregation, followed by precipitation. The globulins can be recovered using centrifugation, leading to a globulin-rich fraction (GLOB) with a protein content of 89.4% (w/w). A drawback of extensive purification is a lower protein recovery of 66.6% (w/w), while MIL had a protein recovery of 79.4% (w/w). The major difference is the loss of albumins in the supernatant after the isoelectric precipitation step, as albumins remain soluble at a large pH range between 2 and 12 (Gonzalez-Perez et al., 2005). Direct utilisation of the albumin-rich supernatant has a potential drawback, as many non-protein components are present, such as salts, saccharides, but also anti-nutritional components, such as lipoxygenases, phytic acids and tannins (Chua & Liu, 2019). However, these solutes were removed using dialysis (or filtration), leading to the albumin-rich fraction (ALB) with a protein

content of 47.1% (w/w). The protein colloid fraction had a protein content of 50.0% (w/w).

Table 4.1 *The protein content (Nx6.25) based on dry matter (% w/w) and protein recovery (expressed as the amount of protein obtained from the FF) of FF (fine fraction), MIL (protein mixture), MPCM (protein colloids), GLOB (globulin fraction), and ALB (albumin fraction). Values are presented as mean ± standard deviation. The values with the same superscript are not significantly different (p > 0.05) from each other.*

	FF	MIL	GLOB	ALB	MPCM
Protein content (%)	25.2 ± 0.4^{a}	58.8 ± 3.2^{c}	89.4 ± 0.6^{d}	47.1 ± 1.5^{b}	50.0 ± 0.5^{b}
Protein recovery (%)	100	79.4	66.6	10.5	80

4.3.2 Protein composition

In the next step, the protein composition was analysed using SDS-PAGE under reducing conditions, where disulphide bonds between protein subunits were broken down (Figure 4.2A). The two major storage protein classes globulin and albumin can be observed in the gel. Globulins in legumins are further divided into two sub-classes: vicilin (VIC) and legumin (LEG) (Mendoza et al., 2001; Tang & Sun, 2010). Native MB vicilin had a molecular weight between 158 – 200 kDa, while MB legumin had a molecular weight of around 360 kDa. For GLOB, there are high-intensity bands between 20 and 30 kDa, at 34 kDa, and between 40 and 55 kDa. Subunits for legumin were previously identified at 24 and 40 kDa, while vicilin had subunits at 26, 32, 48 and 60 kDa (Mendoza et al., 2001). A majority of these bands are prominently present on the lanes of FF, MIL, and GLOB, indicating the presence of both MB vicilin and legumin.

A few typical bands were found for albumins at 25 kDa and between 70 and 95 kDa. The FF and MIL had bands for globulin and albumin subunits, which is expected as FF is unprocessed (obtained after dry fractionation), and both proteins are retained in MIL due to the mild wet fractionation method. Similar protein composition was

also found when performing size exclusion chromatography (SEC) on FF (data shown in Figure S4.2 in the Appendix). The GLOB showed thicker bands for the globulin subunits, and the bands for albumin proteins were (nearly) absent. The opposite was observed for the ALB sample, suggesting a successful separation of both albumin and globulins. The separation of albumin and globulin from MIL into ALB and GLOB was again confirmed using SEC (Figure 4.2B). Here, prominent peaks for legumin (11 min elution time, 660 kDa) and vicilin (12 min, 258 kDa) are present in GLOB, and absent in ALB. The ALB sample showed dominating peaks at 14.5 (113 kDa) and 17 min (32 kDa), showing the major fraction in this isolate are albumins. Also here, the smaller size of albumins compared to globulins (legumin & vicilin) is evident.

MPCM showed both bands for albumins and globulins in the SDS-PAGE gel (Figure 4.2A), but the bands had lower intensity compared to MIL. Fewer proteins might be incorporated in the gel, as the proteins are expected to form large colloids in MPCM that might not have passed into the much smaller pores of the gel. We will evaluate the particle size of the MB protein fractions in the next section.

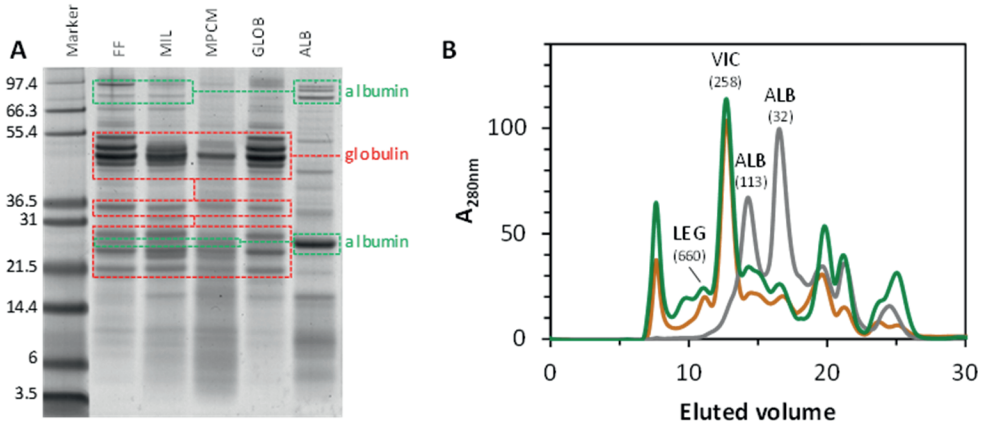

Figure 4.2 (A) *SDS-PAGE profile under reducing conditions of FF (fine fraction), MIL (protein mixture), MPCM (protein colloids), GLOB (globulin fraction), and ALB (albumin fraction).* ***(B)*** *SEC chromatogram with the 280 nm absorbance over eluted volume of MIL (green), ALB (grey) and GLOB (orange). The numbers in brackets indicate the molecular weight (kDa) of the corresponding peak. The calibration curve can be found in the appendix Figure S4.3.*

4.3.3 Protein size distribution

Size distributions of the MB protein fractions obtained from dynamic light scattering are shown in Figure 4.3. The FF had a peak between 100 – 220 nm with a maximum peak height at 164 nm, which are probably protein bodies or starch granule fragments. Large starch granules are not shown in the size distribution of FF, as the sample was filtered over 1.2 µm before analysis. Of course, smaller albumin & globulin proteins might be present in the FF, but the large peak at 100-220 nm is most likely dominating the overall scattering signal. This large material was removed when creating the MIL fraction, which showed a peak at a smaller size between 4 and 20 nm with a maximum peak height at 10 nm. GLOB showed a comparable size distribution with a similar peak at 8.7 nm, while ALB had a peak at 3.6 nm. A smaller size for ALB is expected as albumins are smaller than globulins, as shown in the SDS-PAGE profile & SEC chromatogram (Figure 4.2). Also, the globulins seem to dictate the size distribution of MIL, which could be due to the presence of more globulins than albumins. Based on the protein yield, we expect

roughly 13% of albumins and 87% globulins in the MIL. Finally, the MPCM showed a major peak between 50–800 nm. This confirms the formation and presence of protein colloids.

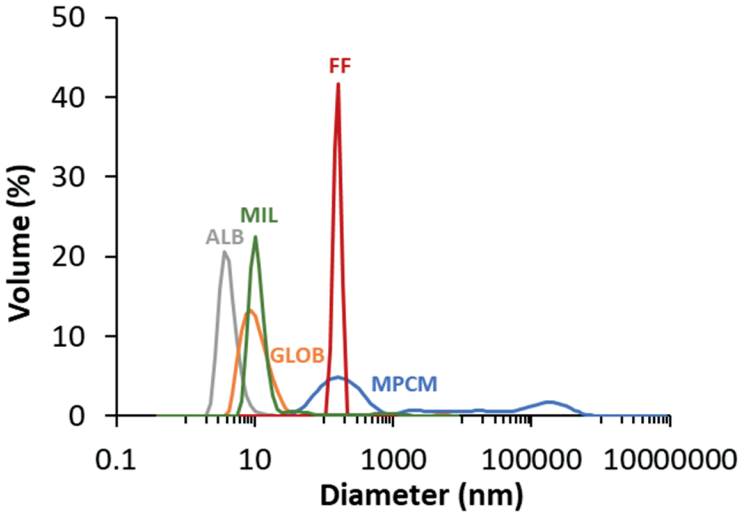

Figure 4.3 *The size distribution of MB protein fractions: FF (fine fraction, filtered over 1.2 µm, red), MIL (protein mixture, filtered over 0.45 µm, green), MPCM (coacervate colloids, unfiltered, blue), GLOB (globulin fraction, filtered over 0.45 µm, orange), and ALB (albumin fraction, filtered over 0.45 µm, grey). For clarity reasons, one representative measurement is shown for each sample, while comparable results were obtained from three replicates.*

4.3.4 Protein heat denaturation properties

Extensive purification or processing of proteins might alter the protein structure. Therefore, the protein thermal properties were evaluated using differential scanning calorimetry (DSC). The denaturation temperatures and enthalpy are shown in Table 4.2. FF had lower denaturation temperatures (T_{onset} and T_{peak} of 70.8 and 76.6 °C) compared to MIL, and also a substantially higher enthalpy (30.2 J/g) due to starch gelatinisation (Hoover et al., 1997). MIL (obtained through removal of starch) had a T_{onset} and T_{peak} of 72.6 and 80.7 °C, respectively. The denaturation behaviour of MIL is most likely dominated by the globulins, as GLOB showed comparable denaturation temperatures, while albumin showed lower ones. However, the denaturation enthalpy of GLOB is about 23% lower compared to MIL.

One could argue that the GLOB fractionation might have altered protein structure, such as increased aggregation, as also found for pea globulins (C. Kornet et al., 2020). This could ultimately lead to the slightly lower enthalpy of GLOB.

Table 4.2 *Protein denaturation temperature and enthalpy of MB protein fractions. Values are presented as mean ± standard deviation.*

	FF	MIL	GLOB	ALB	MPCM
T_{onset} (°C)	70.8 ± 0.8	72.6 ± 0.0	71.2 ± 0.9	67.6 ± 0.3	80.7 ± 0.0
T_{peak} (°C)	76.6 ± 0.1	80.7 ± 0.1	79.4 ± 0.9	76.6 ± 0.1	87.6 ± 0.1
Enthalpy (J/g protein)	30.2 ± 1.0	10.4 ± 0.2	8.0 ± 0.0	2.7 ± 0.0	3.4 ± 0.1

ALB had a substantially lower enthalpy than GLOB, which is related to their tertiary protein structures. From other plant sources, it is known that globulins are folded into (larger) globular structures, while albumins have a more simple structure (Gonzalez-Perez & Vereijken, 2007; Souza, 2020). MPCM had the highest denaturation temperatures, which was expected, as the sample was heated at 80 °C. Even though 80 °C is at the peak denaturation temperature of the globulins, complete denaturation of proteins requires higher temperatures. We expect that a portion of the globulins is not or only partly denatured, which is reflected in the remaining denaturation enthalpy of 3.4 J/g protein for MPCM. In summary, the extensive purification process to obtain GLOB and ALB seemed to slightly alter the protein nativity of the globulins, while heating the colloids resulted in vast alteration of protein structure.

4.3.5 Protein surface hydrophobicity and zeta-potential

The protein surface properties (influenced by hydrophobicity and charge of the protein) are known to affect the protein's interfacial properties. Therefore, we evaluated the relative protein surface hydrophobicity (Table 4.3). In previous studies, globulins of yellow pea, Bambara groundnut and rapeseed were found to have a higher surface hydrophobicity than albumins (C. Kornet et al., 2020; Ntone et al., 2021; Yang, de Wit, et al., 2022). A similar relationship is present in this work,

as the surface hydrophobicity of GLOB is about 45% higher than ALB. FF and MIL showed lower surface hydrophobicity, which could be related to the presence of non-proteinaceous components that cover hydrophobic domains of the protein or interfere with the hydrophobic probe. Another explanation is the slight alteration of protein structure due to the extensive processing, as shown by DSC (Table 4.2). This could lead to higher surface hydrophobicity values for GLOB and ALB in comparison to FF and MIL. The highest surface hydrophobicity was found for MPCM, which is between 3 – 10 times higher than the other MB protein fractions. This finding is not unexpected, as the MPCM sample was heat-denatured to form cross-links, thus leading to more exposed hydrophobic groups on the surface of the coacervate colloids. A second protein surface property of interest is the zeta potential (Table 4.3). Here, we showed a zeta-potential between -14.8 to -22.4 mV for FF, MIL, GLOB and MPCM. These fractions are high in globulins, which probably resulted in comparable surface charges. Albumins showed a substantially lower zeta-potential of -2.3 mV.

Table 4.3 *The relative protein surface hydrophobicity and zeta-potential of FF (fine fraction), MIL (protein mixture), MPCM (protein colloids), GLOB (globulin fraction), and ALB (albumin fraction) dissolved in a sodium phosphate buffer. Values are presented as the mean value ± standard deviation. The means with the same superscript in the same column are not significantly different from each other ($p > 0.05$).*

	Relative protein surface hydrophobicity	Zeta-potential (mV)
FF	0.18 ± 0.01^{b}	-22.4 ± 2.3^{a}
MIL	0.10 ± 0.01^{a}	-19.8 ± 1.8^{a}
GLOB	0.29 ± 0.02^{c}	-14.8 ± 0.9^{b}
ALB	0.20 ± 0.02^{b}	-2.3 ± 1.5^{c}
MPCM	1.00 ± 0.04^{d}	-19.7 ± 1.6^{a}

4.3.6 Interfacial properties

4.3.6.1 Adsorption behavior

All the samples showed an immediate increase of surface pressure at the first measurement point at 1 s (Figure 4.4A). ALB had the highest initial surface pressure increase. The rapid initial adsorption of ALB probably results from the small molecular size, leading to a high diffusional flux towards the interface. The smaller size and low surface charge of albumins can also contribute to a lower energy barrier for adsorption. GLOB showed a much slower initial adsorption compared to ALB, probably due to the higher molecular weight and surface charge. FF and MIL showed higher surface pressure values over the three hours of adsorption time. This could be a contribution of albumins for FF and MIL, as both albumins and globulins are present. We should also keep in mind that many non-proteinaceous components (e.g. phospholipids and phenols) are present in FF and MIL, which can compete with the proteins for the interface, or interact with the proteins, thereby affecting the surface properties of the proteins (Bock et al., 2021; He et al., 2008).

The protein colloids (MPCM) showed a slight surface pressure increase in the initial phase (first 20 s) compared to GLOB, which is surprising, as the protein colloids are much larger (Figure 4.3). Such large colloids (50-800 nm) are not expected to adsorb at the air-water interface due to the high energy barrier against adsorption. In previous work, whey protein colloids were produced, which also did not adsorb at the air-water interface (Yang et al., 2020), while smaller non-cross-linked material also present in the dispersion dictated the interfacial properties. For the MPCM fraction, we also expect the interfacial dominance of non-cross-linked proteins, which might be highly surface-active due to exposure of hydrophobic groups, as shown in the surface hydrophobicity determination (Table 4.3).

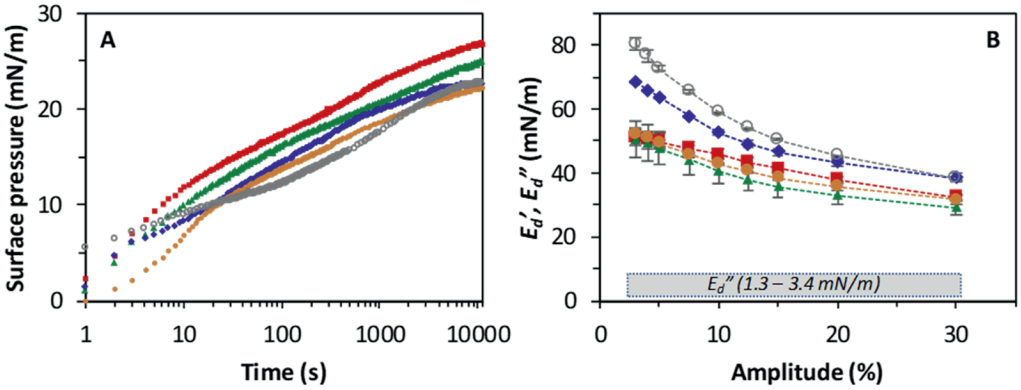

Figure 4.4 (A) *The surface pressure as a function of time of FF (fine fraction, red squares), MIL (protein mixture, green triangles), MPCM (coacervate colloids, blue diamonds), GLOB (globulin fraction, orange circles), and ALB (albumin fraction, white circles). Averages of three replicates are shown, and the standard deviation was below 5%.* ***(B)*** *The surface dilatational moduli versus deformation amplitude of the earlier mentioned MB protein fractions. The E_d' was shown as symbols with a line to guide the eye, while the Ed" of all samples were very low, with values in the grey area. The shown averages and standard deviations are the results of at least three replicates.*

4.3.6.2 Surface dilatational rheology

The mechanical properties of air-water interfacial films stabilised by the MB protein fractions were studied using surface dilatational rheology. Frequency and amplitude sweeps, and step-dilatations were performed.

Frequency sweeps

In frequency sweeps, the deformation amplitude was constant at 3%, while the frequency of the oscillation was varied. The dilatational storage moduli (results not shown) showed a weak power law dependence on frequency, i.e., $E_d' \sim \omega^n$. The n-value are shown in Table 4.4. An n-value of 0.5 was previously related to an interfacial film, where the elasticity is determined by the mass exchange of stabiliser between the bulk and the interface, also known as the Lucassen-Van den Tempel model(Lucassen & Van Den Tempel, 1972). The interfacial layers stabilised by the different MB protein fractions had n-values between 0.08 and 0.17. The

storage modulus was significantly higher than the loss modulus, something typical for soft viscoelastic disordered solids [43,45]. Exchange of material between bulk and interface does not appear to play a significant role in the response, which is more likely governed by in-plane rearrangements and momentum exchange with the bulk phase.

Table 4.4 *The n-value of $E_d' \sim \omega^n$, obtained from frequency sweeps on MB-protein stabilised interfacial films. Values are presented as mean ± standard deviation.*

	n-value
FF	0.17 ± 0.02^b
MIL	0.14 ± 0.03^b
MPCM	0.08 ± 0.03^a
GLOB	0.16 ± 0.03^b
ALB	0.14 ± 0.02^b

Amplitude sweeps

The mechanical properties of the interfacial films were further analysed by performing amplitude sweeps, where the deformation amplitude of the interfacial area is increased from 3 to 30%, while the oscillation frequency is constant (Figure 4.4B). Here, we are interested in the magnitude and amplitude dependence of the surface dilatational elastic moduli *Ed'*. When comparing ALB- and GLOB-stabilised interfaces, the ALB had higher moduli decreasing from 80 to 38 mN/m, while GLOB had lower moduli between 52 and 32 mN/m. This implies the formation of stiffer layers by ALB. The lower amplitude dependence of GLOB indicates there is less disruption of the surface microstructure compared to ALB. The FF- and MIL-stabilised interfacial films had moduli of 51–32 and 51–29 mN/m, respectively, similar to GLOB. This would indicate a globulin-dominated interfacial layer for FF and MIL, probably due to the high concentration of globulins. The moduli of MPCM were between those of GLOB and ALB, with a decrease from 68–38 mN/m. That MPCM formed stiffer interfacial layers than GLOB, FF and MIL could be related to the increased hydrophobic interactions among adsorbed proteins (see Table 4.3).

The microstructure of the interfaces was clearly affected by large deformations, as the E_d' values (Figure 4.4B) decreased with increasing deformation amplitudes, also known as the nonlinear viscoelastic (NLVE) behavior. Disruptions of the interfacial microstructure can lead to nonlinearities in the surface stress/pressure signal. The moduli in Figure 4.4 are obtained by Fourier transforming the surface stress signal and calculated using the intensity and phase of the first harmonic of the obtained Fourier spectrum. Using the first harmonic is reliable only when the deformations are small and in the linear viscoelastic (LVE) regime, where nonlinearities are negligible. Most of the deformations in Figure 4.4B are in the NLVE regime, leading to nonlinearities, thus higher-order harmonics in the Fourier spectrum. These higher-order harmonics (and nonlinearities) are neglected in the E_d' calculation. A qualitative analysis method to incorporate the nonlinearities is plotting the surface pressure as a function of deformation in Lissajous(-Bowditch) plots (Ewoldt et al., 2007; Xia et al., 2022).

Lissajous plots

Lissajous plots of the MB-protein fraction-stabilised interfaces are shown in Figure 4.5. The plots move clockwise, where the interfacial area is extended in the upper part of the cycle, and the opposite (compression) occurs in the bottom part of the cycle. An important characteristic is the width of the plots, which indicates the type of rheological response of the interfacial layer. A straight line (closed plot) reveals a fully elastic response, a circle indicates a viscous response, and an ellipse suggests a viscoelastic response. The angle of the main axis of the plots with the horizontal axis is related to the interfacial stiffness, and a plot that is more tilted towards the vertical axis suggests a stiffer interface. Nonlinearities can lead to asymmetries between the extension and compression cycle, which we will elaborate discuss for the graphs.

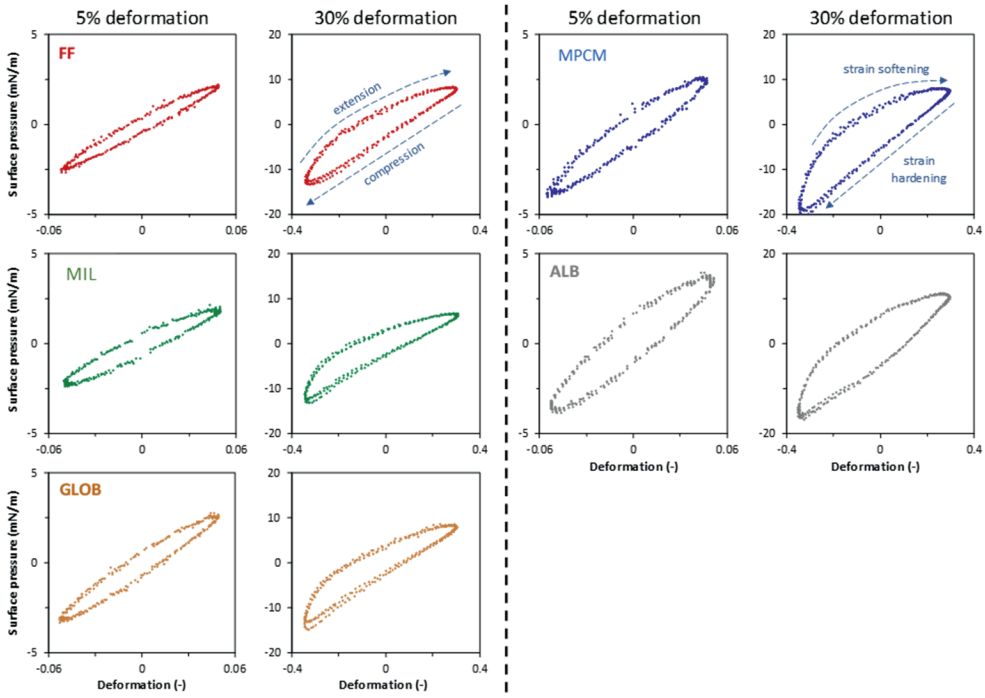

Figure 4.5 *Lissajous plots of surface pressure as a function of deformation. The plots are obtained from the amplitude sweeps of interfacial layers stabilised by the MB protein fractions: FF (fine fraction), MIL (protein mixture), MPCM (coacervate colloids), GLOB (globulin fraction), and ALB (albumin fraction). One representative plot is shown for each sample, while comparable plots were obtained for at least three replicates.*

At 5% deformation, the MPCM- and ALB-stabilised interfaces showed wider plots compared to FF, MIL and GLOB. This indicates a higher energy dissipation upon deformation. Also, the MPCM and ALB are more tilted toward the vertical axis, indicating a stiffer interfacial film. Nonlinear behaviour is clearly present at 30% deformation, as all plots become asymmetric. For both MPCM and ALB, at the start of the extension part of the cycle (bottom-left point), we can observe a relatively fast surface pressure increase, followed by a gradually smaller increase of surface pressure. For MPCM, a nearly flat curve can be observed between a deformation of 0.25–0.30. Such behaviour is called intra-cycle strain softening in extension, revealing a gradual disruption (and softening) of the microstructure. With this, the elastic component of the response diminishes, while the viscous component starts

dominating. On the time scale of a single cycle, there is negligible mass transfer between bulk and interface (as evident from the frequency sweeps). This means the surface density decreases upon expansion, and this may also contribute to the observed softening behaviour.

In the compression cycle, we can observe an opposite phenomenon, as the surface pressure rapidly decreases to values of -18 and -20 mN/m at a deformation of -0.35 for ALB and MPCM. This behaviour is known as intra-cycle strain hardening in compression, as the adsorbed proteins are concentrated upon (extensive) compression, resulting in the jamming of proteins at the interface. The combination of strain softening in extension and strain hardening in compression implies strong in-plane interactions between adsorbed proteins. Such behaviour was previously related to the formation of viscoelastic solid-like interfacial layers (Hinderink et al., 2020; Yang et al., 2020). The ability of albumins to form stiff solid-like interfacial layers was previously related to the small molecular size and low surface charge (Yang, Kornet, et al., 2022). This would allow a closer approach of proteins and more effective coverage, leading to stronger in-plane protein-protein interactions. The proteins in the MPCM might be able to form such layers due to the high surface hydrophobicity (Table 4.3), which can also lead to stronger attractive interaction.

Different behaviour is present for the FF-, MIL- and GLOB-stabilised interfaces, as these protein fractions show narrower 5% deformation plots that are more tilted towards the horizontal axis. At 30%, the asymmetries were less pronounced in comparison to the ALB- and MPCM-stabilised interfaces. This implies that the FF-, MIL- and GLOB-stabilised interfaces formed weak and more easily stretchable interfaces. We also conclude that the globulins dominate the interfacial properties in both FF and MIL, which was also observed for a protein mixture from yellow pea and Bambara groundnut (R. Kornet et al., 2022; Yang, de Wit, et al., 2022). For Bambara groundnut, it is shown explicitly that the legumin dominated the

interfacial properties in a globulin mixture of both legumin and vicilin, probably due to faster adsorption of legumin at the air-water interface than vicilin. The weak interfacial layers formed by MB globulin could be due to their largely aggregated state in combination with high surface charges. As a result, this could lead to a lower and less effective surface coverage, thus weaker in-plane interaction at the interface.

Step-dilatation experiments

The interfacial properties of the MB protein fraction-stabilised interfaces were further investigated by studying the relaxation response. The response was initiated by performing step-dilatations on the air-water interface. The relaxation response was fitted with a combination of a Kohlraus-William-Watts (KWW) stretch exponential and a regular exponential term (Equation 1)(Watts & Davies, 1969).

$$\gamma(t) = ae^{-(t/\tau_1)^{\beta}} + be^{-t/\tau_2} + c \quad (4.2)$$

Here, the stretch exponent β and relaxation time τ_1 are shown in Table 4.5. Other parameters, such as the characteristic time of the second term τ_2 and fitting parameters a, b, and c are shown in Table S4.1 in the Appendix. The KWW is a phenomenological model that was initially used to describe the relaxation responses of disordered systems and later for protein-stabilised interfaces (Klafter & Shlesinger, 1986; Sagis et al., 2019; Watts & Davies, 1969; Yang et al., 2021). A stretch component of β<1 indicates dynamic heterogeneity, which may suggest a wide range of relaxation times due to local variations in the relaxation response. In our work, we show β values varying from 0.53 to 0.63 for all MB protein stabilised interfaces. This reveals the presence of dynamic heterogeneity, which we previously related to the heterogeneous microstructure of a protein-stabilised interface (Yang et al., 2020). Such a microstructure is comprised of proteins clusters, leading to the co-existence of dilute/dense and thicker/thinner regions. Such

dissimilarities could result in local differences in the relaxation response, thus a wide range of relaxation times, and the emergence of dynamic heterogeneity. The relaxation time varies between 19.2 and 34.1 s, which is typical for protein interfaces(Sagis et al., 2019). The relaxation response of these interfacial films indicates the formation of disordered/heterogeneous solid-like materials, as observed for a wide range of protein-stabilised interfacial films (R. Kornet et al., 2022; Rühs et al., 2013; Yang et al., 2020). The findings from the step-dilatation experiment, in combination with the frequency and amplitude sweeps demonstrate the formation of viscoelastic disordered solid-like interfacial films by the MB fractions.

Table 4.5 *The stretch exponent β and characteristic relaxation time τ_1 values obtained from step-dilatation experiments of air-water interfaces stabilised by the MB protein fractions. Values are presented as mean ± standard deviation. The means with the same superscript in the same column are not significantly different from each other (p > 0.05).*

	Extension		Compression	
	β	**T1 (s)**	**β**	**T1 (s)**
FF	0.60 ± 0.03^{a}	32.4 ± 6.9^{b}	0.58 ± 0.01^{a}	27.9 ± 7.1^{ab}
MIL	0.60 ± 0.02^{a}	30.8 ± 8.4^{a}	0.59 ± 0.03^{a}	23.8 ± 4.0^{ab}
MPCM	0.57 ± 0.04^{a}	25.2 ± 5.1^{a}	0.63 ± 0.04^{a}	34.1 ± 8.2^{b}
GLOB	0.54 ± 0.05^{a}	22.2 ± 3.7^{a}	0.60 ± 0.06^{a}	17.3 ± 5.3^{ab}
ALB	0.53 ± 0.03^{a}	19.2 ± 8.0^{a}	0.60 ± 0.05^{a}	18.1 ± 3.5^{ab}

4.3.7 Foams

4.3.7.1 Foamability

The foamability of the MB protein-stabilised foams was evaluated by studying the foam overrun after whipping, and the average air bubble size after sparging with nitrogen gas (Figure 4.6 A & B). The overrun was determined as the foam volume expressed over the initial protein solution volume. The FF, MIL and GLOB, where the globulins dominated the interfacial properties, had the lowest overruns. These values varied from 42 – 75% at 0.1% (w/w) and 200–258 % at 1.0% (w/w) protein. A substantially higher overrun was found for the ALB with values of 307 and 342%.

At 0.1% (w/w) protein, the globulin-dominated fractions (FF, MIL and GLOB) also had much larger air bubble sizes (0.20 – 0.39 mm) than ALB (0.06 mm). Albumins formed higher volumes of foam with smaller air bubbles, which is in line with the initially faster adsorption of ALB compared to FF, MIL and GLOB (Figure 4.4A). The ability to form stiffer interfacial layers by ALB also contributes to a higher foam volume, as the air bubbles are protected against immediate coalescence during foam formation, leading to more and smaller air bubbles, thus higher foam volumes.

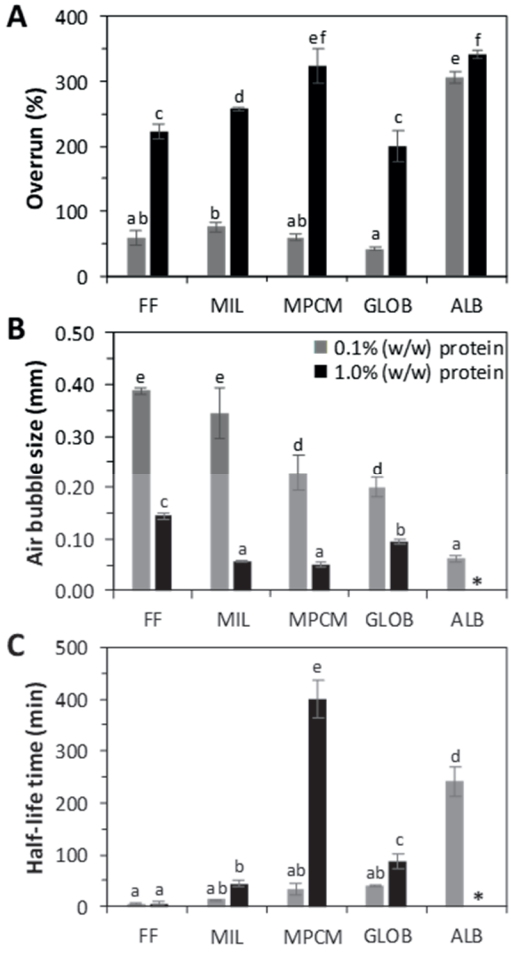

Figure 4.6 (A) *The overrun,* ***(B)*** *average air bubble size directly after foam formation,* ***(C)*** *volume half-life time of foams prepared with FF (fine fraction), MIL (protein mixture), MPCM (coacervate colloids), GLOB (globulin fraction), and ALB (albumin fraction). Foams were created at 0.1% and 1.0% (w/w) protein, shown in grey and black bars, representatively. The averages and standard deviations are the results of at least three replicates. ✳ = 1.0% (w/w) albumin foams were not created for air bubble size and half-life time analysis.*

At 1.0% (w/w) protein, the MIL-stabilised foam had the smallest air bubbles and overrun among the globulin-dominated fractions (FF, MIL and GLOB). MIL is comprised of both albumins and globulins. The albumins in MIL might have contributed to the increased foamability. The FF also contains albumins but has the largest air bubbles. The large starch granules present in this fraction could act as

anti-foaming particles during foam formation. Solid particles may rupture thin films by a mechanism called bridging dewetting (Denkov & Marinova, 2006). Here, the particle is present between two films, and will contact both films upon thinning due to drainage. The particle may dewet the liquid, resulting in the thin film's perforation, and finally, film rupture. As a result, bubbles coalesce, leading to lower foam overrun.

4.3.7.2 Foam stability

The foam stability was determined from the foam half-life time, which is the time required for the foam volume to decay by 50% (Figure 4.6C). The bulk viscosity of the solution can increase foam stability, as higher viscosity might decrease liquid drainage. Therefore, the viscosity of the protein solutions was analysed, which was found to be close to that of water for all samples (shown in Table S4.2 in the Appendix). Therefore, the bulk viscosity is not able to explain the differences in the foaming properties of the different protein fractions.

The FF had the lowest half-life times (below 6 min), which is most likely due to destabilisation by starch granules. Removal of granules results in MIL, with higher foam stability and a half-life time up to 45 min at 1.0% (w/w). GLOB had an even longer half-life time of 87 min at 1.0% (w/w) protein. ALB had substantially higher foam stability with a half-life time of 240 min at 0.1% (w/w), which is probably the result of the formation of smaller air bubbles and stiffer interfacial layers. The smaller and monodisperse distribution of air bubbles reduces the rate of disproportionation, and the stiffer interfacial layers also reduce the rate of disproportionation and the probability of air bubbles coalescence. As shown in previous studies, plant albumins formed stable foams due to their small molecular size and low surface charges, while the highly aggregated globulins resulted in larger air bubbles and weaker interfacial films, thus lower foam stability (Ghumman et al., 2016; Lu et al., 2000; Yang, Kornet, et al., 2022).

Interestingly, the foam stability of MIL did not increase due to the presence of albumins, while the foamability was slightly higher for MIL (in comparison to GLOB). We could argue that the total amount of albumins is too low, only comprising ~13% of the total protein content in MIL (calculated based on protein yield in the current work). The albumins might contribute to the formation of more interfacial area, thus smaller air bubbles and higher foam volumes. However, globulins seem to dictate the mechanical properties of the MIL-stabilised air-water interface, as shown by interfacial rheology (Figure 4.5), which could result in lower foam stability of MIL. With regard to the extent of purification, the FF-, MIL- and GLOB-stabilised foams showed similar foamability. It seems that no or mild purification is sufficient to obtain a foaming ingredient with good foamability. However, more extensive purification does result in higher foam stability. Besides, the side stream of the extensive process (ALB) possesses superior foaming properties. It is worth mentioning that the foaming properties of the ALB were nearly as good as whey protein isolate-stabilised foams, which had a foam half-life time of 258 min (Yang et al., 2021), while ALB had one of 240 min at a similar protein concentration and system conditions (method of foam formation and dissolution buffer).

4.3.7.3 Foaming properties of protein colloids

A final sample in this study are the protein colloids (MPCM). At 0.1% (w/w) MPCM showed a foam overrun of 60%, similar to FF, MIL and GLOB (Figure 4.6A). At 1.0% (w/w), the overrun increased vastly to 324%, nearly as high as ALB. As mentioned in earlier sections, we expect the small non-cross-linked proteins to dominate the interfacial properties of MPCM. With this in mind, the absolute amount of surface active non-cross-linked proteins is low at 0.1% (w/w), but increases by tenfold at 1.0% (w/w). This was also reflected in the average air bubble size (Figure 4.6B), which was found to be 0.05 mm, even smaller than air bubbles of 1.0% (w/w) MIL-stabilised foams. The most prominent improvement is the foam stability, with a half-life time of 400 min at 1.0% (w/w). Turning MIL into MPCM resulted in a foam

stability increase of roughly 12 times. The high foam stability could result from the formation of stiff interfacial layers, as shown in interfacial rheology (Figure 4.5). In addition, the colloids could also contribute to the foam stability, as particles can cause pinning in the foam. In this process, the colloids are trapped in the lamellae and plateau borders between the air bubbles. This process can vastly reduce the drainage and increase thin film stability, thus slowing down the coalescence of air bubbles. Such a phenomenon was previously shown for casein particles and dairy protein aggregates (Chen et al., 2017; Dhayal et al., 2015; Rullier et al., 2008). In conclusion, the formation of coacervate colloids is a promising and controlled method to significantly enhance the foaming properties of mung bean proteins.

4.4 Conclusion

In this work, the physical-chemical, interface and foam stabilising properties of five mung bean protein fractions were evaluated. The interfacial properties of the dry fractionated fine fraction (FF), the protein mixture (MIL) and globulin-rich fraction (GLOB) were similar, suggesting that globulins dominated the interfacial films for FF and MIL. Physical-chemical analysis showed large (and aggregated) proteins with high zeta-potential. This could lead to an ineffective surface coverage with weak in-plane protein-protein interactions. As a result, the globulin proteins formed weak and more easily stretchable interfacial layers, leading to low foamability and stability for FF, MIL and GLOB.

The other major protein in mung bean are the albumins (ALB), which are smaller proteins with lower zeta-potential values. More proteins fit on the interface that can also approach each other closer, giving a stiff interfacial film due to strong protein-protein in-plane interactions. The result is an high performance in foaming properties with nearly two times higher foam volumes and five times higher stability compared to GLOB-stabilised foams. The albumins present in FF and MIL slightly increased the foamability compared to GLOB, but their foam stability is

substantially than GLOB. Mild purification yields FF and MIL with the highest protein nativity and also presence of albumins, but these traits were not sufficient to boost their foaming performance. An underlaying reason could be the presence of more impurities in FF and MIL. Further purification into GLOB increases the foam stability, and yields excellent foam stabiliser ALB as a side-stream.

Another promising ingredient are the protein coacervate colloids MPCM, which showed similar foamability, and even higher foam stability than ALB. We expect that the formed coacervate colloids with sizes between 50 and 800 nm can block the lamellae or/and plateau borders between the air bubbles. As a result, the drainage and destabilisation processes are slowed down, leading to extraordinarily high foam stability (> 400 min). Simple coacervation is, relatively simple method to form protein colloids with good foaming properties. In addition, proteins in MPCM were able to form stiff interfacial films, which could be related to more hydrophobic interactions at the interface between the more hydrophobic MPCM. The exact interface and foam stabilising mechanism requires analysis in future studies.

In this work, we have shown the high potential of mung bean proteins as foam stabilisers. The ability to form and stabilise foam is intimately related to the fractionation used, as this affects the protein purity, protein aggregated state and protein composition. Exploring the different mild and sustainable protein fractionation routes to obtain protein ingredients with useful functional properties, can contribute to the creation of plant-based alternatives, thereby contributing to the current plant protein transition.

References

Anwar, F., Latif, S., Przybylski, R., Sultana, B., & Ashraf, M. (2007). Chemical composition and antioxidant activity of seeds of different cultivars of mungbean. *Journal of Food Science*, *72*(7), 503–510.

Barać, M. B., Pešić, M. B., Stanojević, S. P., Kostić, A. Z., & Čabrilo, S. B. (2015). Techno-functional properties of pea (Pisum sativum) protein isolates-a review. *Acta Periodica Technologica*, *46*, 1–18.

Bock, A., Steinhäuser, U., & Drusch, S. (2021). Partitioning Behavior and Interfacial Activity of Phenolic Acid Derivatives and their Impact on β-Lactoglobulin at the Oil-Water Interface. *Food Biophysics*, *16*, 191–202.

Brishti, F. H., Zarei, M., Muhammad, S. K. S., Ismail-Fitry, M. R., Shukri, R., & Saari, N. (2017). Evaluation of the functional properties of mung bean protein isolate for development of textured vegetable protein. *International Food Research Journal*, *24*(4), 1595–1605.

Chen, M., Sala, G., Meinders, M. B. J., van Valenberg, H. J. F., van der Linden, E., & Sagis, L. M. C. (2017). Interfacial properties, thin film stability and foam stability of casein micelle dispersions. *Colloids and Surfaces B: Biointerfaces*, *149*, 56–63.

Chéreau, D., Videcoq, P., Ruffieux, C., Pichon, L., Motte, J. C., Belaid, S., Ventureira, J., & Lopez, M. (2016). Combination of existing and alternative technologies to promote oilseeds and pulses proteins in food applications. *OCL - Oilseeds and Fats, Crops and Lipids*, *41*(1).

Chua, J. Y., & Liu, S. Q. (2019). Soy whey: More than just wastewater from tofu and soy protein isolate industry. *Trends in Food Science and Technology*, *91*, 24–32.

Denkov, N. D., & Marinova, K. G. (2006). Antifoam effects of solid particles, oil drops and oil–solid compounds in aqueous foams. In *Colloidal Particles at Liquid Interfaces* (pp. 383–444).

Dhayal, S. K., Delahaije, R. J. B. M., de Vries, R. J., Gruppen, H., & Wierenga, P. A. (2015). Enzymatic cross-linking of α-lactalbumin to produce nanoparticles with increased foam stability. *Soft Matter*, *11*(40), 7888–7898.

Du, M., Xie, J., Gong, B., Xu, X., Tang, W., Li, X., Li, C., & Xie, M. (2018). Extraction, physicochemical characteristics and functional properties of Mung bean protein. *Food Hydrocolloids*, *76*, 131–140.

Ewoldt, R. H., Hosoi, A. E., & McKinley, G. H. (2007). New measures for characterizing nonlinear viscoelasticity in large amplitude oscillatory shear. *Journal of Rheology*, *52*(6), 1427–1458.

Ganesan, K., & Xu, B. (2018). A critical review on phytochemical profile and health promoting effects of mung bean (Vigna radiata). *Food Science and Human Wellness*, *7*(1), 11–33.

Geerts, M. E. J., Nikiforidis, C. V., van der Goot, A. J., & van der Padt, A. (2017). Protein nativity explains emulsifying properties of aqueous extracted protein components from yellow pea. *Food Structure*, *14*, 104–111.

Ghumman, A., Kaur, A., & Singh, N. (2016). Functionality and digestibility of albumins and globulins from lentil and horse gram and their effect on starch rheology. *Food Hydrocolloids*, *61*, 843–850.

Gonzalez-Perez, S., & Vereijken, J. M. (2007). Sunflower proteins: overview of their physicochemical, structural and functional properties. *Journal of the Science of Food and Agriculture*, *87*, 2173–2191.

González-Pérez, S., Vereijken, J. M., Van Koningsveld, G. A., Gruppen, H., & Voragen, A. G. J. (2005). Formation and stability of foams made with sunflower (Helianthus annuus) proteins. *Journal of Agricultural and Food Chemistry*, *53*(16), 6469–6476.

Gonzalez-Perez, S., Vereijken, J. M., van Koningsveld, G. A., Gruppen, H., & Voragen, A. G. J. (2005). Physicochemical Properties of 2S albumins and the corresponding protein isolate from Sunflower (Helianthus annuus). *Food Chemistry and Toxicology*, *70*(1), C98–C103.

He, Q., Zhang, Y., Lu, G., Miller, R., Möhwald, H., & Li, J. (2008). Dynamic adsorption and characterization of phospholipid and mixed phospholipid/protein layers at liquid/liquid interfaces. *Advances in Colloid and Interface Science*, *140*(2), 67–76.

Hinderink, E. B. A., Sagis, L., Schroën, K., & Berton-Carabin, C. C. (2020). Behavior of plant-dairy protein blends at air-water and oil-water interfaces. *Colloids and Surfaces B: Biointerfaces*, *192*, 111015.

Hoover, R., Li, Y. X., Hynes, G., & Senanayake, N. (1997). Physicochemical characterization of mung bean starch. *Food Hydrocolloids*, *11*(4), 401–408.

Inthavong, W., Chassenieux, C., & Nicolai, T. (2019). Viscosity of mixtures of protein aggregates with different sizes and morphologies. *Soft Matter*, *15*(23), 4682–4688.

Karaca, O. B., Güven, M., Yasar, K., Kaya, S., & Kahyaoglu, T. (2009). The functional, rheological and sensory characteristics of ice creams with various fat replacers. *International Journal of Dairy Technology*, *62*(1), 93–99.

Klafter, J., & Shlesinger, M. F. (1986). On the Relationship among Three Theories of Relaxation in Disordered. *Proceedings of the National Academy of Sciences of the United States of America*, *83*(4), 848–851.

Kornet, C., Venema, P., Nijsse, J., van der Linden, E., van der Goot, A. J., & Meinders, M. (2020). Yellow pea aqueous fractionation increases the specific volume fraction and viscosity of its dispersions. *Food Hydrocolloids*, *99*, 105332.

Kornet, R., Yang, J., Venema, P., van der Linden, E., & Sagis, L. (2022). Optimizing pea protein fractionation to yield protein fractions with a high foaming and emulsifying capacity. *Food Hydrocolloids*, *126*, 107456.

Kudre, T. G., Benjakul, S., & Kishimura, H. (2013). Comparative study on chemical compositions and properties of protein isolates from mung bean, black bean and bambara groundnut. *Journal of the Science of Food and Agriculture*, *93*(10), 2429–2436.

Lam, A. C. Y., Can Karaca, A., Tyler, R. T., & Nickerson, M. T. (2018). Pea protein isolates: Structure, extraction, and functionality. *Food Reviews International*, *34*(2), 126–147.

Lie-Piang, A., Braconi, N., Boom, R. M., & van der Padt, A. (2021). Less refined ingredients have lower environmental impact – A life cycle assessment of protein-rich ingredients from oil- and starch-bearing crops. *Journal of Cleaner Production*, *292*, 126046.

Liu, H., Liu, H., Yan, L., Cheng, X., & Kang, Y. (2015). Functional properties of 8S globulin fractions from 15 mung bean (Vigna radiata (L.) Wilczek) cultivars. *International Journal of Food Science and Technology*, *50*(5), 1206–1214.

Loveday, S. M. (2020). Plant protein ingredients with food functionality potential. *Nutrition Bulletin*, *45*(3), 321–327.

Lu, B. Y., Quillien, L., & Popineau, Y. (2000). Foaming and emulsifying properties of pea albumin fractions and partial characterisation of surface-active components. *Journal of the Science of Food and Agriculture*, *80*(13), 1964–1972.

Lucassen, J., & Van Den Tempel, M. (1972). Dynamic measurements of dilational properties of a liquid interface. *Chemical Engineering Science*, *27*(6), 1283–1291.

Mariotti, F., Tomé, D., & Mirand, P. P. (2008). Converting nitrogen into protein - Beyond 6.25 and Jones' factors. *Critical Reviews in Food Science and Nutrition*, *48*(2), 177–184.

Mendoza, E. M. T., Adachi, M., Bernardo, A. E. N., & Utsumi, S. (2001). Mungbean [Vigna radiata (L.) Wilczek] globulins: Purification and characterization. *Journal of Agricultural and Food Chemistry*, *49*(3), 1552–1558.

Möller, A. C., van der Padt, A., & van der Goot, A. J. (2021). From raw material to mildly refined ingredient – Linking structure to composition to understand fractionation processes. *Journal of Food Engineering*, *291*.

Mubarak, A. E. (2005). Nutritional composition and antinutritional factors of mung bean seeds (Phaseolus aureus) as affected by some home traditional processes. *Food Chemistry*, *89*(4), 489–495.

Ntone, E., Wesel, T. Van, Sagis, L. M. C., Meinders, M., Bitter, J. H., & Nikiforidis, C. V. (2021). Adsorption of rapeseed proteins at oil / water interfaces. Janus-like napins dominate the interface. *Journal of Colloid And Interface Science*, *583*, 459–469.

Osborne, T. B. (1924). The vegetable proteins. In *Longmans green and co*.

Pelgrom, P. J. M., Boom, R. M., & Schutyser, M. A. I. (2014). Functional analysis of mildly refined fractions from yellow pea. *Food Hydrocolloids*, *44*, 12–22.

Pernollet, J. C. (1978). Protein bodies of seeds: Ultrastructure, biochemistry, biosynthesis and degradation. *Phytochemistry*, *17*(9), 1473–1480.

Rühs, P. A., Affolter, C., Windhab, E. J., & Fischer, P. (2013). Shear and dilatational linear and nonlinear subphase controlled interfacial rheology of β-lactoglobulin fibrils and their derivatives. *Journal of Rheology*, *57*(3), 1003–1022.

Rullier, B., Axelos, M. a V, Langevin, D., & Novales, B. (2009). β-Lactoglobulin aggregates in foam films: Correlation between foam films and foaming properties. *Journal of Colloid and Interface Science*, *336*(2), 750–755.

Rullier, B., Novales, B., & Axelos, M. A. V. (2008). Effect of protein aggregates on foaming properties of β-lactoglobulin. *Colloids and Surfaces A: Physicochemical and Engineering Aspects*, *330*(2–3), 96–102.

Sagis, L. M. C., Liu, B., Li, Y., Essers, J., Yang, J., Moghimikheirabadi, A., Hinderink, E., Berton-Carabin, C., & Schroen, K. (2019). Dynamic heterogeneity in complex interfaces of soft interface-dominated materials. *Scientific Reports*, *9*(1), 1–12.

Sağlam, D., Venema, P., De Vries, R., & Van Der Linden, E. (2013). The influence of pH and ionic strength on the swelling of dense protein particles. *Soft Matter*, *9*(18), 4598–4606.

Sandoval-Castilla, O., Lobato-Calleros, C., Aguirre-Mandujano, E., & Vernon-Carter, E. J. (2004). Microstructure and texture of yogurt as influenced by fat replacers. *International Dairy Journal*, *14*(2), 151–159.

Shewan, H. M., & Stokes, J. R. (2013). Review of techniques to manufacture micro-hydrogel particles for the food industry and their applications. *Journal of Food Engineering*, *119*(4), 781–792.

Souza, P. F. N. (2020). The forgotten 2S albumin proteins: Importance, structure, and biotechnological application in agriculture and human health. *International Journal of Biological Macromolecules*, *164*, 4638–4649.

Tamayo Tenorio, A., Kyriakopoulou, K. E., Suarez-Garcia, E., van den Berg, C., & van der Goot, A. J. (2018). Understanding differences in protein fractionation from conventional crops, and herbaceous and aquatic biomass - Consequences for industrial use. *Trends in Food Science and Technology*, *71*(November 2017), 235–245.

Tang, C. H., & Sun, X. (2010). Physicochemical and structural properties of 8S and/or 11S globulins from mungbean [Vigna radiata (L.) Wilczek] with various polypeptide constituents. *Journal of Agricultural and Food Chemistry*, *58*(10), 6395–6402.

Watts, C., & Davies, E. (1969). Non-Symmetrical Dielectric Relaxation Behaviour Arising from a Simple Empirical Decay Function. *Transactions of the Faraday Society*, *66*(1), 80–85.

Xia, W., Botma, T., Sagis, L. M. C., & Yang, J. (2022). Selective proteolysis of β-conglycinin as a tool to increase air-water interface and foam stabilising properties of soy proteins. *Food Hydrocolloids*, *130*, 107726.

Yang, J., de Wit, A., Diedericks, C. F., Venema, P., van der Linden, E., & Sagis, L. M. C. (2022). Foaming and emulsifying properties of extensively and mildly extracted Bambara groundnut proteins: a comparison of legumin, vicilin and albumin protein. *Food Hydrocolloids*, *123*, 107190.

Yang, J., Kornet, R., Diedericks, C. F., Yang, Q., Berton-Carabin, C. C., Nikiforidis, C. V., Venema, P., van der Linden, E., & Sagis, L. M. C. (2022). Rethinking plant protein extraction: albumin — from side stream to an excellent foaming ingredient. *Food Structure*, *31*, 100254.

Yang, J., Lamochi Roozalipour, S. P., Berton-Carabin, C. C., Nikiforidis, C. V., van der Linden, E., & Sagis, L. M. C. (2021). Air-water interfacial and foaming properties of whey protein - sinapic acid mixtures. *Food Hydrocolloids*, *112*, 106467.

Yang, J., Thielen, I., Berton-Carabin, C. C., van der Linden, E., & Sagis, L. M. C. (2020). Nonlinear interfacial rheology and atomic force microscopy of air-water interfaces stabilized by whey protein beads and their constituents. *Food Hydrocolloids*, *101*, 105466.

Yi-Shen, Z., Shuai, S., & Fitzgerald, R. (2018). Mung bean proteins and peptides: Nutritional, functional and bioactive properties. *Food and Nutrition Research*, *62*, 1–11.

Zhang, Y., Chang, Z., Luo, W., Gu, S., Li, W., & An, J. (2015). Effect of starch particles on foam stability and dilational viscoelasticity of aqueous-foam. *Chinese Journal of Chemical Engineering*, *23*(1), 276–280.

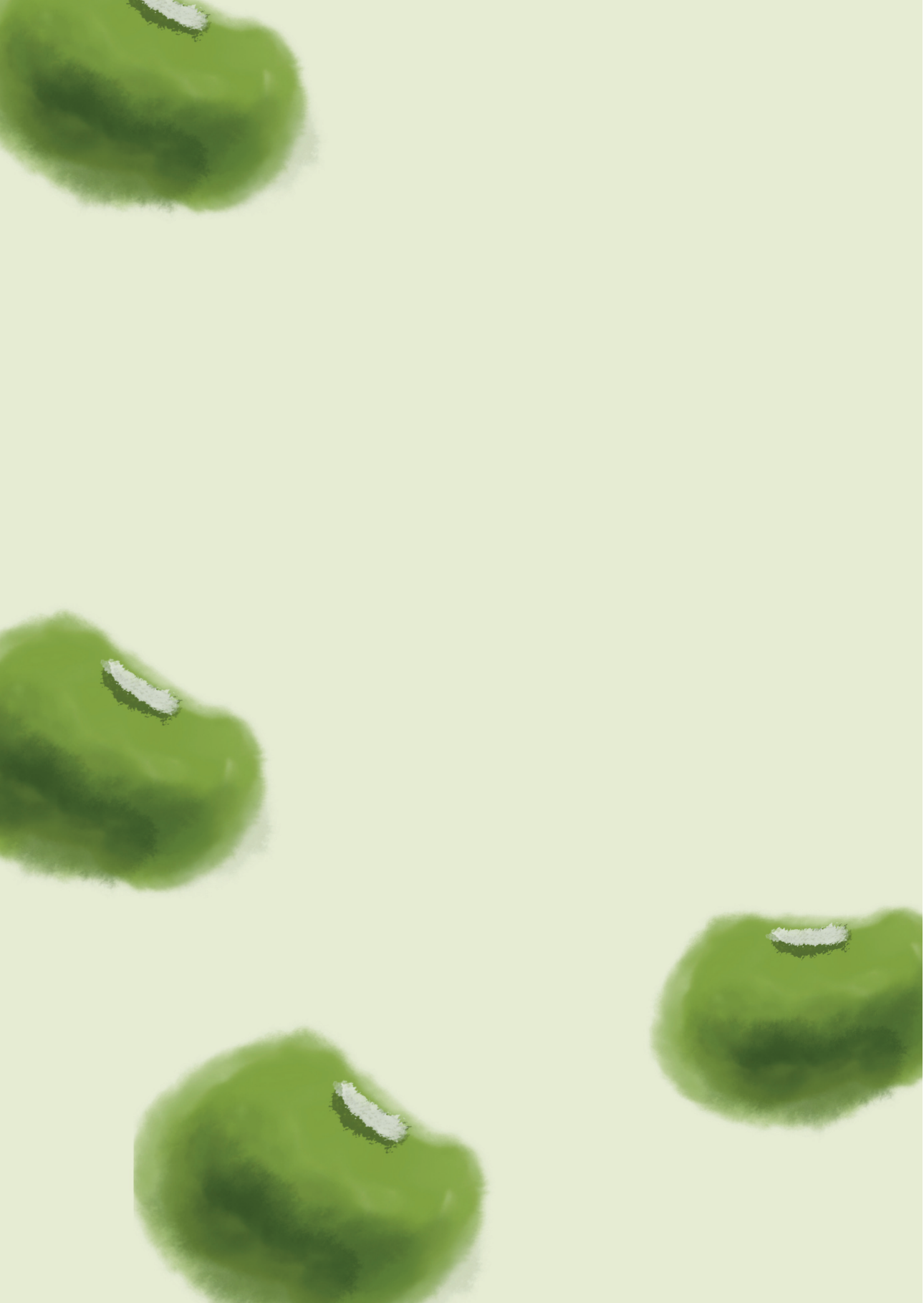

5

Mung bean protein colloids mixtures and fractions - a novel and excellent foam stabiliser

This chapter has been submitted as:

Yang, Q., Yang, J.*, Waterink, B., Sagis, L. M. C., de Vries, R. & Venema, P., Mung bean protein colloids mixtures and their fractions - a novel and excellent foam stabiliser*

(the authors have contributed equally to this work)*

Abstract

Protein aggregates are known to enhance foam stability by either increasing the thin film viscosity or by blocking the lamellae of a foam. In a previous study we observed that the mung bean protein colloids mixture (MPCM) was a promising foam stabiliser. However, the stabilisation mechanism was not clearly identified. Therefore, several mung bean protein fractions from the MPCM were studied for their contribution for creating a stable foam with a high overrun. The MPCM were produced by heating the protein coacervates that were formed by liquid-liquid phase separation. Three different mung bean protein fractions were included in this study. 1) The fraction containing only the protein colloids (COL). 2) The fraction containing only the proteins that are present in the continuous phase of the MPCM (SUP) and 3) a protein fraction that was obtained by a mild purification of the mung bean flour (MIL). The foam stabilising properties of the three protein fractions were studied by measuring the adsorption rate, interfacial rheology and surface microstructure. Also, the foam capacity, foam stability and air bubble size were measured. It was found that the highest foam capacity was observed for the SUP fraction by generating stiffer interfaces, in addition, it also brought high foam stability to MPCM. The other factor resulted in a long lasting MPCM foam is COL fraction. The COL fraction was found to form a viscoelastic thin film between air bubbles, thereby decreasing the drainage and destabilisation rate of the foam. In brief, SUP and COL fractions co-operate in the formation of highly stable MPCM foam leading to a promising plant-derived candidate for producing stable foams in food products.

5.1 Introduction

As an alternative for animal-based proteins, plant-based proteins have been given considerable attention in terms of their functionalities. Besides currently prevalent topic meat analogue, plant derived proteins can be considered as a replacement for dairy or egg proteins as well. Among these alternatives, mung bean is an upcoming and promising plant-based protein source (Wang et al., 2022; M. Yang et al., 2021). The main reasons for this rising interest are sustainability and well-balanced amino acid (Hou et al., 2019) of mung bean proteins. In terms of sustainability, mung bean is allowed to culture with less water usage and without fertilizers. In addition, it is widely cultured not only in traditional mung bean consuming countries (Asia), but also Southern Europe, and Northern American.

A key functionality for which people looking to replace animal proteins is foaming. The main focus is on soybean and pea proteins, unfortunately, both of them showed barely satisfied interfacial behaviour as compared to animal-derived proteins. The foaming capacity of these plant proteins were observed lower (Brishti et al., 2017; Kornet, Yang, et al., 2022; Ma et al., 2011; Xia et al., 2022) than whey protein isolates in many cases (Nicorescu et al., 2009; J. Yang, R. Kornet, et al., 2022). As for mung bean proteins, rather limited investigations have been conducted on their interfacial stabilising properties, they were found present better foam capacity with a lower stability than soybean (Brishti et al., 2017; Liu et al., 2022). However, the foaming stabilisation mechanism behind mung bean proteins is still unknown.

It has been shown that mild processes can produce plant protein ingredients with altered functionalities (Assatory et al., 2019; Kornet, Yang, et al., 2022; Pelgrom, Boom, et al., 2015a; Jack Yang, Iris Faber, et al., 2021; Q. Yang et al., 2022). Nevertheless, extensive processing not always led to a worse functional behaviour. Heating induced colloids and aggregates were found able to increase the stability

of protein stabilised foams. So far, majority of these research focus on thermal aggregation generated by animal-based globular proteins due to their high solubility and presence forms of monomers and dimers in dispersions (Nicolai, 2016). Aggregates of whey protein isolates (Nicorescu et al., 2009; Nicorescu et al., 2010; Schmitt et al., 2007) , whey protein microgels (Nicolai, 2016), casein micelle (Chen et al., 2018), and β-lactoglobulins (Rullier et al., 2009, 2010; Rullier et al., 2008) were extensively studied at both acidic and neutral pH, they were proved to efficiently enhance the foam stability only with the company of sufficient amount of non-aggregated proteins. Based on these studies, aggregates have been revealed enhance foam stability in two ways: either by increasing the viscosity of the thin film or by acting as blockage in the lamellae or plateau borders, resulting in slowing down the drainage rate and leading to more stable foam (Chen et al., 2018; Rullier et al., 2009; Rullier et al., 2008). Unfortunately, the implementation of these mechanisms on plant-based aggregates is still limited.

Soybean protein is a typical plant-derived protein which has been extensively studied in terms of its functionalities. By heating soybean protein isolates at various temperatures from 80 ˚C to 100 ˚C, Guo et al. (2015) produced soluble aggregates of medium-size (670 to 1000 kDa) and large-size (> 1000 kDa). Medium-size aggregates appeared to be essential to enhance foaming capacity due to a supportive effect provided by their loose structure, while large proportion (> 50%) of large-size aggregates presented would form films with increased thickness, leading to promoted foaming stability. This improvement in foaming stability could be resulted in by the thin film stabilisation mechanism mentioned before.

Except for aggregates size, the impact of protein composition and processing on aggregates foam stabilising properties has been revealed. Heat-induced pea protein aggregates have been produced to evaluate the influence of heating and drying on their foaming properties at two food systems related pH (J. Yang, H. C. M.

Mocking-Bode, et al., 2022). It was shown that independent of drying methods, the stiffest layers were formed by the pea protein aggregates. Heating induced the surface activity of globulin aggregates, thereby they were hampered to adsorb to interfaces. In the meanwhile, albumins remain soluble and got enriched relatively by globulin aggregation, dominating interface and foaming properties of the heated pea protein stabilised foams. However, these cases still unable to be demonstrated by the stabilisation mechanisms obtained from dairy protein aggregates.

Previously, we produced mung bean protein colloids which are suitable for beverages due to their high internal protein content, low intrinsic viscosity and weak heat-induced gelation behaviour in Chapter 3. Surprisingly, an extraordinary interface behaviour was observed in our previous study as well. The colloidal mung bean protein dispersions formed exceptionally highly stable foams (half-life time around 400 min) with high capacity (overrun around 325%), it is dramatically higher than foam stabilised by pea protein aggregates which showed a half-life time app. 4 min. It would be worthy to mention that, mung bean protein colloids even can generate foams with unexpectedly higher stability than whey protein isolates which presented a half-life time around 260 min (Jack Yang, Sarah P. Lamochi Roozalipour, et al., 2021). However, the reasons resulted in such an excellent foaming behaviour of mung bean protein colloids are still unknown. Since functionality of plant-based proteins are different from source to source, the role of fractions of thermal induced plant protein aggregates in foam stabilisation still needs to be validated for legumes other than yellow pea and soybean. Additionally, exploring the stabilisation mechanism of mung bean protein colloids to develop it as a highly functional plant-derived ingredient would be favoured by food industry.

Hence, to determine the stabilising mechanism of colloids mixtures as well as the role of aggregates and non-aggregates fractions in foam stabilisation, MPCM (mung bean protein colloids mixture) fractions were obtained by fractionated MPCM

solutions in the present study. The interfacial behaviour including adsorption rate, surface oscillatory dilatational rheology and surface microstructure of fractions were investigated. Also, the foam abilities including foam capacity, foam stability and air bubble size were measured, the stabilisation mechanism were revealed by determining the stability curves of fractions and albumin mixtures. We then proved the potential of MPCM to be developed into a sustainable and highly functional plant-protein foaming agent in food systems.

5.2 Materials and methods

5.2.1. Materials

Dry mung bean seeds (Golden Chief, Thailand) were purchased from the online Asian store MyEUShop (Nieuw-Vennep, The Netherlands). All chemicals (Sigma-Aldrich, USA) were used as received. The solutions were prepared in ultrapure water (MilliQ Purelab Ultra, Darmstadt, Germany).

5.2.2 Sample preparation

5.2.2.1 Preparation of mung bean protein colloids

The mung bean protein fine fraction (FF) was obtained by dry fractionation as described earlier (Yang et al., 2022). A 20% wt. suspension was produced by dispersing the FF fraction in 15 mM sodium metabisulfite solution, where the pH of the suspension was adjusted to 8.5 using 1M NaOH. After 1h stirring at room temperature, the suspension was centrifuged at 10,000 g for 30 min to remove starch granules and insolvable fragments and the supernatant was collected. Afterwards, the pH of the supernatant was adjusted to 6.75 to induce the formation of the liquid nearly spherical protein coacervates. The proteins in the coacervates were cross-linked by a heating step at 80˚C for 20 minutes, while stirring to obtain the so-called mung bean protein colloids mixture (MPCM). Subsequently, the MPCM were freeze dried to be used for the present investigations.

5.2.2.2. Fractionation of mung bean proteins and colloids

All samples were prepared based on weight-based protein content (% w/w) in a 20 mM PO_4-buffer, pH 7.0, while stirring for at least 4 hrs at room temperature. Samples were prepared in a protein concentration range from 0.1 to 1.0% (w/w). In order to obtain different fractions, a 1% MPCM suspension was prepared and centrifuged at 20000g for 30min. The supernatant obtained from the first centrifugation step was obtained as a sample and referred to as supernatant (SUP). The buffer was added to resuspend the pellet and the centrifugation and washing step was repeated three times to finally obtain the purified pellet (COL). Additionally, a mildly purified protein mixture (MIL) was obtained by dispersing FF in water followed by a centrifugation step to remove the starch granules and cellular debris. More details were presented in Figure 5.1.

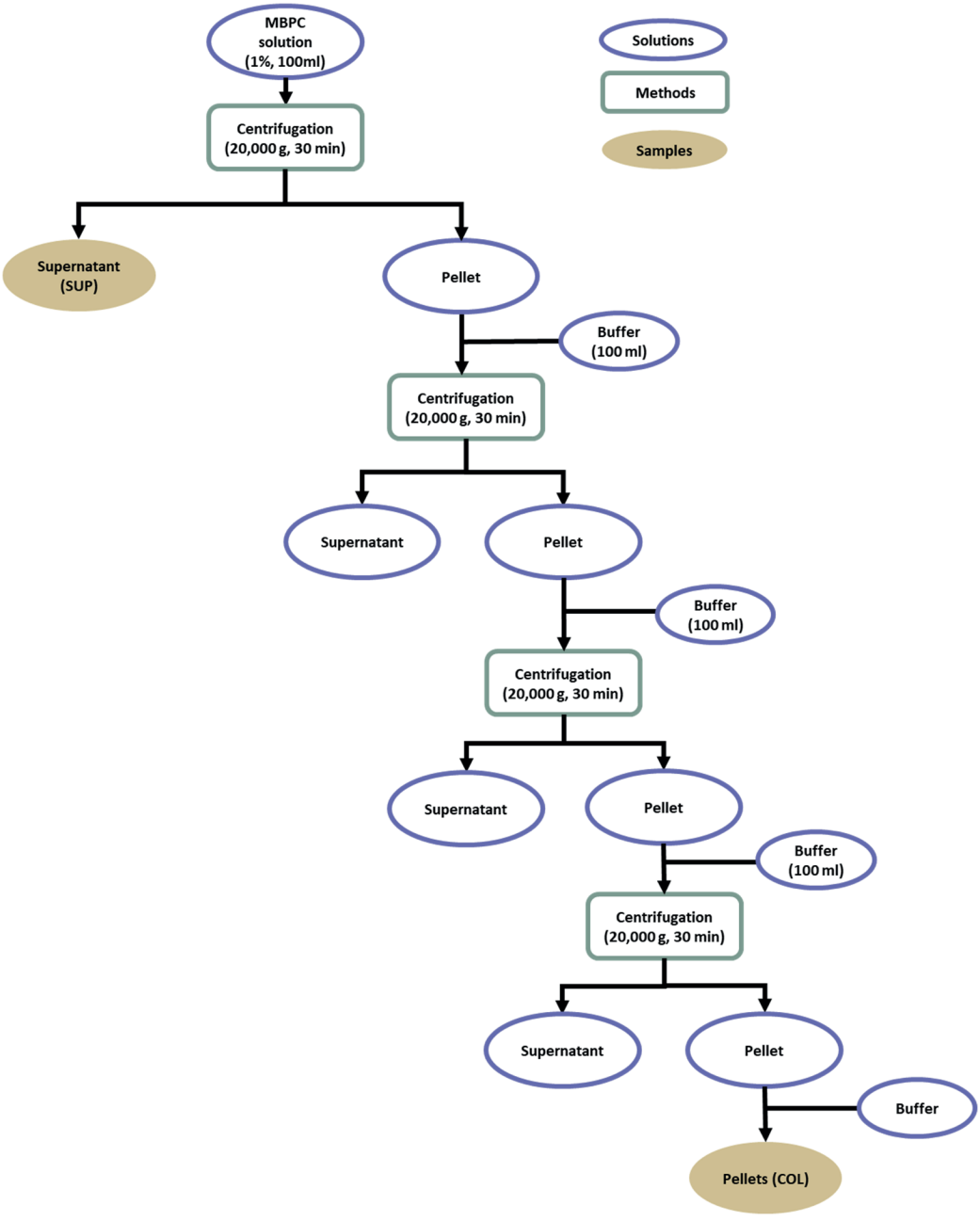

Figure 5.1 *Schematic overview of the sample fractionation. Purple circles represent the different solutions during fractionation, the green boxes represent methods used and the yellow circles indicating the final samples for analysis.*

5.2.3 Size exclusion chromatography

Size exclusion chromatography (SEC) was carried out by an an ÄKTA pure 25 system (Cytiva, Marlborough, MA, USA) equipped with Superdex® 200 10/300 GL column. Protein solutions with protein concentrations of 0.1% (w/w) were centrifuged at 15000 g for 10 min. Subsequently, 50 µL supernatant was injected into the system which has sodium phosphate buffer (20 mM, pH 7.0) containing 50 mM NaCl as the eluent. The flow rate was set at 0.5 mL/min and the elution was recorded with UV absorbance at 280 nm.

5.2.4 Particle size distribution

The particle size distribution of MIL, SUP and COL were analysed using dynamic light scattering (Zetasizer Nano ZS, Malvern Instruments Ltd., United Kingdom). Dispersions with 0.1 % (w/w) protein were injected in a DTS1070 Zetasizer cell. Prior to analysis, the cell containing sample was equilibrated for 2 min at 20 °C, followed by a size distribution measurement, where 12 scans were performed in automatic mode, of which an average was calculated. For MPCM samples, particle size distributions were measured using static light scattering (Mastersizer 2000, Malvern instruments, United Kingdom), setting the particle refractive index to 1.48. All measurements were at least performed in triplicate.

5.2.5 Protein surface hydrophobicity

The protein surface hydrophobicity was determined using 8-anilino-1-napthalenesulfonic acid ammonium salt (ANSA) as a fluorescence agent. MPCM fractions are dissolved in a phosphate buffer at protein concentrations varying from 0.005 – 0.04 % (w/w). Protein dispersions were loaded in double-sided transparent plastic cuvettes, and 25 µL of 8 mM ANSA solution were added in each cuvette. Next, the samples were mixed using a vortex mixer and incubated for 1 hr in dark environment to prevent deterioration of the ANSA reagent. After incubation, the fluorescence of samples was determined by an LS 50B luminescence spectrometer

(Perkin Elmer, USA), the excitation wavelength was 390 nm and the emission wavelength was set at 470 nm. The buffer solution was used as a blank. The initial slope of the fluorescence intensity versus protein concentration was used as measure of surface hydrophobicity (H_0). The relative surface hydrophobicity was calculated to compare hydrophobicity among the samples. All samples were studied in triplicate.

5.2.6 Surface tension and surface dilatational properties

The mechanical properties of the air-water interface were studied by performing surface dilatational rheology in a drop tensiometer PAT-1M (Sinterface Technologies, Germany). A 0.1% (w/w) protein solution was used to form a hanging droplet with a surface area of 20 mm^2 at the tip of a hollow needle. The surface tension was calculated by fitting the Young-Laplace equation to the shape of the droplet. Three types of oscillatory deformation measurements were performed, and prior to the start of each of these analyses, the droplets were equilibrated for 3 hrs. Frequency sweeps were performed at a constant amplitude of 3%, and a frequency series, which increased from 0.002 to 0.1 Hz. Amplitude sweeps were performed at a constant frequency of 0.02 Hz, and an amplitude series, which increased from 3 to 30% deformation amplitude. In these oscillatory deformations, five cycles were performed for each frequency or amplitude step. The relaxation behaviour of the interface was also studied by performing step-dilations, where the interface was subjected to a 10% rapid compression or extension (2s step time) of the area. All measurements were performed at least in triplicate at 20 °C.

5.2.7 Rheology data analysis

The raw data of the amplitude sweeps were transformed into Lissajous plots by plotting the surface stress (γ-γ_0) against the deformation ((A-A_0)/A_0). The γ and A are the surface tension and area of the deformed interface, and γ_0 and A_0 are the

surface tension and area of the non-deformed interface. The plots were generated using the middle three of five oscillations.

5.2.8 Preparation of Langmuir-Blodgett films

Langmuir-Blodgett films of the interfacial films were created using a Langmuir trough (243 mm^2 Langmuir-Blodgett Trough KN 2002, KSV NIMA/Biolin Scientific Oy, Finland). First, the trough was filled with the subphase, a 20 mM PO_4 buffer at pH 7.0. The surface was carefully cleaned using a vacuum pump. Afterwards, 200 µL of 0.01% protein (w/w) solution of MIL and MPCM was injected at the bottom of the trough using a gas-tight syringe. The proteins were allowed to adsorb at the interface for 10800 s, while the surface pressure was monitored using a Wilhelmy plate (platinum, perimeter 20 mm, height 10 mm). After equilibration, the interface was compressed by Teflon barriers at a moving speed of 5 mm/min. The interfacial films were compressed to a target surface pressure 15 or 25 mN/m, and the protein film was deposited on a freshly cleaved mica substrate (Highest Grade V1 Mica, Ted Pella, USA) using the Langmuir-Blodgett deposition at a withdraw speed of 1 mm/min. The Langmuir-Blodgett films were dried for two days and were further analysed using atomic force microscopy. All films were produced in duplicate at 20 °C.

5.2.9 Determination of the interfacial structure by AFM

Atomic force microscopy (AFM) was applied to study the topography of the interfacial microstructure of Langmuir-Blodgett films. The AFM (Multimode 8-HR, Bruker, USA) was equipped with a Scanasyst-air model non-conductive pyramidal silicon nitride probe (Bruker, USA) with a normal spring constant of 0.40 mN/m. The films were recorded in tapping mode at a lateral frequency of 0.977 Hz, and an area of 2x2 μm^2 were analysed with a lateral resolution of 512x512 $pixels^2$. All films were recorded on at least two locations to ensure good representativeness, and the images were analysed using Nanoscope Analysis software v1.5 (Bruker, USA).

5.2.10 Determination of foam properties

5.2.10.1 Ability and stability of foams created by whipping

Foams were created by whipping 15 mL of 0.1 – 1.0% protein (w/w) solutions with an overhead stirrer equipped with an aerolatte foam head at 2,000 rpm for 2 min in a plastic container (34 mm diameter). The foam ability was determined by marking the bottom and upper level of the foam, of which the height was measured and recalculated into the maximum foam volume using the radius of the container. From this, the overrun was calculated by equation 1.

$$Foam\ overrun\ (\%) = \frac{Maximum\ foam\ volume\ (mL)}{Initial\ solution\ volume\ (15\ mL)}\ x\ 100\ \% \quad (5.1)$$

After determining the maximum foam volume, the foam sample was transferred into a 50 mL volumetric glass cylinder. The liquid and foam height of the sample was determined from 1 min after foam formation, until the foam volume decayed by half. All measurements were performed in triplicate at 20 °C.

5.2.10.2 Stability of foams created by sparging

Sparged foams were created in a Foam scan foaming device (Tecles IT-concept, France). A glass cylinder (60 mm diameter) was filled with 40 ml of sample and gas was sparged through a metal frit (27 µm pore size, 100 µm distance between centres of pores, square lattice) at a flow rate of 400 mL/min. The generated foam in the tube was studied by image analysis to obtain a foam volume, and the foams were sparged to a volume of 400 mL. Afterwards, the foam volume was monitored until a 50% decay of volume, which is known as the foam volume half-life time. A second camera recorded a detailed image of the air bubbles, which was analysed using a custom Matlab script with a DIPlip and DIPimage analysis software package (TU Delft, NL) to determine an average bubble size. All experiments were at least performed in duplicate at 20 °C.

5.3 Results and discussion

5.3.1 Characterization of the different protein fractions

In Chapter 4, we have showed that MPCM possess a superior foam capacity and stability. In order to reveal the mechanism behind, MPCM were fractionated into SUP and COL by centrifugation, several washing steps and redispersing. The protein content and dry matter content of these fractions were determined. As shown in Table 5.1, the majority of proteins in MPCM ended up in SUP, consequently led to a higher dry matter content.

Table 5.1 *Protein content and dry matter of supernatant and pellets fractionated from mung bean protein colloids solutions.*

	Amount of protein of MPCM in SUP or COL (%)	Amount of dry matter of MPCM in SUP or COL (%)
SUP	67.2 ± 2.3	72.1 ± 0.3
COL	32.8 ± 2.3	27.7 ± 0.5

SEC (size exclusion chromatography) was performed to investigate the protein composition pf different Mung bean fractions. As shown in Figure 5.2, a major peak for legumin was observed around an elution volume of 11 mL, representing proteins with molecular weight of 660 kDa in MIL. Also, several minor peaks for vicilin (around 12 mL, 261 kDa) and albumin (around 14.5 and 16 mL, 113 and 35 kDa, respectively) were observed in MIL, while only vicilin was tracked in SUP. The absence of legumin in SUP suggested that most of them ended up in COL. A similar observation was reported by Kornet, Roozalipour, et al. (2022) and (Lui, Litster, & White, 2007), where most of the vicilin remained in the continuous phase, while most of the legumin (approx. 70%) were found in the coacervates of pea and soy proteins. The SEC result imply that the protein composition in coacervates of legume proteins may dominated by legumins.

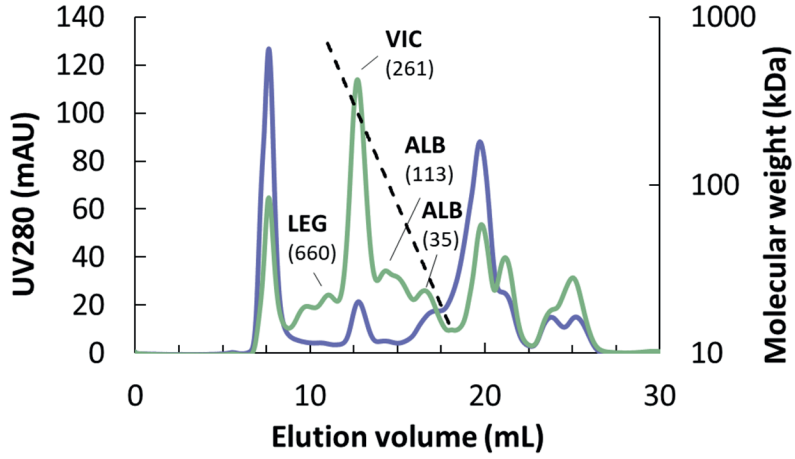

Figure 5.2 *SEC chromatogram of the 280 nm absorbance as a function of eluted volume of MIL (mildly purified protein mixture, green) and SUP (supernatant of MPCM, purple). The number in rackets represent the molecular weight (kDa) of the corresponding peak. The dashed line represents the calibration curve.*

The size distribution results of MPCM fractions and mildly purified MB proteins mixtures (MIL) were obtained from dynamic light scattering and static light scattering (MPCM) and presented in Figure 5.3. MIL sample showed a smallest average diameter around 10 nm attributed to mildly purification. SUP was found have a peak at 30 nm and a shoulder between 50 -700 nm. On another hand, COL showed the largest average diameter around 1000nm while MPCM showed a particle size distribution between SUP and COL as expected. The average size of MPCM is around 150 nm, and a second peak around 100000 nm were observed. These are few number of aggregates can be neglected based on volume distribution.

The protein foam properties are largely impacted by protein surface properties such as hydrophobicity. As an index of the number of hydrophobic groups on the surface of proteins, the relative protein H_0 (surface hydrophobicity) was determined by using ANSA. As shown in Table 5.2, COL seems dominate the H_0 of MPCM since they show a comparable hydrophobicity. Nevertheless, COL showed a relative hydrophobicity higher than SUP, indicating more surface exposed hydrophobic groups of COL. It should be noted that these MPCM fractions showed

significantly higher hydrophobicity values than mildly processed MIL samples. This would be attributed to heating induced structure alteration during protein coacervates crosslink. These heat induced increases in surface hydrophobicity have been reported widely by previous researchers, in terms of soybean proteins (Shen & Tang, 2012; Z. Wang et al., 2014). The other possible reason for this increase in H_0 is the freeze-drying method applied. As shown by Brishti et al. (2020), freeze-drying resulted a higher H_0 of MB proteins than other drying methods. H_0 of freeze-dried MB protein samples are consequently higher than MIL which was mildly extracted and not experienced any drying process yet.

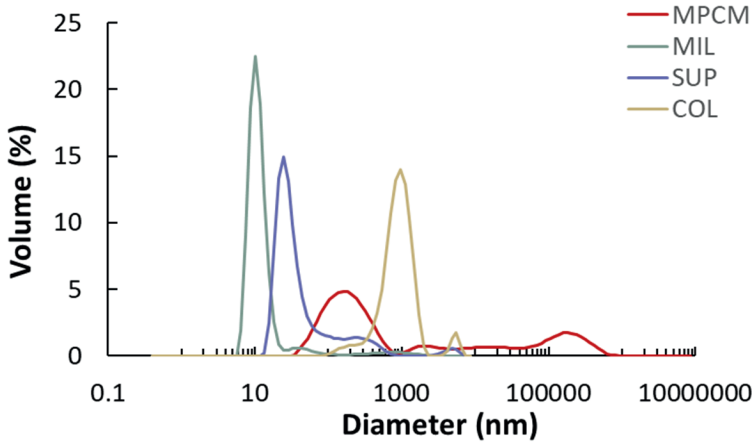

Figure 5.3 *The size distribution of mung bean protein colloids mixtures (MPCM, red), mildly purified protein mixtures (MIL, green), supernatant of MPCM (SUP, purple) and pellets of MPCM (COL, yellow). All measurements were carried out in triplicate.*

Table 5.2 *Relative hydrophobicity of MB protein COL (Pellets) and Sup (Supernatant) fractionated from mung bean protein colloids solutions, and MIL (Mildly purified protein mixtures) obtained from MB fine fraction. The hydrophobicity was calculated based on result of MPCM.*

	Hydrophobicity
MPCM	1.00 ± 0.03
COL	0.96 ± 0.03
SUP	0.62 ± 0.02
MIL	0.24 ± 0.01

5.3.2 Interfacial properties of MB fractions

5.3.2.1 Adsorption behavior

Since foams normally form in a short period (a couple of seconds), the adsorption behaviour of proteins to the interface is an imperative factor to be determined. In Figure 5.4, the highest adsorption rate was presented by MIL, this would be attributed to its smallest particle size as shown in Figure 5.3. Considering to particle size of MPCM is much larger than MIL, MPCM showed an unexpected comparable adsorption behaviour as MIL during the whole process. This could reveal that MPCM are exceedingly surface-active due to exposure of hydrophobic domains. According to previous report, the presence of smaller non-cross-linked particles in whey protein colloids dispersion mainly responsible for ruling interfacial properties (Yang et al., 2020). To investigate the role of these smaller particles in the MPCM suspension, a centrifugation process was carried out to separate smaller particles (SUP) from larger pellets. The interfacial properties of MPCM were found beneficial from both SUP and COL. Smaller particle size of SUP brought a rapid increase in surface pressure in the initial phase (first 30 s) compared to COL, as they were allowing to move agiler toward the interface. After 5 min, when the increase in surface pressure of SUP slowing down, COL started to enter a considerable increasing period. This probably can be linked to its highly hydrophobic surface as shown in Table 5.2. Therefore, we presume that the contribution of SUP in the initial phase and of COL in the later phase, together have a synergy effect on interfacial properties of MPCM. The assumption was further investigated in foam properties tests.

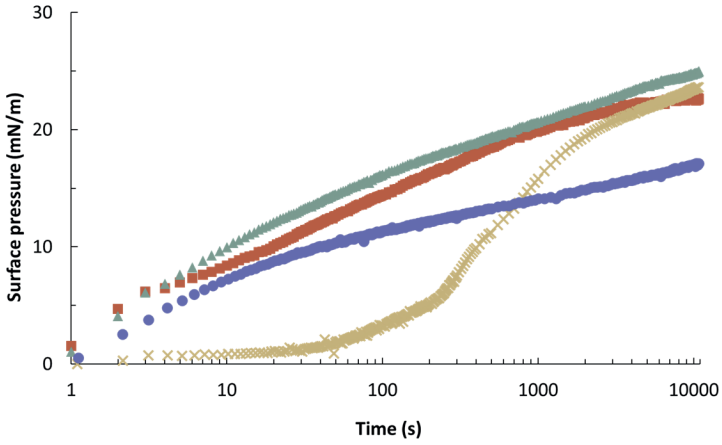

Figure 5.4 *Surface pressure as a function of time of MPCM (colloids, red squares), MIL (mildly purified protein mixture, green triangles), COL (pellets, yellow crosses) and SUP (supernatant, purple circles). All measurements were conducted at least in triplicate.*

5.3.2.2 Surface oscillatory dilatational rheology

Amplitude sweeps

To gain an insight on the stability and strength of the interfacial films upon deformation, amplitude sweeps were performed with an interfacial area range from 3 % - 30% at a constant frequency. MPCM and SUP showed almost identical behaviours upon increasing amplitudes. The Ed' (dilatational elastic moduli) of both samples decreased from 70 to 37 mN/m approximately, whereas COL had a lower modulus ranged between 41 - 29 mN/m. Suggesting stiffer interface microstructures formed by MPCM and SUP and more stretchable layers obtained from COL, therefore, SUP may dominate dilatational behaviour of MPCM. To investigate the influence of processing on MB protein interfacial behaviour, mildly purified protein mixtures MIL was measured as well. The Ed' of MIL was found located between 51 - 29 mN/m, showing a comparable amplitude dependency as MPCM. Hence, the mildly purification process cannot be related to a stiffer or a more stretchable interfacial microstructure.

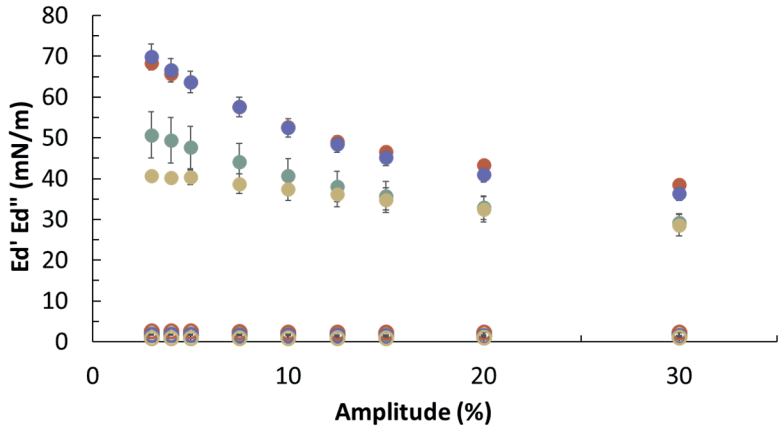

Figure 5.5 *Surface dilatational moduli as a function of deformation amplitude of MPCM (mung bean protein colloids mixture, red), MIL (mildly purified protein mixtures, green), SUP (supernatant, purple) and COL (pellets, yellow). All measurements were conducted in triplicate.*

Disruption of the interfacial microstructure caused by deformation could lead nonlinear viscoelastic behaviours. As shown in Figure 5.5, all surfaces stabilised by MB fractions are in the NLVE (non-linear regime) as Ed' obviously decreased at higher amplitudes. It brings higher-order harmonics into the Fourier spectrum of the stress response. However, the moduli shown in Figure 5.5 are obtained based on the first harmonic of the Fourier spectrum, where nonlinear behaviour are negligible, these transformed values are only dependable if the limited deformations and linear viscoelastic regime applied. To reveal this neglected nonlinear data, a qualitative analysis was conducted, and the results were plotted as Lissajous plots.

Lissajous plots

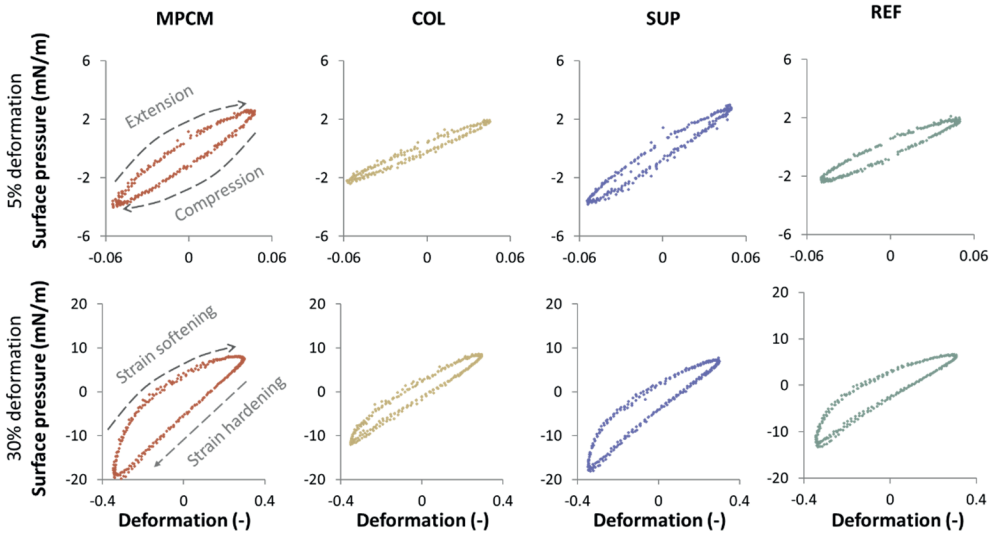

Figure 5.6 *Lissajous plots of deformation versus surface pressure. The plots are obtained from the amplitude sweeps of the mung bean MIL (mildly purified protein mixture, green), MPCM (mung bean protein colloids mixtures, red), COL (MPCM pellets, yellow) and SUP (MPCM supernatants, purple) stabilised interfacial layers. All measurements were conducted at least in triplicate and one representative plot is presented for each sample.*

In order to evaluate nonlinear deformations more accurately, Lissajous plots were plotted in Figure 5.6 as surface pressure over deformation. The movement of Lissajous plots is clockwise, where the interfacial area of the MPCM fractions stabilised interfaces are extended in the upper part of the cycle and are compressed in the lower part of the cycle.

As shown in Figure 5.6, all plots are symmetric at 5% deformation, suggesting almost linear response upon deformation. Only COL showed a narrower plot, which indicates a more elastic response of the COL stabilised interface. Other fractions presented wider ellipse shapes, which indicates more viscous response behaviours and higher energy dissipation upon deformation than COL. SUP and MPCM were found more tilted toward the vertical axis, indicating formation of stiffer interfacial films than MIL and COL. This is in line with the results of amplitude sweeps.

When deformation increased to 30%, except for COL, other samples all showed significant nonlinear behaviour upon deformation as revealed by their asymmetric plots. Relatively fast surface pressure increases were found for MIL, MPCM and SUP at the beginning of the extension phase of the cycle. Subsequently, mild increases in surface pressure were observed. In which intra-cycle strain softening phenomena happened, revealing a gradual disruption of the microstructure. This should be attributed to the interfacial layer dilution. The interfacial is stretched upon extension, and extra proteins are probably cannot be included, therefore, the adsorbed proteins were diluted resulted in softening. Whereas in the compression phase, MIL, MPCM and SUP all presented steep increases in surface pressure upon deformation. The density effect of stabilisers contributes to this phenomenon. It was reported by previous research (Yang et al., 2020) that compression can concentrate stabilisers and generate jammed adsorbed proteins at the interface, led to intra-cycle hardening in compression. The presence of softening in extension and hardening in compression can be considered as a consequence of in-plane interactions between adsorbed proteins.

COL was found show obviously different interfacial behaviour from others. The larger angle it presented with horizontal axis and the less asymmetries suggesting that weak and more stretchable film was stabilised by COL. And the larger width of the plots indicating less energy dissipation upon deformation. This observation was supported by amplitude sweep test as shown in Figure 5.5, where lower moduli of COL than MIL, SUP and MPCM were found. The weak and more stretchable interlayers formed by COL could be a result of its relatively larger particle size, less effective surface coverage was reached, and weaker in-plane interaction was established. Comparing to SUP, COL seems possess less dominance in interfacial behaviour. This is relevant to slower adsorption speed COL showed at interface (as shown in Figure 5.4), thus, the behaviour of MPCM is mainly dependent on SUP in nonlinear phase. Nevertheless, the difference between MPCM and SUP suggesting

that more than one fraction contributed to the interfacial behaviour of MPCM. Therefore, we propose that both SUP and COL contributed to the interfacial properties of MPCM, further investigations were conducted to reveal the cooperation between different fractions.

5.3.3 Interfacial microstructure of MB fractions

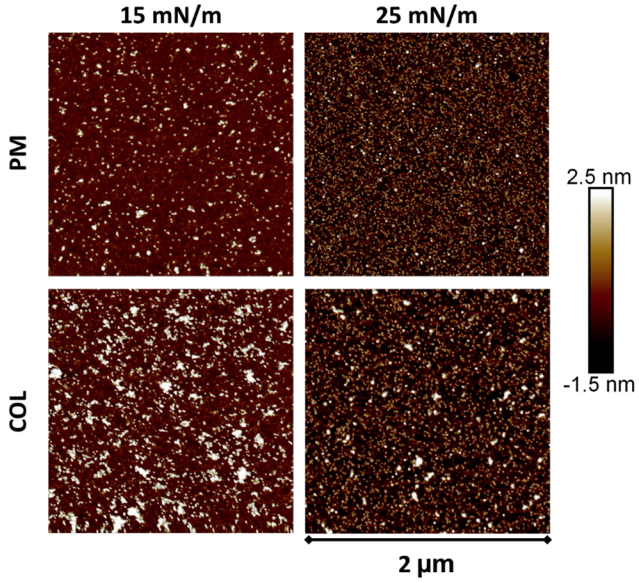

Figure 5.7 *Atomic Force Microscopy (AFM) images of Langmuir-Blodgett films prepared by MIL (mildly purified mung bean protein mixtures) and MPCM (mung bean protein colloids mixture) stabilised air-water interfaces. The surface pressure designates the conditions applied during the film sampling.*

To obtain detailed insights into the interfacial microstructure of MPCM and MIL stabilised interfaces, the topography of these interfaces was examined by atomic force microscopy (AFM). The protein stabilised interfacial layers were transferred onto a solid substrate with assistance of Langmuir-Blodgett (LB) deposition. As shown in Figure 5.7, both MIL and MPCM presented structures with obvious heterogeneity (white dots) at a surface pressure of 15 mN/m, higher density thicker regions were observed in MPCM, indicating more and larger cluster presented in MPCM film. These clusters should be protein clusters considering to heating process applied during MPCM preparation. This finding is in line with previous

report, these clusters were proved to be protein clusters by Sagis et al. (2019). Larger protein clusters presented by MPCM is also a result of particle size, larger sizes it possesses compared to MIL bring more relatively larger clusters at the interface.

With increased surface pressure of 25 mN/m, same phenomenon can be observed for both MIL and MPCM. Upon higher compression, fewer large protein clusters were visible whereas more smaller protein dense regions were found surrounded by thinner regions, suggesting denser films formation. This result can be attributed to stiffness of interface formed by MIL and MPCM, according to J. Yang, R. Kornet, et al. (2022), the protein which can form stiff and cohesive layers can lead to a denser film, due to strong in-plane interactions, proteins can still remain on the interface after compression. It is not a behaviour only has been observed in mung bean proteins, other protein stabilised interfaces show this denser layer after compression as well, for example, pea proteins(Kornet, Yang, et al., 2022), rapeseed proteins (Jack Yang, Iris Faber, et al., 2021), and even animal-based proteins such as whey proteins (Rühs et al., 2013) and bovine serum albumin (Sah & Kundu, 2017).

5.3.4 Foam properties

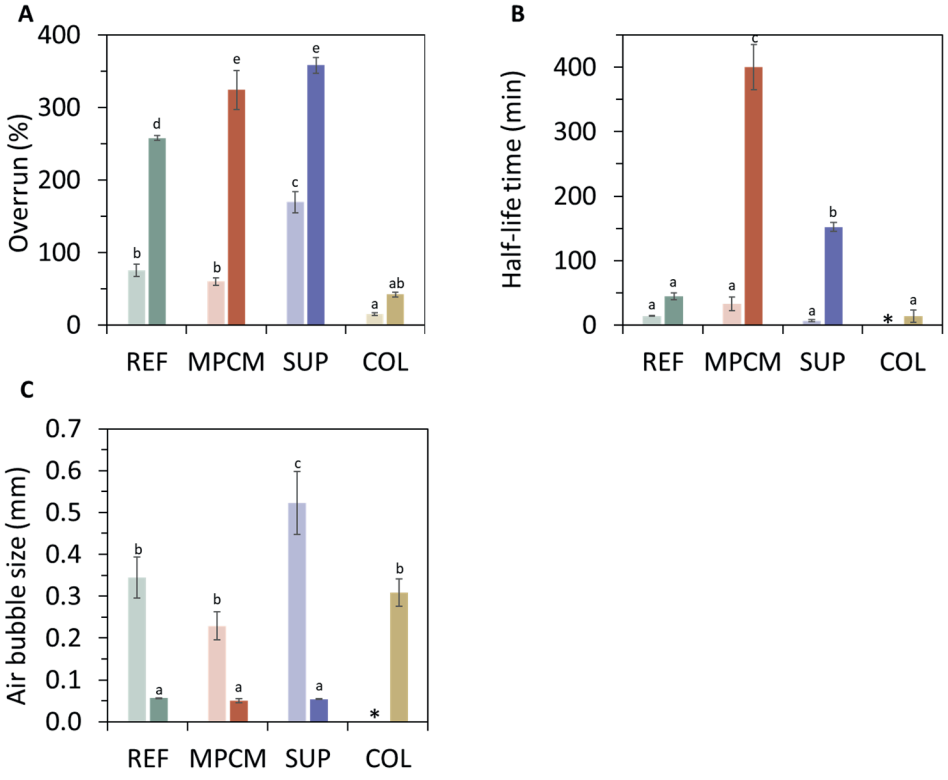

Figure 5.8 *The* ***(A)*** *overrun,* ***(B)*** *half-life time and* ***(C)*** *air bubble size ($d_{3,2}$) of MIL (mildly purified mung bean protein mixture), MPCM (mung bean protein colloids mixture), SUP (supernatant) and COL (pellets) stabilised foam. Foams were prepared at protein concentration of 0.1 wt% (light colour bars) and 1 wt% (dark colour bars). The average and standard deviations were obtained from at least 3 replicates. * 0.1 wt% COL foams were not created for half-life time and air bubble size analysis.*

To evaluate foaming properties of various mung bean protein fractions, the foam overrun, half-life time and air bubble size of the foam were obtained. The foam overrun was determined by whipping the fraction solutions and characterised as the foam volume over the initial solution volume. To evaluate foam stability, different mung bean protein fraction stabilised foams were prepared by sparging, 50% decay time was recorded by a foam scan, afterwards, the air bubble size was analysed by Matlab package.

Foam capacity

The most considerable increase in overrun was observed for MPCM, it increased vastly from 60 % to 324 % when the protein concentration increased from 0.1 wt% to 1 wt%. Even though COL has the most comparable surface activity as MPCM, the foamability of MPCM seems dominated by SUP. According to Figure 5.8, COL barely can make foam itself, the lowest overrun was observed for both protein concentrations. It could be related to its lagged adsorption and significantly larger air bubble size compared to SUP at 1 wt%. This was also revealed by results of air bubble size, increased protein concentration introduced enough rapid adsorbed oligomers at the interfaces, thus brought smaller air bubble size to MPCM and contribute to a higher overrun. Additionally, the relatively stiffer interfacial layers SUP formed can also play a role, it would prevent air bubbles from collapse, consequently, a higher foam volume. Considering to relatively lower absolute number of oligomers presented in MPCM, the foam capacity is weaker than SUP is logical. The same finding was previously reported by Kornet, Yang, et al. (2022) for pea protein fractions. It should be noted that, MIL (mildly purified protein mixture) did not show a better foamability than SUP although it has the smaller particle size (around 10 nm) than SUP, and a rapid adsorption rate. This unexpecting could be attributed to its lowest surface activity and bland interfacial layer stiffness, the latter cannot afford accumulation of air bubbles, hence, foam would start to collapse after a while.

Foam stability

Another foam property should be assessed is the foam stability, half-life time was used to reflect the stability of foams stabilised by different mung bean protein fractions. The MPCM showed a superior foam stability than others, while SUP and COL only showed less pronounced increase in half-life time with increased protein concentration. On the other hand, a better foam stability can be introduced by smaller air bubble size. Since no significant difference in bubble size was observed

for different fractions stabilised foams at 1 % w/w, it suggests that there is the synergy effect between different fractions as reported by (Burke et al., 2014). To explore the mechanism behind this effect, the whipping tests were performed on different fractions and their mixtures to obtain foam stability curves (Figure 5.9). 0.1% w/w albumins were mixed with fractions to eliminate the influence of varied initial foam volume.

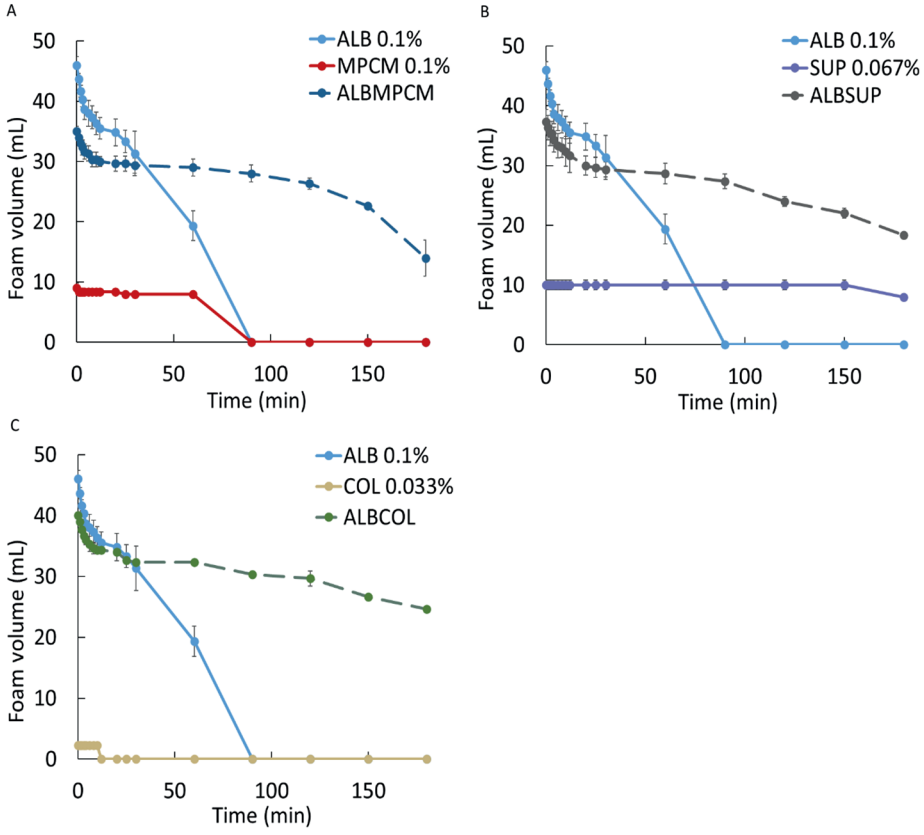

Figure 5.9 *Foam volume as a function of time of A) 0.1% w/w ALB (albumin), 0.1% w/w MPCM (mung bean protein colloids mixtures) and ALBMPCM (mixture of 0.1% w/w albumin and 0.1% w/w mung bean protein colloids mixture) stabilised foam, B) 0.1% w/w ALB (albumin), 0.067% w/w SUP (supernatant separated from 0.1% MPCM) and ALBSUP (mixture of 0.1% w/w albumin and 0.067% w/w Supernatant) and C) 0.1% w/w ALB (albumin), 0.033% w/w COL (colloids, pellets separated from 0.1% MPCM) and ALBCOL (mixture of 0.1% w/w albumin and 0.033% w/w colloids). All measurements were conducted at least in triplicate.*

As reported previously (Rullier et al., 2008; Saint-Jalmes et al., 2005; Schmitt et al., 2007), there are two mechanisms can explain the enhanced foam stability, either by confinement of protein aggregates in the Plateau borders or by the formation of viscoelastic layers in the thin film. It is possible that large particles act as blockages in the lamellae and Plateau boarders, hence slow down the drainage and destabilisation of the foam. However, COL possess the largest particle size, whereas they were unable to provide the highest stability among others, we found MPCM, SUP and COL showed similar foam stability curves in Figure 5.9. It reveals that COL may form viscoelastic layers in the thin film and contribute to the stabilisation of the foam. This finding was confirmed by Lissajous plots as well; the most elastic interface was found formed by COL (Figure 5.6). Consequently, we presume that SUP and COL both are essential to maintain MPCM foam stable as shown in Figure 5.10. SUP possess smaller particles which are able to generate stiffer interfacial layers as shown in rheology results (Figure 5.6), on the other hand, COL can form viscoelastic layers in the thin film, thus extraordinarily high foam stability established as a result of this collaboration.

In summary, SUP and COL collaborate greatly in the formation of highly stable foam. SUP has the small particle size enable them to move to interfaces rapidly, contributing to foam accumulation and leading to a high foam capacity. Additionally, the relatively small particles of SUP than COL can produce stiffer interfaces, leading to a high foam stability. COL as a stabiliser in thin film between air bubbles due to formation of viscoelastic layers, competently slow down the drainage and destabilisation, hence, contribute to a long-lasting foam.

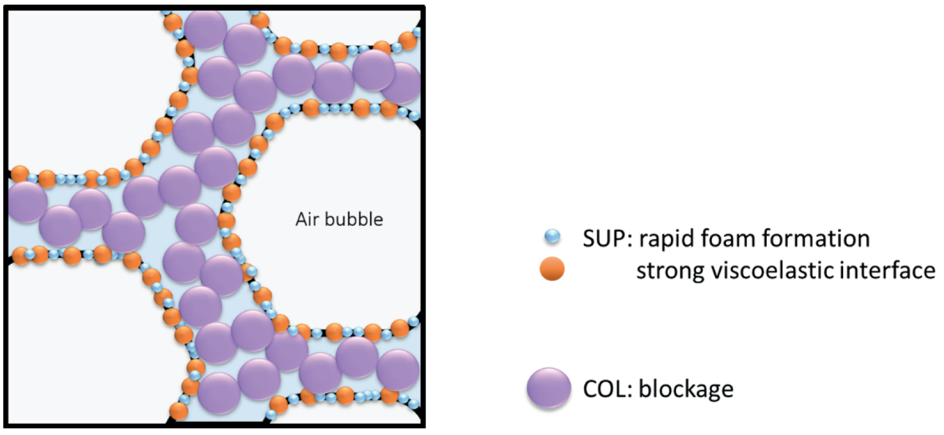

Figure 5.10 *Simplified schematic overview of MPCM (mung bean protein colloids mixtures) stabilised foam. Smaller blue and orange spheres represent SUP (Supernatant) and larger purple spheres represent COL (Colloids).*

5.4 Conclusion

The interfacial stabilising behaviour of mung bean protein colloids mixtures and its fractions were studied to reveal the mechanism behind MPCM foaming stability phenomenon. SUP seems dominate interfacial behaviour of MPCM, since they both were found form stiffer layers with strong in-plane interactions at the air-water interface. COL presented a distinctly more stretchable interfaces compared to SUP, it could be attributed to its relatively larger particle size resulted in less effective coverage, therefore, weaker in-plane interactions. MIL sample was unable to show any superior interfacial stabilising properties even though it possesses smallest particle size and the most rapid adsorption rate, a relatively lower foam capacity and poorer foam stability indicating that mild purification process cannot yield a better foaming behaviour for mung bean proteins.

Additionally, the role of various fractions was investigated. It should be noticed that the high foam stability was not achieved by sacrificing foam capacity as other plant-based proteins, MPCM was observed presented both high foam capacity (app. 325%) and foam stability (app. 400 min). Due to rapid moving speed, the highest foam capacity was observed for SUP like other unaggregated proteins. Furthermore,

by generating stiffer interfaces, it also brought high foam stability to MPCM. The other factor resulted in long lasting MPCM foam is COL. It was found form viscoelastic thin film between air bubbles, thereby decrease the drainage and destabilisation rate. In brief, SUP and COL co-operate greatly in the formation of highly stable MPCM foam. Heat-induced aggregates can enhance the foaming stability of mung bean proteins as other previously reported plant-based proteins and dairy proteins, and also lead to a foam with high capacity. Hence, MPCM can be considered as a promising and novel foaming agent for plant-based food products, for example, protein fortified beverages.

References

Adebiyi, A. P., & Aluko, R. E. (2011). Functional properties of protein fractions obtained from commercial yellow field pea (Pisum sativum L.) seed protein isolate. *Food Chemistry*, *128*(4), 902-908.

Aiking, H. (2011). Future protein supply. *Trends in Food Science & Technology*, *22*(2-3), 112-120.

Amonsou, E., Taylor, J., & Minnaar, A. (2011). Microstructure of protein bodies in marama bean species. *LWT - Food Science and Technology*, *44*(1), 42-47.

Assatory, A., Vitelli, M., Rajabzadeh, A. R., & Legge, R. L. (2019). Dry fractionation methods for plant protein, starch and fiber enrichment: A review. *Trends in Food Science & Technology*, *86*, 340-351.

Avila Ruiz, G., Arts, A., Minor, M., & Schutyser, M. (2016). A Hybrid Dry and Aqueous Fractionation Method to Obtain Protein-Rich Fractions from Quinoa (Chenopodium quinoa Willd). *Food and Bioprocess Technology*, *9*(9), 1502-1510.

Aydemir, L. Y., & Yemenicioğlu, A. (2013). Potential of Turkish Kabuli type chickpea and green and red lentil cultivars as source of soy and animal origin functional protein alternatives. *LWT - Food Science and Technology*, *50*(2), 686-694.

Beran, M., Drahorad, J., Vltavsky, O., Urban, M., Laknerova, I., Fronek, M., Sova, J., Ondracek, J., Ondrackova, L., Kralova, M., & Formankova, S. (2018). Pilot-Scale Production and Application of Microparticulated Plant Proteins. *Journal of Nutrition & Food Sciences*, *08*(01).

Boye, J., Zare, F., & Pletch, A. (2010). Pulse proteins: Processing, characterization, functional properties and applications in food and feed. *Food Research International*, *43*(2), 414-431.

Brishti, F. H., Zarei, M., Muhammad, S. K. S., Ismail-Fitry, M. R., Shukri, R., & Saari, N. (2017). Evaluation of the functional properties of mung bean protein isolate for development of textured vegetable protein. *International Food Research Journal*, *24*(4), 1595–1605.

Brishti, F. H., Chay, S. Y., Muhammad, K., Ismail-Fitry, M. R., Zarei, M., Karthikeyan, S., & Saari, N. (2020). Effects of drying techniques on the physicochemical, functional, thermal, structural and rheological properties of mung bean (Vigna radiata) protein isolate powder. *Food Res Int*, *138*(Pt B), 109783.

Brückner-Gühmann, M., Kratzsch, A., Sozer, N., & Drusch, S. (2021). Oat protein as plant-derived gelling agent: Properties and potential of modification. *Future Foods*, *4*.

Burke, J., Cox, A., Petkov, J., & Murray, B. S. (2014). Interfacial rheology and stability of air bubbles stabilized by mixtures of hydrophobin and β-casein. *Food Hydrocolloids*, *34*, 119-127.

Carbonaro, M., Maselli, P., & Nucara, A. (2015). Structural aspects of legume proteins and nutraceutical properties. *Food Research International*, *76*, 19-30.

Chen, M., Feijen, S., Sala, G., Meinders, M. B. J., van Valenberg, H. J. F., van Hooijdonk, A. C. M., & van der Linden, E. (2018). Foam stabilized by large casein micelle aggregates: The effect of aggregate number in foam lamella. *Food Hydrocolloids*, *74*, 342-348.

Chen, N., Zhao, M., Nicolai, T., & Chassenieux, C. (2017). Exploiting Salt Induced Microphase Separation To Form Soy Protein Microcapsules or Microgels in Aqueous Solution. *Biomacromolecules*, *18*(7), 2064-2072.

Chen, N., Zhao, Z., Wang, Y., & Dimova, R. (2020). Resolving the Mechanisms of Soy Glycinin Self-Coacervation and Hollow-Condensate Formation. *ACS Macro Letters*, *9*(12), 1844-1852.

Cochereau, R., Nicolai, T., Chassenieux, C., & Silva, J. V. C. (2019). Mechanism of the spontaneous formation of plant protein microcapsules in aqueous solution. *Colloids and Surfaces A: Physicochemical and Engineering Aspects*, *562*, 213-219.

Coffmann, C. W., & Garciaj, V. V. (1977). Functional properties and amino acid content of a protein isolate from mung bean flour*. *International Journal of Food Science & Technology*, *12*(5), 473-484.

Daubert, C. R., Hudson, H. M., Foegeding, E. A., & Prabhasankar, P. (2006). Rheological characterization and electrokinetic phenomena of charged whey protein dispersions of defined sizes. *LWT - Food Science and Technology*, *39*(3), 206-215.

de Kruif, C. G., Weinbreck, F., & de Vries, R. (2004). Complex coacervation of proteins and anionic polysaccharides. *Current Opinion in Colloid & Interface Science*, *9*(5), 340-349.

Delcour, J., & Hoseney, R. C. (2010). Principles of cereal science and technology authors provide insight into the current state of cereal processing. *Cereal Foods World*, *55*(1), 21-22.

Du, M., Xie, J., Gong, B., Xu, X., Tang, W., Li, X., Li, C., & Xie, M. (2018). Extraction, physicochemical characteristics and functional properties of Mung bean protein. *Food Hydrocolloids*, *76*, 131-140.

Eissa, A. S., Mohamed, D. M., Uoness, K. S., Azab, M. M., Abed, N. S., & El-Aish, D. A. (2013). Characterization of Rheological and Molecular Properties of Whey Protein Thickeners. *International Journal of Food Properties*, *17*(3), 570-586.

Godfray, H. C., Crute, I. R., Haddad, L., Lawrence, D., Muir, J. F., Nisbett, N., Pretty, J., Robinson, S., Toulmin, C., & Whiteley, R. (2010). The future of the global food system. *Philos Trans R Soc Lond B Biol Sci*, *365*(1554), 2769-2777.

Guo, F., Xiong, Y. L., Qin, F., Jian, H., Huang, X., & Chen, J. (2015). Surface properties of heat-induced soluble soy protein aggregates of different molecular masses. *J Food Sci*, *80*(2), C279-287.

Hou, D., Yousaf, L., Xue, Y., Hu, J., Wu, J., Hu, X., Feng, N., & Shen, Q. (2019). Mung Bean (Vigna radiata L.): Bioactive Polyphenols, Polysaccharides, Peptides, and Health Benefits. *Nutrients*, *11*(6).

Itoh, T., Garcia, R. N., Adachi, M., Maruyama, Y., Tecson-Mendoza, E. M., Mikami, B., & Utsumi, S. (2006). Structure of 8Salpha globulin, the major seed storage protein of mung bean. *Acta Crystallogr D Biol Crystallogr*, *62*(Pt 7), 824-832.

Khattab, R. Y., Arntfield, S. D., & Nyachoti, C. M. (2009). Nutritional quality of legume seeds as affected by some physical treatments, Part 1: Protein quality evaluation. *LWT - Food Science and Technology*, *42*(6), 1107-1112.

Kornet, C., Venema, P., Nijsse, J., van der Linden, E., van der Goot, A. J., & Meinders, M. (2020). Yellow pea aqueous fractionation increases the specific volume fraction and viscosity of its dispersions. *Food Hydrocolloids*, *99*.

Kornet, R., Roozalipour, S. L., Venema, P., van der Goot, A. J., Meinders, M. B. J., & van der Linden, E. (2022). Coacervation in pea protein solutions: The effect of pH, salt, and fractionation processing steps. *Food Hydrocolloids*, *125*.

Kornet, R., Yang, J., Venema, P., van der Linden, E., & Sagis, L. M. C. (2022). Optimizing pea protein fractionation to yield protein fractions with a high foaming and emulsifying capacity. *Food Hydrocolloids*, *126*.

Kudre, T. G., Benjakul, S., & Kishimura, H. (2013). Comparative study on chemical compositions and properties of protein isolates from mung bean, black bean and bambara groundnut. *J Sci Food Agric*, *93*(10), 2429-2436.

Lazko, J., Popineau, Y., & Legrand, J. (2004). Soy glycinin microcapsules by simple coacervation method. *Colloids and Surfaces B: Biointerfaces*, *37*(1), 1-8.

Li, X., & de Vries, R. (2018). Interfacial stabilization using complexes of plant proteins and polysaccharides. *Current Opinion in Food Science*, *21*, 51-56.

Li, X., Erni, P., Van Der Gucht, J., & De Vries, R. (2020). Encapsulation Using Plant Proteins: Thermodynamics and Kinetics of Wetting for Simple Zein Coacervates. *ACS Applied Materials & Interfaces*, *12*(13), 15802-15809.

Liu, F. F., Li, Y. Q., Wang, C. Y., Liang, Y., Zhao, X. Z., He, J. X., & Mo, H. Z. (2022). Physicochemical, functional and antioxidant properties of mung bean protein enzymatic hydrolysates. *Food Chem*, *393*, 133397.

Liu, J., Shim, Y. Y., Shen, J., Wang, Y., & Reaney, M. J. T. (2017). Whey protein isolate and flaxseed (Linum usitatissimum L.) gum electrostatic coacervates: Turbidity and rheology. *Food Hydrocolloids*, *64*, 18-27.

Lui, D. Y. M., Litster, J. D., & White, E. T. (2007). Precipitation of soy proteins: Particle formation and protein separation. *AIChE Journal*, *53*(2), 514-522.

Ma, Z., Boye, J. I., Simpson, B. K., Prasher, S. O., Monpetit, D., & Malcolmson, L. (2011). Thermal processing effects on the functional properties and microstructure of lentil, chickpea, and pea flours. *Food Research International*, *44*(8), 2534-2544.

MordorIntelligence. (2022). *Protein ingredients market size, share, trends: 2022 - 27*. Mordor Intelligence. Retrieved 23 November from https://www.mordorintelligence.com/industry-reports/protein-ingredients-market?gclid=CjwKCAiApvebBhAvEiwAe7mHSCGuLLg--J9ytWjcSyx8MJ_t60x-RwynZu62Sz5UmOdjJNGk_et-EBoCfCkQAvD_BwE

Nicolai, T. (2016). Formation and functionality of self-assembled whey protein microgels. *Colloids and Surfaces B: Biointerfaces*, *137*, 32-38.

Nicorescu, I., Loisel, C., Riaublanc, A., Vial, C., Djelveh, G., Cuvelier, G., & Legrand, J. (2009). Effect of dynamic heat treatment on the physical properties of whey protein foams. *Food Hydrocolloids*, *23*(4), 1209-1219.

Nicorescu, I., Vial, C., Loisel, C., Riaublanc, A., Djelveh, G., Cuvelier, G., & Legrand, J. (2010). Influence of protein heat treatment on the continuous production of food foams. *Food Research International*, *43*(6), 1585-1593.

Opazo-Navarrete, M., Freire, D. T., Boom, R. M., Janssen, A. E. M., & Schutyser, M. A. I. (2018). Dry fractionation of quinoa sweet varieties Atlas and Riobamba

for sustainable production of protein and starch fractions. *Journal of Food Composition and Analysis*, *74*, 95-101.

Pathak, J., Priyadarshini, E., Rawat, K., & Bohidar, H. B. (2017). Complex coacervation in charge complementary biopolymers: Electrostatic versus surface patch binding. *Advances in Colloid and Interface Science*, *250*, 40-53.

Pelgrom, P. J. M., Berghout, J. A. M., van der Goot, A. J., Boom, R. M., & Schutyser, M. A. I. (2014). Preparation of functional lupine protein fractions by dry separation. *LWT - Food Science and Technology*, *59*(2), 680-688.

Pelgrom, P. J. M., Boom, R. M., & Schutyser, M. A. I. (2015a). Functional analysis of mildly refined fractions from yellow pea. *Food Hydrocolloids*, *44*, 12-22.

Pelgrom, P. J. M., Boom, R. M., & Schutyser, M. A. I. (2015b). Method Development to Increase Protein Enrichment During Dry Fractionation of Starch-Rich Legumes. *Food and Bioprocess Technology*, *8*(7), 1495-1502.

Pelgrom, P. J. M., Vissers, A. M., Boom, R. M., & Schutyser, M. A. I. (2013). Dry fractionation for production of functional pea protein concentrates. *Food Research International*, *53*(1), 232-239.

Pelgrom, P. J. M., Wang, J., Boom, R. M., & Schutyser, M. A. I. (2015). Pre- and post-treatment enhance the protein enrichment from milling and air classification of legumes. *Journal of Food Engineering*, *155*, 53-61.

Popello, I. A., Suchkov, V. V., Grinberg, V. Y., & Tolstoguzov, V. B. (1992). Effects of pH upon the liquid-liquid phase equilibria in solutions of legumins and vicilins from broad beans and peas. *Food Hydrocolloids*, *6*(2), 147-152.

Ringgenberg, E., Alexander, M., & Corredig, M. (2013). Effect of concentration and incubation temperature on the acid induced aggregation of soymilk. *Food Hydrocolloids*, *30*(1), 463-469.

Rühs, P. A., Affolter, C., Windhab, E. J., & Fischer, P. (2013). Shear and dilatational linear and nonlinear subphase controlled interfacial rheology of β-lactoglobulin fibrils and their derivatives. *Journal of Rheology*, *57*(3), 1003-1022.

Rullier, B., Axelos, M. A., Langevin, D., & Novales, B. (2009). Beta-lactoglobulin aggregates in foam films: correlation between foam films and foaming properties. *J Colloid Interface Sci*, *336*(2), 750-755.

Rullier, B., Axelos, M. A., Langevin, D., & Novales, B. (2010). Beta-lactoglobulin aggregates in foam films: effect of the concentration and size of the protein aggregates. *J Colloid Interface Sci*, *343*(1), 330-337.

Rullier, B., Novales, B., & Axelos, M. A. V. (2008). Effect of protein aggregates on foaming properties of β-lactoglobulin. *Colloids and Surfaces A: Physicochemical and Engineering Aspects*, *330*(2-3), 96-102.

Sagis, L. M. C., Liu, B., Li, Y., Essers, J., Yang, J., Moghimikheirabadi, A., Hinderink, E., Berton-Carabin, C., & Schroen, K. (2019). Dynamic heterogeneity in complex interfaces of soft interface-dominated materials. *Sci Rep*, *9*(1), 2938.

Sağlam, D., Venema, P., de Vries, R., Shi, J., & van der Linden, E. (2013). Concentrated whey protein particle dispersions: Heat stability and rheological properties. *Food Hydrocolloids*, *30*(1), 100-109.

Saglam, D., Venema, P., de Vries, R., van Aelst, A., & van der Linden, E. (2012). Relation between gelation conditions and the physical properties of whey protein particles. *Langmuir*, *28*(16), 6551-6560.

Sah, B. K., & Kundu, S. (2017). Modification of hysteresis behaviors of protein monolayer and the corresponding structures with the variation of protein surface charges. *Colloids Surf B Biointerfaces*, *159*, 696-704.

Saint-Jalmes, A., Peugeot, M. L., Ferraz, H., & Langevin, D. (2005). Differences between protein and surfactant foams: Microscopic properties, stability and coarsening. *Colloids and Surfaces A: Physicochemical and Engineering Aspects*, *263*(1-3), 219-225.

Saricay, Y., Wierenga, P. A., & de Vries, R. (2016). Rheological properties of dispersions of enzymatically cross-linked apo-α-lactalbumin. *Food Hydrocolloids*, *56*, 344-351.

Schmidt, S. R. (2013). Protein bodies in nature and biotechnology. *Mol Biotechnol*, *54*(2), 257-268.

Schmitt, C., Bovay, C., Rouvet, M., Shojaei-Rami, S., & Kolodziejczyk, E. (2007). Whey Protein Soluble Aggregates from Heating with NaCl: Physicochemical, Interfacial, and Foaming Properties. *Langmuir*, *23*(8), 4155-4166.

Schutyser, M. A. I., & van der Goot, A. J. (2011). The potential of dry fractionation processes for sustainable plant protein production. *Trends in Food Science & Technology*, *22*(4), 154-164.

Shen, L., & Tang, C.-H. (2012). Microfluidization as a potential technique to modify surface properties of soy protein isolate. *Food Research International*, *48*(1), 108-118.

Shen, Y., Tang, X., & Li, Y. (2021). Drying methods affect physicochemical and functional properties of quinoa protein isolate. *Food Chem*, *339*, 127823.

Taherian, A. R., Mondor, M., Labranche, J., Drolet, H., Ippersiel, D., & Lamarche, F. (2011). Comparative study of functional properties of commercial and membrane processed yellow pea protein isolates. *Food Research International*, *44*(8), 2505-2514.

Tang, C. H., & Sun, X. (2010). Physicochemical and structural properties of 8S and/or 11S globulins from mungbean [Vigna radiata (L.) Wilczek] with various polypeptide constituents. *J Agric Food Chem*, *58*(10), 6395-6402.

Teng, Z., Luo, Y., & Wang, Q. (2012). Nanoparticles Synthesized from Soy Protein: Preparation, Characterization, and Application for Nutraceutical Encapsulation. *Journal of Agricultural and Food Chemistry*, *60*(10), 2712-2720.

Tombs, M. P. (1967). Protein bodies of the soybean. *Plant Physiol*, *42*(6), 797-813.

USDA. (2019). *FoodData Central*. Retrieved July 20 from https://fdc.nal.usda.gov/

Wang, J., de Wit, M., Schutyser, M. A. I., & Boom, R. M. (2014). Analysis of electrostatic powder charging for fractionation of foods. *Innovative Food Science & Emerging Technologies*, *26*, 360-365.

Wang, J., Smits, E., Boom, R. M., & Schutyser, M. A. I. (2015). Arabinoxylans concentrates from wheat bran by electrostatic separation. *Journal of Food Engineering*, *155*, 29-36.

Wang, J., Zhao, J., de Wit, M., Boom, R. M., & Schutyser, M. A. I. (2016). Lupine protein enrichment by milling and electrostatic separation. *Innovative Food Science & Emerging Technologies*, *33*, 596-602.

Wang, Y., Zhao, J., Zhang, S., Zhao, X., Liu, Y., Jiang, J., & Xiong, Y. L. (2022). Structural and rheological properties of mung bean protein emulsion as a liquid egg substitute: The effect of pH shifting and calcium. *Food Hydrocolloids*, *126*.

Wang, Z., Li, Y., Jiang, L., Qi, B., & Zhou, L. (2014). Relationship between Secondary Structure and Surface Hydrophobicity of Soybean Protein Isolate Subjected to Heat Treatment. *Journal of Chemistry*, *2014*, 1-10.

Wouters, A. G. B., Rombouts, I., Fierens, E., Brijs, K., & Delcour, J. A. (2016). Relevance of the Functional Properties of Enzymatic Plant Protein Hydrolysates in Food Systems. *Compr Rev Food Sci Food Saf*, *15*(4), 786-800.

Xia, W., Botma, T. E., Sagis, L. M. C., & Yang, J. (2022). Selective proteolysis of β-conglycinin as a tool to increase air-water interface and foam stabilising properties of soy proteins. *Food Hydrocolloids*, *130*.

Yang, J., Faber, I., Berton-Carabin, C. C., Nikiforidis, C. V., van der Linden, E., & Sagis, L. M. C. (2021). Foams and air-water interfaces stabilised by mildly purified rapeseed proteins after defatting. *Food Hydrocolloids*, *112*.

Yang, J., Kornet, R., Diedericks, C. F., Yang, Q., Berton-Carabin, C. C., Nikiforidis, C. V., Venema, P., van der Linden, E., & Sagis, L. M. C. (2022). Rethinking plant protein extraction: Albumin—From side stream to an excellent foaming ingredient. *Food Structure*, *31*.

Yang, J., Lamochi Roozalipour, S. P., Berton-Carabin, C. C., Nikiforidis, C. V., van der Linden, E., & Sagis, L. M. C. (2021). Air-water interfacial and foaming properties of whey protein - sinapic acid mixtures. *Food Hydrocolloids*, *112*.

Yang, J., Mocking-Bode, H. C. M., van den Hoek, I. A. F., Theunissen, M., Voudouris, P., Meinders, M. B. J., & Sagis, L. M. C. (2022). The impact of heating and freeze or spray drying on the interface and foam stabilising properties of pea protein extracts: Explained by aggregation and protein composition. *Food Hydrocolloids*, *133*.

Yang, J., Thielen, I., Berton-Carabin, C. C., van der Linden, E., & Sagis, L. M. C. (2020). Nonlinear interfacial rheology and atomic force microscopy of air-water interfaces stabilized by whey protein beads and their constituents. *Food Hydrocolloids*, *101*.

Yang, M., Li, N., Tong, L., Fan, B., Wang, L., Wang, F., & Liu, L. (2021). Comparison of physicochemical properties and volatile flavor compounds of pea protein and mung bean protein-based yogurt. *Lwt*, *152*.

Yang, Q., Eikelboom, E., van der Linden, E., de Vries, R., & Venema, P. (2022). A mild hybrid liquid separation to obtain functional mungbean protein. *Lwt*, *154*.

Zhao, H., Guo, M., Ding, T., Ye, X., & Liu, D. (2020). Exploring the mechanism of hollow microcapsule formation by self-assembly of soy 11s protein upon heating. *Food Hydrocolloids*, *108*, 105379.

Zhu, Y., Sun, S., & FitzGerald, R. (2018). Mung bean proteins and peptides: nutritional, functional and bioactive properties. *Food Nutr Res*, *62*.

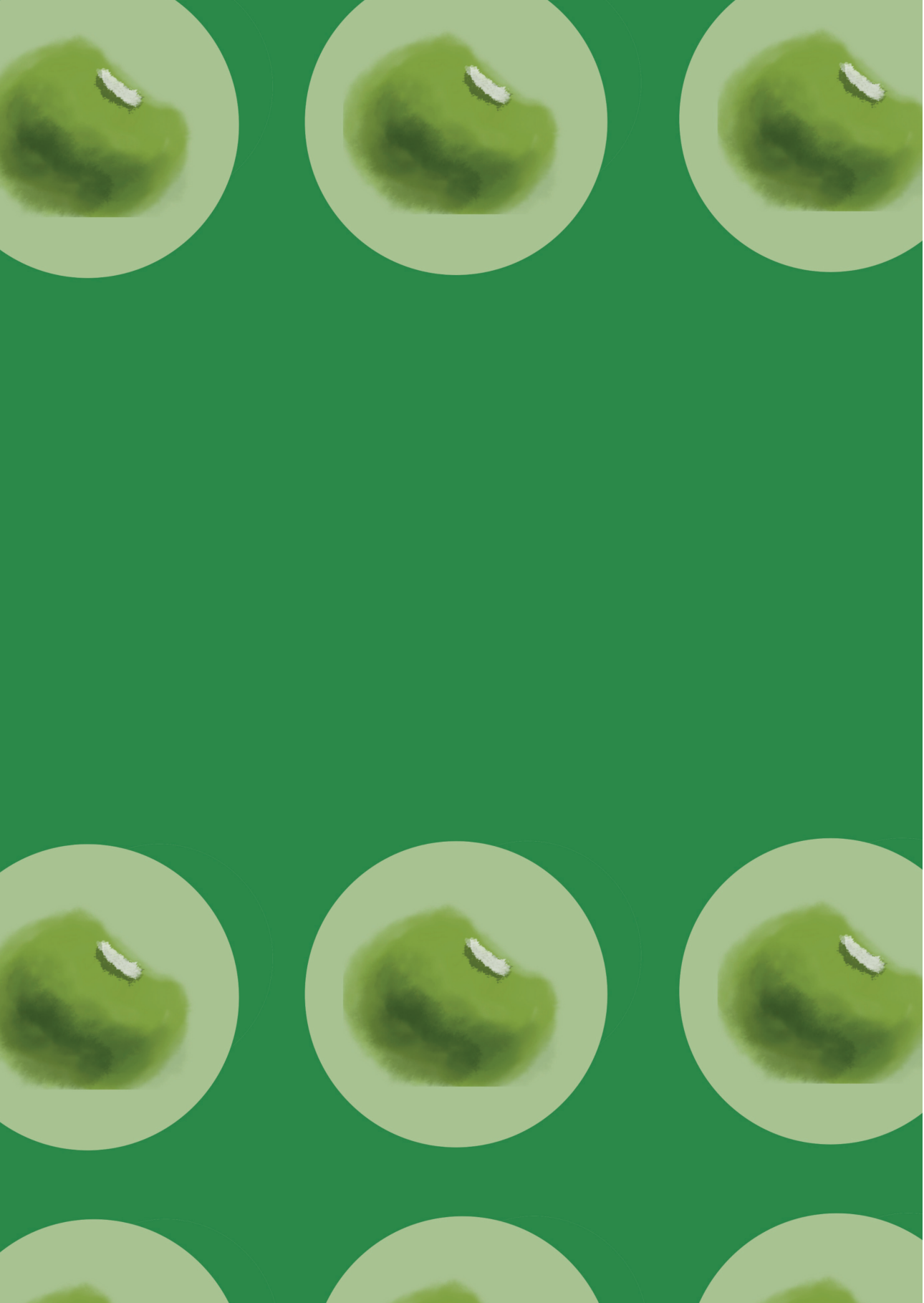

6

General discussion

6.1 Introduction

Mung bean proteins are well known for their well-balanced amino acid composition, their sustainable production and promising possible replacement for soybean proteins. Hitherto, the available research mostly focuses on mung bean protein isolates obtained by traditional isoelectric precipitation approaches. This method produces highly pure protein fractions at the expense of losing part of the protein functionality. In contrast, milder fractionation methods usually require less water and energy input, retain native protein functionalities, but typically yield ingredients with lower protein content. In the current work, we start from protein-rich mung bean fractions (MBFF) obtained by dry fractionation.

In brief, in this thesis, in **Chapter 2** we performed an aqueous-phase sedimentation-based separation to further increase protein content of MBFF. We investigated protein yield and purity for this method, as well as the resulting bulk functionalities of the mildly extracted proteins. Alternatively, in **Chapter 3**, to further increase protein content of MBFF, we used liquid-liquid phase separation, also called simple coacervation, to create dispersions of submicron droplets concentrated in Mung Bean protein. By heating this dispersion, Mung bean protein colloids mixtures (MPCM) were produced. Functional properties of MPCM were investigated in terms of bulk behaviour (**Chapter 3**) and interfacial behaviour (**Chapters 4 & 5**). An overview of the research in this thesis using various mung bean protein fractions is shown in Figure 6.1.

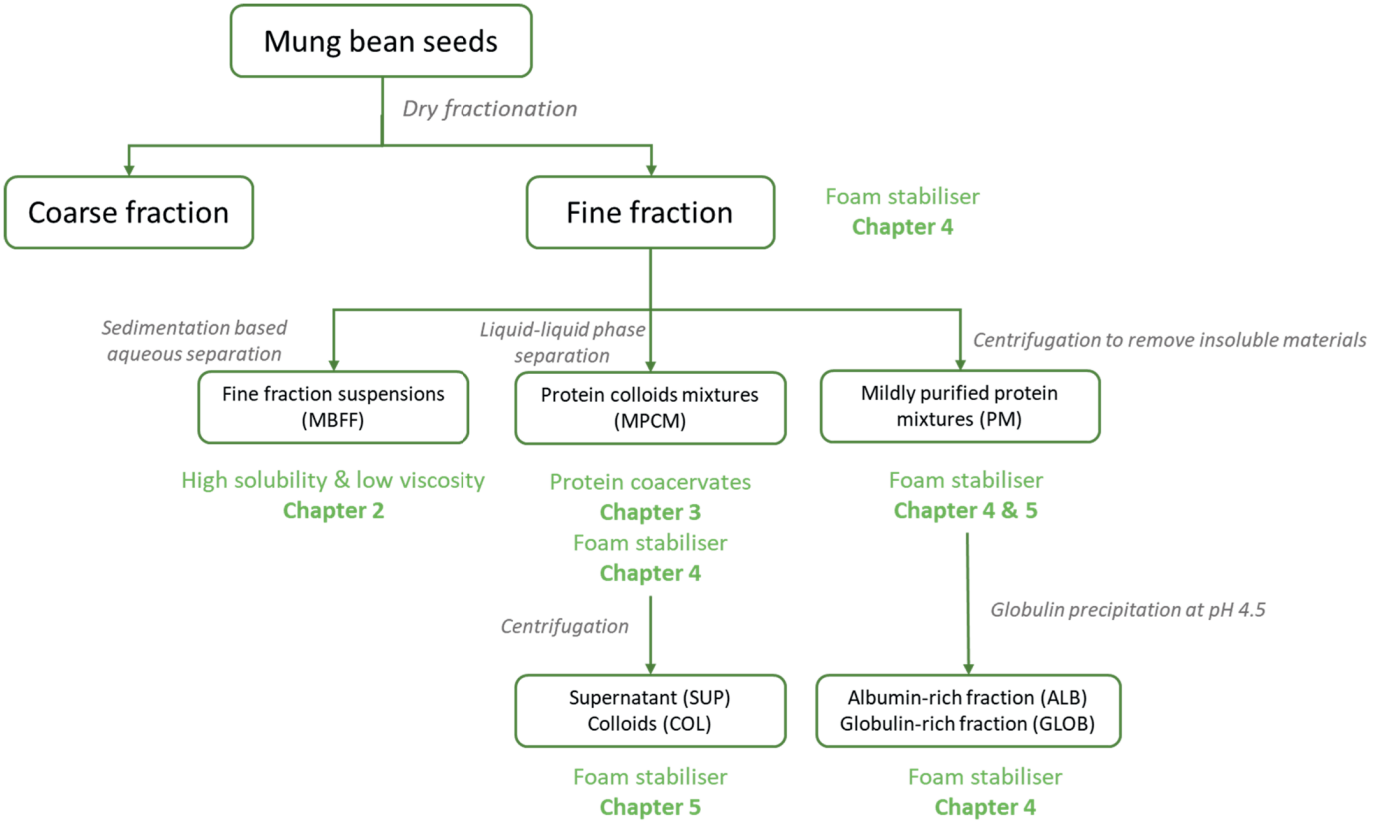

Figure 6.1 *Overview of the methods used to process various mung bean fractions in the present thesis and the corresponding functional properties (in green) investigated in relevant chapters.*

6.2 Perspective on protein colloid formation methods

To provide a broader perspective on protein colloids, in the present section, we review methods to produce them. Some of the routes are already widely used while others are new and not yet used widely developed.

Emulsification

Emulsification methods (Joye & McClements, 2014) can be used for producing proteinaceous particles with colloidal sizes. For example, emulsification of a dense aqueous protein solution in an oil phase was followed by thermal gelation, was used to produce solid like proteinaceous particles in oil that were subsequently separated from the oil (Sağlam et al., 2013). This process resulting in dense protein particles. In work of Saglam et al., spherical whey protein particles with diameters larger than 1 µm were obtained with a high internal protein content (e.g. 20 v/v %). The need to use the oil soluble stabilizer PGPR in this process makes the production of food-grade protein particles by this process unattractive, since food producers are trying to minimize or eliminate the use of this stabilizers in their product. Therefore, next we discuss an alternative method for protein colloid preparation, based on simple coacervation. This method may result in smaller particle sizes than the protein colloids prepared with emulsification (Purwanti et al., 2013).

Coacervation

Coacervation is a synonym for liquid-liquid phase separation for the special case that the liquid which is undergoing phase separation is a polymer solution. Polymers or polymer mixtures in solution may undergo liquid-liquid phase separation into a polymer dense and a polymer dilute phase. The dense phase is typically called the coacervate, the dilute phase is typically called the excess phase, and the phase separation process is referred to as “coacervation” (de Kruif et al., 2004). Dispersions of droplets of the dense phase in the excess phase are also often referred to as coacervates.

According to previous research, the pH, ionic strength and temperature are the main parameters controlling the coacervation of biopolymers, including proteins. Since phase separation is spontaneous, preparing protein coacervates require little energy input (Cho & Jones, 2019) the process is scalable, the size distribution of coacervate droplets can be simply monitored and, last but not least, these resulting protein colloids can be used to tune the rheological properties of food products (Amin et al., 2014; Ru et al., 2012; Shewan & Stokes, 2013). Therefore, coacervation is an attractive method for the food industry to produce functional protein-rich colloids.

Two distinct coacervation methods, simple and complex coacervation can be distinguished (Table 6.1). Simple coacervation is also referred to as self-coacervation or liquid-liquid (micro) phase separation (Chen et al., 2020). It is an approach to produce colloids from a single protein type (Figure 1) and it is this process which has been studied in this thesis (**Chapter 3, 4 and 5**).

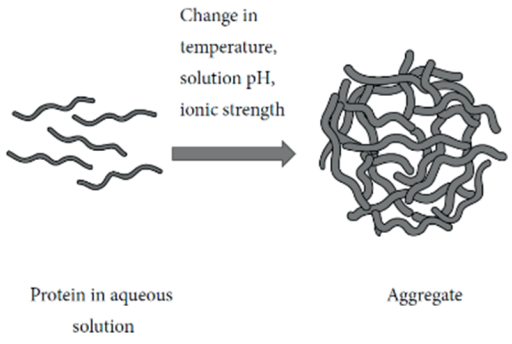

Figure 6.2 *Preparation of protein colloids by simple coacervation (Lohcharoenkal et al., 2014).*

Simple coacervation is induced by changing the solvent conditions of the protein solutions by the addition of salt or ethanol or a change in pH or temperature (Chen et al., 2017; Joye et al., 2019; Shewan & Stokes, 2013). This approach was applied using animal-derived proteins, such as, albumin, casein and gelatin. The plant proteins used to produce coacervates, where mainly soy glycinin (Chen et al., 2017),

pea protein (Cochereau et al., 2019), gliadin, zein and kafirin (Chen et al., 2020). More examples and more details for simple coacervation are presented in Table 6.2.

Simple coacervation was reported to occur within a narrow range of pH and salt concentrations (Van Megen, 1974) and to depend on the type of protein used. Indeed, we found that the optimal pH for mung bean coacervate formation is around pH 6.7 (**Chapter 3**), whereas for alkaline extracted soy flour the optimal pH values were reported to be between pH 5.7 and 6.2 (Lui et al., 2007). As for temperature, it is interesting to note that coacervate formation could be enhanced at low temperatures, since the critical pH was found to be above neutral pH at 5 °C (Cochereau et al., 2019). Thus, a low temperature probably accelerates coacervation more than ambient or higher temperature. Indeed, a similar phenomenon was observed in **Chapter 3**. By storing the mung bean protein coacervates at 4 °C overnight, we found a distinctive phase separation into a clear (dilute) and an opaque (concentrated) layer. In contrast, no such phase separation was observed when the sample was stored overnight at room temperature.

It should be noted that protein coacervate formation is typically reversible (Yan & Zhang, 2014), hence the coacervate droplets may re-dissolve when solution conditions are changed. Therefore, to form true "protein colloids" that are stable against environmental changes as required by most food applications, the protein coacervate droplets need to be solidified or gelled in some way, or in other words, the proteins inside the droplets need to be (irreversibly) aggregated.

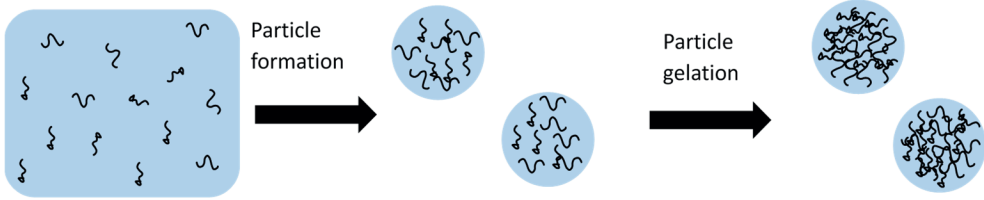

Figure 6.3 *Schematic overview of the two-step microgel formation (McClements, 2017).*

In general, particle gelation can be induced by heat treatment or cold gelation (Figure 6.3). According to previous research, especially thermal treatment is a simple and practical method to induce plant protein coacervation gelation (see Table 6.2). Stable heat-induced microgels (resistant towards dilution in water) were prepared by simple coacervation of pea protein isolates with an approximate size between 4.9 and 7.2 µm (Cochereau et al., 2019). These are much larger than our MPCM as observed in **Chapter 3** (app. 0.15 µm). This difference in size could be caused by the difference in intrinsic properties of mung bean fine fraction versus the pea protein isolate fractions used there. Some studies have shown that, when dispersed in aqueous solutions, the microgel particles tend to sediment rapidly as a result of their relatively high density and large size (Jonassen et al., 2012; Matalanis & McClements, 2013; Zhang, Zhang, Chen, et al., 2016; Zhang, Zhang, Zou, et al., 2016). When applying microgels in low viscosity products, it is therefore important to ensure that the microgels have small dimensions in order to prevent sedimentation. Fortunately, the smaller size of MPCM indeed avoids sedimentation, making MPCM suitable to be used in beverages.

Microgels of globular plant proteins, obtained by irreversibly cross-linking protein-rich droplets, could indeed have promising applications in plant-based protein beverages. However, no successful application has yet been reported for legume globular proteins, presumably since large-scale production of stable dispersions of suitable plant protein colloids has not yet been achieved, and possibly also due to unawareness to the concept of “protein colloids” as a food ingredient (Shewan & Stokes, 2013).

Table 6.1 *Overview of the techniques for protein colloids formation*

	Technology	Advantage	Disadvantage	Protein sources	Colloids size range	Reference
Coacervation	**Simple coacervation**	-Can be implemented in large scale production -Residing insoluble neutral polysaccharides can be incorporated in the complex -Resistant towards aggregation	-Only suitable for batchwise production rather than continuously. -Reversible	-Pea vicilin -Pea legumin -Gelatin -Whey proteins	1 – 800 µm	(Jahanshahi & Babaei, 2008; Oxley, 2014; Shewan & Stokes, 2013)
	Complex coacervation	-Can be implemented in large scale production	-Applicable just for charged biopolymers (complex) -Only suitable for batchwise production rather than continuously. -Reversible	-SPI -WPI -Pea proteins	0.1 – 500 µm	(Nori et al., 2011; O'Neill et al., 2014; Oxley, 2014; Shewan & Stokes, 2013; Zhang et al., 2012)
Nano-/micro-particulation	**Cold gelation**	-Suitable for temperature-sensitive compounds -Can be implemented for large scale production	-Not applicable for all proteins	-Soy proteins	0.1 – 1 µm	(Cochereau et al., 2019; Zhang et al., 2012)
	Heat-induced gelation	-Can be implemented for large scale productions -Tendency of protein aggregation is reduced -Digestibility of proteins is increased	-It is not recommended to heat sensitive compounds	-Soy proteins -Whey proteins -lysozyme & ovalbumin	0.1 – 1 µm	(Oxley, 2014; Schmitt et al., 2011; Shewan & Stokes, 2013; Yu et al., 2006)

Table 6.2 *An overview of plant-based functional colloids with their corresponding preparation method, interactions involved and characteristics.*

Functional colloid	Preparation method	Interactions	Characterisation	Particle size	Stability	Reference(s)
Coacervation						
Defatted soy flour	Simple coacervation, ionic strength	Electrostatic	DLS, microstructure, rheology	6 – 10 µm	Up to several months at 4°C	(Lui et al., 2007)
SPI	Simple coacervation, chemical cross-linking	Electrostatic, hydrophobic, hydrogen bonds, disulphide bonds	DLS, microstructure, particle charge	201.5 nm	Moderate to good stability in solution	(Teng et al., 2012)
Micro-gelation						
Soy glycinin	Simple coacervation, thermal gelation	Electrostatic, hydrophobic, hydrogen bonds, disulphide bonds	Microstructure, particle charge, solubility	2.8 – 6.6 µm	Improved solubility when cross-linked	(Zhao et al., 2020)
SPI	Simple coacervation, thermal gelation	Electrostatic, hydrophobic, hydrogen bonds, disulphide bonds	DLS, turbidity, microstructure	1.3 – 1.9 µm	Resistant against dilution in water	(Chen et al., 2020)
SPI	Simple coacervation, thermal gelation	Electrostatic, hydrophobic, hydrogen bonds, disulphide bonds	Microstructure, turbidity, solubility	3 – 30 µm	Resistant against dilution in water	(Chen et al., 2017)
Soy glycinin	Simple coacervation, thermal gelation	Electrostatic, hydrophobic, hydrogen bonds, disulphide bonds	Microstructure	4 – 24 µm	Integrity of microcapsules remained intact between pH 1 and 11.5	(Chen et al., 2018)

6.3 Fractionation methods of plant-based proteins

The functionalities of proteins depend on the processing conditions used during their fractionation. Here we will discuss the influence of the fractionation methods used, on the functional properties of plant proteins. To place our study on Mung Bean proteins in a broader perspective, other legume proteins are also included in the discussion.

6.3.1 Current research status of fractionation methods

6.3.1.1 Traditional isoelectric precipitation

Relatively harsh conditions are used in industry in order to produce ingredients with high protein content (e.g. > 80% for protein concentrates) (Assatory et al., 2019; Pelgrom, Boom, et al., 2015a). At this moment mainly wet fractionation, in particular isoelectric precipitation, is used to obtain protein-rich fractions originating from mung beans (Brishti et al., 2020; Brishti et al., 2021; Du et al., 2018; Wang et al., 2022). Wet fractionation is essential to food industry, because plant proteins are much less hydrophilic than proteins from milk or eggs and often cannot be extracted easily from the raw plant material in their native state (Li & de Vries, 2018).

Firstly, aqueous extraction processes typically require pre-treatments such as dehulling, milling and defatting. Next, soluble proteins and other components are extracted by dispersing the flour in an alkaline solution followed by centrifugation. The pH of the supernatant is then adjusted to the isoelectric point of the protein to induce precipitation of the majority of the proteins. Finally, the precipitated proteins are spray-dried into a powder. The main advantage of this technique is that it produces protein isolates with high protein purities. However, the functionality of the proteins is often compromised, because of the iso-electric precipitation and, possibly, also by the spray drying process. Additionally, it requires a large input of energy, water, and chemicals. These factors work against the

current trend towards a more sustainable processing in the food industry. Therefore, an alternative for isoelectric precipitation could be of benefit for the food industry.

6.3.1.2 Dry fractionation

Dry fractionation is milder and more sustainable for protein ingredients production from legumes, although generally, the purities obtained are lower (Pelgrom, Boom, et al., 2015a). A major advantage of dry fractionation is that the native functional properties of the proteins are retained (Avila Ruiz et al., 2016). Although mild processing results in a lower protein purity due to the presence of impurities e.g. carbohydrates, salts, phenols and oil, the overall functionality may be equal or even better than a highly purified protein isolate (Kornet et al., 2020).

Dry fractionation usually consists of two steps. The first step is fine milling of the seeds to release the protein bodies and starch granules from seeds. The second step is the dry separation of the flour in fractions based on particle size and particle density using air classification and/or electrostatic separation. The dissociation of seed components is critical to enable separation and is dependent on seed structure and the milling conditions (Pelgrom, Boom, et al., 2015b). This technique is not designed for oil-rich legumes, such as soybeans and lupines, since lipids make it difficult to freely disperse millings of crops into the air, even after the oil extraction with hexane (Schutyser & van der Goot, 2011). Unfortunately, studies using dry fractionation to extract mung bean proteins are still very limited. We have shown it is possible to use dry fractionation to obtain protein enriched mung bean protein fine fractions (MBFF) in **Chapter 2**. Fine fractions with protein contents around 24 g/ 100 g flour were obtained after air classification at a classifier wheel speed of 2500 rpm.

6.3.1.3 Mild hybrid fractionation

The main disadvantage of the dry fractionation is the relatively low protein purity as compared to wet fractionation. Hence, additional wet processing steps may still be required to obtain ingredients with the higher protein contents required for many industrial applications. We have investigated two mild steps that can be used to further increase protein content. In **Chapter 2** we used aqueous sedimentation-based separation, and in **Chapter 3** we used liquid-liquid phase separation or simple coacervation. We have found that these mild methods better preserve the native functionalities of the proteins than traditional isoelectric precipitation. The relation between processing and functionality for legume proteins will be discussed in more detail in the following section.

6.3.2 The influence of fractionation and processing on plant-based protein functionalities

In general, extensive fractionation is associated with a higher degree of denaturation of the proteins, which in turn is closely related to protein functionalities (Kudre et al., 2013; van der Goot et al., 2016). In this section, we will discuss the influence of fractionation methods on protein functionalities such as viscosity, solubility, gelation and interfacial properties. This discussion will not only focus on mung bean proteins, but also include some other legume proteins as a comparison.

6.3.2.1 Bulk functional properties

Solubility

Especially for beverage applications, a key functional property of proteins is their solubility. The solubility of a protein as a function of pH is commonly measured, because it is a key factor allowing (or disallowing) formulations with the required level of protein in food products. When a globular protein denatures, its hydrophobic patches, that are mainly folded towards the centre of the protein,

become exposed to the solvent leading to a reduced solubility. Therefore, reduced protein solubility can be considered as a practical indicator for the denaturation introduced by fractionation. Replacing harsh isolation methods by milder ones, like the replacement of wet fractionation for dry fractionation, can result in a protein retaining more native protein structure, resulting in improved water solubility. For example, Pelgrom et al. (2013) show that milled and air-classified pea protein concentrates are highly soluble in water, making them an interesting ingredient for preparing liquid foods that are high in protein content. This statement is in line with Kornet, Shek, et al. (2021), where it was observed that a mild aqueous fractionation can yield highly soluble pea proteins.

One should take into consideration however, that heating is often applied during processing of beverages. In general, heating leads to protein denaturation, affecting the solubility of the protein. However, Tang and Sun (2010) indicated that additional heating of mung bean protein isolates could also increase protein solubility, which was attributed to increases in the charged residues on the protein surface, as a result of protein denaturation and/or unfolding. In our case, to obtain mung bean protein colloids (MPCM), simple coacervates were heated to arrive at a crosslinked internal structure, as described in **Chapter 3**. Nevertheless, the MPCM retained a high solubility (47%), even close to the Mung Bean protein isoelectric point (pH 4-5).

Viscosity

Similar to solubility, the viscosity of a protein solution is also strongly influenced by the fractionation method used. It is reasonable to assume, that protein aggregates formed during extensive processing could increase the viscosity of the protein solutions, thereby limiting their application window. For example, high viscosity beverages are particularly undesired for liquid medical formulations (Streimikyte et al., 2020). In contrast, Boye et al. (2010) claimed that high starch and fibre contents

of legumes make them less suitable for beverage applications, where low viscosities are desired. Extensive fractionation that resulted in a globulin-rich fraction, was able to form soluble aggregates, that probably cause the high viscosity of pea protein isolates dispersions (Kornet et al., 2020). The effect of mild fractionation on the viscosity of mung bean proteins is discussed in **Chapter 2** and **3**. The viscosity of mung bean proteins purified by aqueous sedimentation-based separation was found lower compared to commercial mung bean protein concentrates at comparable protein concentrations. Likewise, in **Chapter 3**, lower viscosities compare to commercial mung bean protein concentrates were also observed for MPCM obtained by mild liquid-liquid phase separation. These colloids produced by simple coacervation had an intrinsic viscosity around 15 mL/g, which is significantly lower than general protein-based food thickeners, while still possessing an internal protein concentration of 17 % wt.

Gelation

Except for solubility and viscosity, gelation is another functional property that can be considerably affected by protein aggregation generated during fractionation. More aggregates introduced by either isoelectric precipitation or spray-drying were found to lead to a more heterogeneous gel network in the heat induced gels, resulting in more softer and brittle gels compare to mildly fractionated pea protein gels (Kornet, Linden, et al., 2021). However, Pelgrom, Boom, et al. (2015a) observed that dry fractionated pea protein formed softer gels than commercial pea proteins. To confirm this observation, more investigation is needed. In terms of least gelation concentration (LGC), dry fractionated pea protein showed the highest LGC compared to extensive extraction protein fractions (Jingqi Yang et al., 2021). In contrast, dry fractionation does not seem to lead to mung bean protein fractions with a higher LGC. Schlangen et al. (2022) reported that fine fraction of mung bean has LGC around 7.5% (w/w), which is significantly lower than value of mung bean protein isolates (12% (w/w)) as reported by Brishti et al. (2017) and the 10% (w/w)

as reported by Coffmann and Garciaj (1977). Except for LGC measurements, also rheology was used to determine the gelation of protein fractions. It seems that dry fractionation leads to a higher storage modulus (G') after thermal treatment. In **Chapter 2**, we observed that the final G' of MBFF was 34000 Pa, whereas Brishti et al. (2020) reported that no gelation occurred for mung bean protein isolates. Our finding is in line with Schlangen et al. (2022), where a much higher G' (12250 Pa) for the mung bean fine fraction was found after heating. Additionally, liquid-liquid phase separation was found to weaken the gelation after thermal treatment. In **Chapter 3**, a lower final G' of 1000 Pa was observed in MPCM samples in comparison to commercial mung bean protein concentrate M65 (G' = 6660 Pa). The difference in gelation of these mung bean fractions reveal that, by adjusting the processing steps, the gelling properties of mung bean fractions could be tuned to fit a wide range of applications. It is suggested that dry fractionated and aqueous phase separated mung bean fractions would be valuable candidates for products where a strong gel network is preferred, such as gelled dairy alternatives and meat analogues. Alternatively, MPCM with a lower G' after heat treatment might be a good candidate for plant-based drinks, where gelation is not desired.

6.3.2.2 Interfacial functional properties

To better understand the behaviour of emulsions and foams, the interfacial behaviour of the proteins should be studied. In this thesis we only focus on the foaming properties of the mildly fractionated mung bean proteins.

Foaming

In general, the foaming capacity (or foamability) and foam stability are chosen as parameters to characterize the behaviour of a foam. One conclusion that follows from literature is that commercial pea protein isolates show worse foaming properties compared to pea protein isolates obtained by other techniques (Kornet, Linden, et al., 2021). In **Chapter 4**, it was found that the foaming capacity of MPCM is 324 % at 1 w/w % protein concentration, whereas mung bean isolates only show

a foam capacity of 26 % (Du et al., 2018) and 90 % (Brishti et al., 2017) even at a higher protein concentration. Therefore, we conclude that simple coacervation- or liquid-liquid phase separation - would be a valuable technique to produce a mung bean protein ingredient with excellent foaming behaviour.

6.4 Summary and outlook

We showed that the functionalities of mung bean protein can be tuned over a wide range of applicability by adjusting fractionation and processing methods leading to a different mung bean protein fractions. In particular, dry fractionation followed by simple coacervation is a promising route towards plant-derived ingredients. This route is also more sustainable than the traditional processing methods. Subsequent gelation of the coacervate droplets into Mung Bean Protein Colloid Mixtures (MPCM), results in a mildly purified Mung Bean protein ingredient that is highly functional and suitable e.g. for plant protein-fortified beverages.

Due to promising surface properties (e.g., surface hydrophobicity and emulsifying properties), colloidally sized biopolymer particles have also been studied for applications in Pickering emulsions (Liu & Tang, 2014; Zhang et al., 2020; Zhu et al., 2017). Therefore, it would be interesting to determine if MPCM could also be good Pickering stabilizers of emulsions. In addition, we would recommend studying the relation between the gelation behaviour of the gels made by MPCM, including gel strength, elasticity, water holding capacity *etc.* together with the processing conditions used to induce gelation (e.g., temperature, time, rate of heating, high pressure treatment *etc*). In this case, not only the application range of mildly fractionated mung bean proteins would be broadened, but also valuable guidelines of systematic mildly fractionation methods for other legumes could be provided.

In this thesis it has been shown that MPCM can be considered as a promising plant-based protein ingredient considering its excellent functional properties in terms of stability, solubility, thickening, emulsification and foaming properties. In the

General Discussion we conclude that the routes and their possibilities for fine tuning, as investigated in this thesis, towards MPCM from Mung bean, lead to a wide applicability window for relevant functionalities of gelation, foaming and emulsification. Some similarities with results from other research were also identified, but no systematic approach for using MPCM was addressed before.

The routes towards MCPM will apply to other plant-based ingredient sources, with according finetuning capabilities. As such, this thesis provides a systematic basis for exploring plant-based ingredients that are minimally processed and sustainable, and exhibit a wide range of applicability.

At the same time, the formation of such other and novel MPCM, of other ingredients, needs to be understood in terms of microstructural changes that occur during their formation, and the relations between the internal microstructure and composition versus the functional properties of such MPCM need to be established.

References

Amin, S., Barnett, G. V., Pathak, J. A., Roberts, C. J., & Sarangapani, P. S. (2014). Protein aggregation, particle formation, characterization & rheology. *Current Opinion in Colloid & Interface Science*, *19*(5), 438-449.

Assatory, A., Vitelli, M., Rajabzadeh, A. R., & Legge, R. L. (2019). Dry fractionation methods for plant protein, starch and fiber enrichment: A review. *Trends in Food Science & Technology*, *86*, 340-351.

Avila Ruiz, G., Arts, A., Minor, M., & Schutyser, M. (2016). A Hybrid Dry and Aqueous Fractionation Method to Obtain Protein-Rich Fractions from Quinoa (Chenopodium quinoa Willd). *Food and Bioprocess Technology*, *9*(9), 1502-1510.

Boye, J., Zare, F., & Pletch, A. (2010). Pulse proteins: Processing, characterization, functional properties and applications in food and feed. *Food Research International*, *43*(2), 414-431.

Brishti, F. H., Chay, S. Y., Muhammad, K., Ismail-Fitry, M. R., Zarei, M., Karthikeyan, S., & Saari, N. (2020). Effects of drying techniques on the physicochemical, functional, thermal, structural and rheological properties of mung bean (Vigna radiata) protein isolate powder. *Food Res Int*, *138*(Pt B), 109783.

Brishti, F. H., Chay, S. Y., Muhammad, K., Ismail-Fitry, M. R., Zarei, M., & Saari, N. (2021). Texturized mung bean protein as a sustainable food source: Effects of extrusion on its physical, textural and protein quality. *Innovative Food Science & Emerging Technologies*, *67*.

Brishti, F. H., Zarei, M., Muhammad, S. K. S., Ismail-Fitry, M. R., Shukri, R., & Saari, N. (2017). Evaluation of the functional properties of mung bean protein isolate for development of textured vegetable protein. *International Food Research Journal*, *24*(4), 1595-1605.

Chen, M., Feijen, S., Sala, G., Meinders, M. B. J., van Valenberg, H. J. F., van Hooijdonk, A. C. M., & van der Linden, E. (2018). Foam stabilized by large casein micelle aggregates: The effect of aggregate number in foam lamella. *Food Hydrocolloids*, *74*, 342-348.

Chen, N., Zhao, M., Nicolai, T., & Chassenieux, C. (2017). Exploiting Salt Induced Microphase Separation To Form Soy Protein Microcapsules or Microgels in Aqueous Solution. *Biomacromolecules*, *18*(7), 2064-2072.

Chen, N., Zhao, Z., Wang, Y., & Dimova, R. (2020). Resolving the Mechanisms of Soy Glycinin Self-Coacervation and Hollow-Condensate Formation. *ACS Macro Letters*, *9*(12), 1844-1852.

Cho, Y.-H., & Jones, O. G. (2019). Chapter Two - Assembled protein nanoparticles in food or nutrition applications. In L.-T. Lim & M. Rogers (Eds.), *Advances in Food and Nutrition Research* (Vol. 88, pp. 47-84). Academic Press.

Cochereau, R., Nicolai, T., Chassenieux, C., & Silva, J. V. C. (2019). Mechanism of the spontaneous formation of plant protein microcapsules in aqueous solution. *Colloids and Surfaces A: Physicochemical and Engineering Aspects*, *562*, 213-219.

Coffmann, C. W., & Garciaj, V. V. (1977). Functional properties and amino acid content of a protein isolate from mung bean flour. *International Journal of Food Science & Technology*, *12*(5), 473-484.

de Kruif, C. G., Weinbreck, F., & de Vries, R. (2004). Complex coacervation of proteins and anionic polysaccharides. *Current Opinion in Colloid & Interface Science*, *9*(5), 340-349.

Du, M., Xie, J., Gong, B., Xu, X., Tang, W., Li, X., Li, C., & Xie, M. (2018). Extraction, physicochemical characteristics and functional properties of Mung bean protein. *Food Hydrocolloids*, *76*, 131-140.

Jahanshahi, M., & Babaei, Z. (2008). Protein nanoparticle: A unique system as drug delivery vehicles. *AFRICAN JOURNAL OF BIOTECHNOLOGY*, *7*.

Jonassen, H., Kjøniksen, A.-L., & Hiorth, M. (2012). Stability of Chitosan Nanoparticles Cross-Linked with Tripolyphosphate. *Biomacromolecules*, *13*(11), 3747-3756.

Joye, I. J., Corradini, M. G., Duizer, L. M., Bohrer, B. M., LaPointe, G., Farber, J. M., Spagnuolo, P. A., & Rogers, M. A. (2019). Chapter One - A comprehensive perspective of food nanomaterials. In L.-T. Lim & M. Rogers (Eds.), *Advances in Food and Nutrition Research* (Vol. 88, pp. 1-45). Academic Press.

Joye, I. J., & McClements, D. J. (2014). Biopolymer-based nanoparticles and microparticles: Fabrication, characterization, and application. *Current Opinion in Colloid & Interface Science*, *19*(5), 417-427.

Kornet, C., Venema, P., Nijsse, J., van der Linden, E., van der Goot, A. J., & Meinders, M. (2020). Yellow pea aqueous fractionation increases the specific volume fraction and viscosity of its dispersions. *Food Hydrocolloids*, *99*.

Kornet, R., Linden, E. v. d. P. d., Goot, A. J. v. d. P. d., Venema, P. D., Meinders, M. D., Kornet, R., Linden, E. v. d. P. d., Goot, A. J. v. d. P. d., Venema, P. D., & Meinders, M. D. (2021). *Pea protein functionality : tailor-made through fractionation* Wageningen University]. WorldCat.org. Wageningen.

Kornet, R., Shek, C., Venema, P., Jan van der Goot, A., Meinders, M., & van der Linden, E. (2021). Substitution of whey protein by pea protein is facilitated by specific fractionation routes. *Food Hydrocolloids*, *117*.

Kudre, T. G., Benjakul, S., & Kishimura, H. (2013). Comparative study on chemical compositions and properties of protein isolates from mung bean, black bean and bambara groundnut. *J Sci Food Agric*, *93*(10), 2429-2436.

Li, X., & de Vries, R. (2018). Interfacial stabilization using complexes of plant proteins and polysaccharides. *Current Opinion in Food Science*, *21*, 51-56.

Liu, F., & Tang, C.-H. (2014). Emulsifying Properties of Soy Protein Nanoparticles: Influence of the Protein Concentration and/or Emulsification Process. *Journal of Agricultural and Food Chemistry*, *62*(12), 2644-2654.

Lohcharoenkal, W., Wang, L., Chen, Y. C., & Rojanasakul, Y. (2014). Protein nanoparticles as drug delivery carriers for cancer therapy. *Biomed Res Int*, *2014*, 180549.

Lui, D. Y. M., Litster, J. D., & White, E. T. (2007). Precipitation of soy proteins: Particle formation and protein separation. *AIChE Journal*, *53*(2), 514-522.

Matalanis, A., & McClements, D. J. (2013). Hydrogel microspheres for encapsulation of lipophilic components: Optimization of fabrication & performance. *Food Hydrocolloids*, *31*(1), 15-25.

McClements, D. J. (2017). Designing biopolymer microgels to encapsulate, protect and deliver bioactive components: Physicochemical aspects. *Adv Colloid Interface Sci*, *240*, 31-59.

Nori, M. P., Favaro-Trindade, C. S., Matias de Alencar, S., Thomazini, M., de Camargo Balieiro, J. C., & Contreras Castillo, C. J. (2011). Microencapsulation of propolis extract by complex coacervation. *LWT - Food Science and Technology*, *44*(2), 429-435.

O'Neill, G. J., Egan, T., Jacquier, J. C., O'Sullivan, M., & Dolores O'Riordan, E. (2014). Whey microbeads as a matrix for the encapsulation and immobilisation of riboflavin and peptides. *Food Chemistry*, *160*, 46-52.

Oxley, J. (2014). Chapter 4 - Overview of Microencapsulation Process Technologies. In A. G. Gaonkar, N. Vasisht, A. R. Khare, & R. Sobel (Eds.), *Microencapsulation in the Food Industry* (pp. 35-46). Academic Press.

Pelgrom, P. J. M., Boom, R. M., & Schutyser, M. A. I. (2015a). Functional analysis of mildly refined fractions from yellow pea. *Food Hydrocolloids*, *44*, 12-22.

Pelgrom, P. J. M., Boom, R. M., & Schutyser, M. A. I. (2015b). Method Development to Increase Protein Enrichment During Dry Fractionation of Starch-Rich Legumes. *Food and Bioprocess Technology*, *8*(7), 1495-1502.

Pelgrom, P. J. M., Vissers, A. M., Boom, R. M., & Schutyser, M. A. I. (2013). Dry fractionation for production of functional pea protein concentrates. *Food Research International*, *53*(1), 232-239.

Purwanti, N., Peters, J. P., & van der Goot, A. J. (2013). Protein micro-structuring as a tool to texturize protein foods. *Food Funct*, *4*(2), 277-282.

Ru, Q., Wang, Y., Lee, J., Ding, Y., & Huang, Q. (2012). Turbidity and rheological properties of bovine serum albumin/pectin coacervates: Effect of salt concentration and initial protein/polysaccharide ratio. *Carbohydrate Polymers*, *88*(3), 838-846.

Sağlam, D., Venema, P., de Vries, R., & van der Linden, E. (2013). The influence of pH and ionic strength on the swelling of dense protein particles. *Soft Matter*, *9*(18), 4598-4606.

Schlangen, M., Taghian Dinani, S., Schutyser, M. A. I., & van der Goot, A. J. (2022). Dry fractionation to produce functional fractions from mung bean, yellow pea and cowpea flour. *Innovative Food Science & Emerging Technologies*, *78*.

Schmitt, C., Bovay, C., Vuilliomenet, A.-M., Rouvet, M., & Bovetto, L. (2011). Influence of protein and mineral composition on the formation of whey protein heat-induced microgels. *Food Hydrocolloids*, *25*(4), 558-567.

Schutyser, M. A. I., & van der Goot, A. J. (2011). The potential of dry fractionation processes for sustainable plant protein production. *Trends in Food Science & Technology*, *22*(4), 154-164.

Shewan, H. M., & Stokes, J. R. (2013). Review of techniques to manufacture micro-hydrogel particles for the food industry and their applications. *Journal of Food Engineering*, *119*(4), 781-792.

Streimikyte, P., Kersiene, M., Eisinaite, V., Jasutiene, I., Lesauskaite, V., Damuleviciene, G., Knasiene, J., & Leskauskaite, D. (2020). Formulating

protein-based beverages for the dysphagia diets of the elderly: viscosity, protein quality, in vitro digestion, and consumers acceptability. *J Sci Food Agric*, *100*(10), 3895-3901.

Tang, C. H., & Sun, X. (2010). Physicochemical and structural properties of 8S and/or 11S globulins from mungbean [Vigna radiata (L.) Wilczek] with various polypeptide constituents. *J Agric Food Chem*, *58*(10), 6395-6402.

Teng, Z., Luo, Y., & Wang, Q. (2012). Nanoparticles Synthesized from Soy Protein: Preparation, Characterization, and Application for Nutraceutical Encapsulation. *Journal of Agricultural and Food Chemistry*, *60*(10), 2712-2720.

van der Goot, A. J., Pelgrom, P. J. M., Berghout, J. A. M., Geerts, M. E. J., Jankowiak, L., Hardt, N. A., Keijer, J., Schutyser, M. A. I., Nikiforidis, C. V., & Boom, R. M. (2016). Concepts for further sustainable production of foods. *Journal of Food Engineering*, *168*, 42-51.

Van Megen, W. H. (1974). Solubility behavior of soybean globulins as a function of pH and ionic strength. *Journal of Agricultural and Food Chemistry*, *22*(1), 126-129.

Wang, Y., Zhao, J., Zhang, S., Zhao, X., Liu, Y., Jiang, J., & Xiong, Y. L. (2022). Structural and rheological properties of mung bean protein emulsion as a liquid egg substitute: The effect of pH shifting and calcium. *Food Hydrocolloids*, *126*.

Yan, C., & Zhang, W. (2014). Chapter 12 - Coacervation Processes. In A. G. Gaonkar, N. Vasisht, A. R. Khare, & R. Sobel (Eds.), *Microencapsulation in the Food Industry* (pp. 125-137). Academic Press.

Yang, J., Zamani, S., Liang, L., & Chen, L. (2021). Extraction methods significantly impact pea protein composition, structure and gelling properties. *Food Hydrocolloids*, *117*.

Yu, S., Yao, P., Jiang, M., & Zhang, G. (2006). Nanogels prepared by self-assembly of oppositely charged globular proteins, *Biopolymers*, *83*(2), 148-158.

Zhang, J., Liang, L., Tian, Z., Chen, L., & Subirade, M. (2012). Preparation and in vitro evaluation of calcium-induced soy protein isolate nanoparticles and their formation mechanism study. *Food Chemistry*, *133*(2), 390-399.

Zhang, S., Holmes, M., Ettelaie, R., & Sarkar, A. (2020). Pea protein microgel particles as Pickering stabilisers of oil-in-water emulsions: Responsiveness to pH and ionic strength. *Food Hydrocolloids*, *102*.

Zhang, Z., Zhang, R., Chen, L., & McClements, D. J. (2016). Encapsulation of lactase (β-galactosidase) into κ-carrageenan-based hydrogel beads: Impact of environmental conditions on enzyme activity. *Food Chemistry*, *200*, 69-75.

Zhang, Z., Zhang, R., Zou, L., & McClements, D. J. (2016). Protein encapsulation in alginate hydrogel beads: Effect of pH on microgel stability, protein retention and protein release. *Food Hydrocolloids*, *58*, 308-315.

Zhao, H., Guo, M., Ding, T., Ye, X., & Liu, D. (2020). Exploring the mechanism of hollow microcapsule formation by self-assembly of soy 11s protein upon heating. *Food Hydrocolloids*, *108*, 105379.

Zhu, X.-F., Zheng, J., Liu, F., Qiu, C.-Y., Lin, W.-F., & Tang, C.-H. (2017). The influence of ionic strength on the characteristics of heat-induced soy protein aggregate nanoparticles and the freeze–thaw stability of the resultant Pickering emulsions, *Food & Function*, *8*(8), 2974-2981.

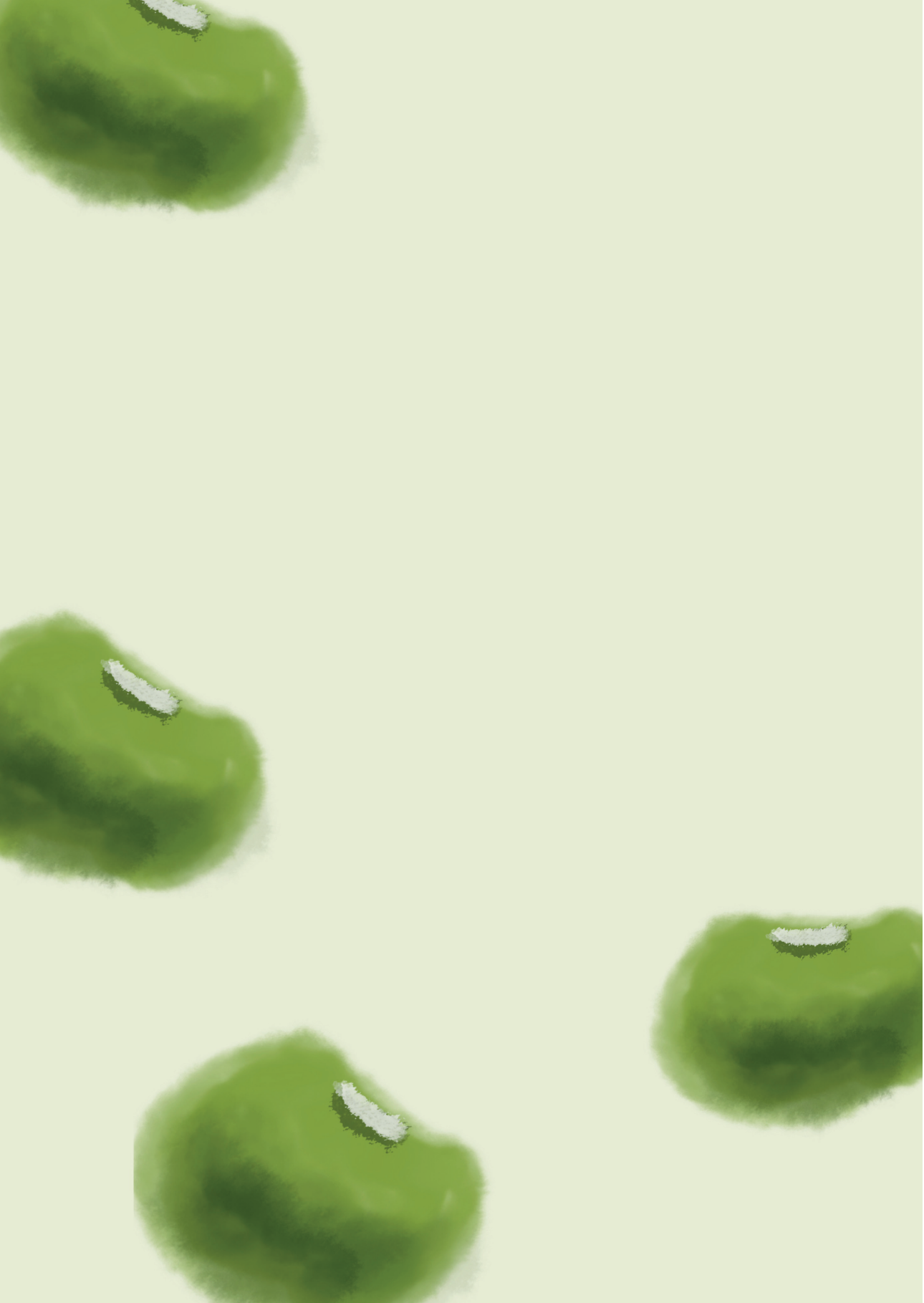

Summary

Two current challenges for the food industry are to achieve (1) a shift from the use of high purity ingredients to the use of less purified ingredients, and (2) a shift from the use of (mainly) animal-based proteins, to the use of (mainly) plant-based proteins. The present study connects to both these transitions by focusing on developing new, mildly purified Mung Bean protein ingredients with good functionality. **Chapters 2 & 3** mainly focus on protein extraction and ingredient formulation, whereas **Chapters 4 & 5**, focus mostly on the functionality of the new protein ingredients.

In **Chapter 2** we used air-classification and sedimentation-based separation to obtain mildly purify mung bean proteins with minimal denaturation with good yield and protein content. Most of the protein concentrated in a single layer (Layer 1) during the sedimentation-based separation. For this layer, protein yields were 72% and 81%, respectively, and protein contents were 65% and 64%, respectively, when extracting either at pH 6.5 or at pH 8. The mildly extracted mung bean proteins showed a higher solubility and lower viscosity as compared to a reference commercial mung bean protein concentrate (M65), which we attribute to the (relative) absence of protein aggregates in the mildly extracted Mung bean proteins. Indeed, from light scattering we found that the average particle diameters of mung bean fine fraction (MBFF) Layer 1 and M65 dispersions were 0.2 and 120 µm, respectively. While viscosities of the mildly purified protein were low as compared to those of the M65 reference isolate, we found that heat-set gelation of the mildly purified Mung Bean proteins and the M65 reference isolate leads to hydrogels with very similar rheological characteristics. We conclude therefore that the mildly purified mung bean protein obtained here may be useful in food products which require high protein solubility and low product viscosity, for example, protein rich plant-based beverages.

Next, in **Chapter 3** instead of sedimentation-based separation, we use simple coacervation to further increase the protein content when starting from air-classified Mung Bean flour. The simple coacervation leads to the formation of tiny concentrated droplets rich in protein, which we heat-set to form Mung Bean Protein Colloids (MBPC).

From viscosimetry we found that, as a protein ingredient, MBPC has a significantly lower intrinsic viscosity (15 mL/g) as compared to typical food thickeners (30 – 150 mL/g). The internal protein concentration of the MBPC particles is found to be quite high, around 17% wt. The MBPC particles can be dried using freeze-drying and spray drying. Both types of powders readily redisperse to the original particle sizes. Dispersed, freeze dried mung bean protein colloids (FDMBPC) have much weaker heat-induced gelation and lower viscosity as compared to commercial Mung Bean protein isolate reference M65. Hence, in combination the with good stability of MBPC dispersions against sedimentation, we believe MBPC could be an interesting new protein ingredient for protein-rich plant-based beverages.

In **Chapter 4** we compare the interfacial properties of a range of different mung bean protein fractions: mung bean fine fraction (FF), mung bean protein mixture (PM, obtained by removing insoluble materials from FF), mung bean globulin-rich extract (GLOB), mung bean albumin-rich extract (ALB), and finally our mung bean protein colloids (COL). We found that FF or PM already stabilise foams to some extent. By comparison to the more purified GLOB and ALB samples, we conclude that is mostly the globulins that dominate the interfacial properties of FF and PM. The globulins form weak and stretchable interfacial layers however. In contrast, ALB was found to be an excellent foaming agent, forming stiffer and more solid-like interfaces with strong in-plane interactions. The longer-term stability of the ALB foams was not very good. Somewhat surprisingly, the COL samples appear to combine the best of both worlds: they are not highly purified yet have similar

foamability as ALB. Best of all, the longer-term stability of the COL foams was found to be excellent, much better than for ALB.

To explain the remarkably good foaming functionality of the COL samples, in **Chapter 5**, we separate the MBPC dispersions into two parts using centrifugation. We find that the supernatant (SUP), dominates interfacial behaviour of MBPC, forming stiff layers with strong in-plane interactions at the air-water interfaces, like ALB. The particles from the (redispersed) precipitate on the other hand, form much more stretchable interfaces by themselves compared to SUP, are crucial to obtain the long-term stability of the foams as well. Presumably, the larger particles stabilize the foams by forming viscoelastic thin films between air bubbles that decrease drainage and decrease the destabilisation rate of the foam.

Finally, in **Chapter 6**, the results of the thesis are placed in a broader scientific context via a discussion of the application potential in food products of the mildly purified Mung Bean protein ingredients that we have developed. We also discuss the further work that still needs to be done to realize such applications. Finally, we point out and discuss the possible extensions of our approach to proteins from other legumes.

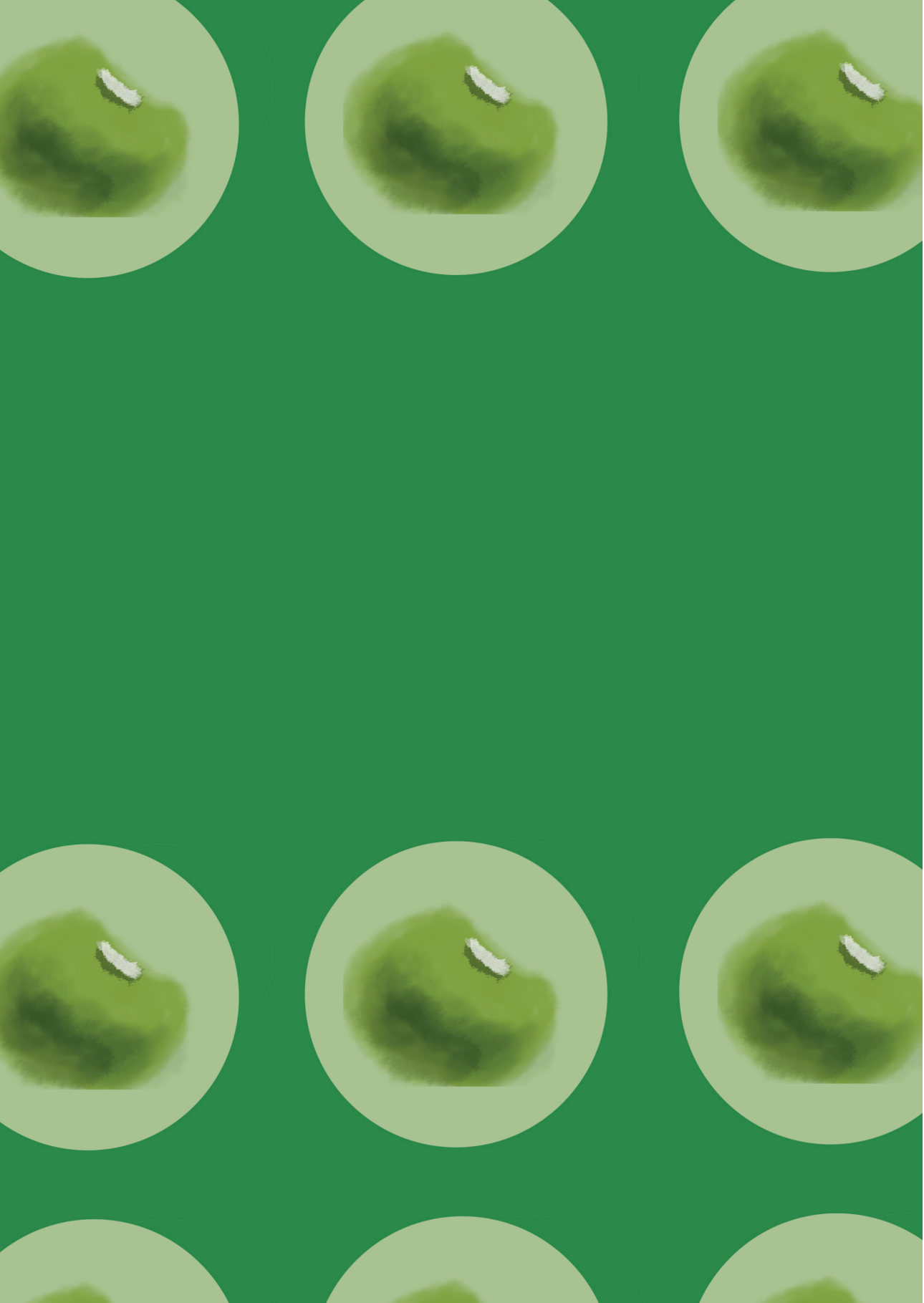

Appendix

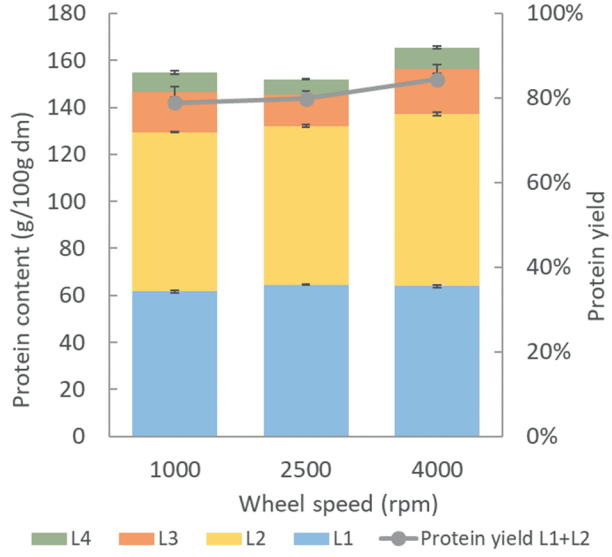

Figure S2.1 *Protein content and yield of 1000, 2500 and 4000 rpm mung bean fine fraction after aqueous phase separation with 10 min stirring.*

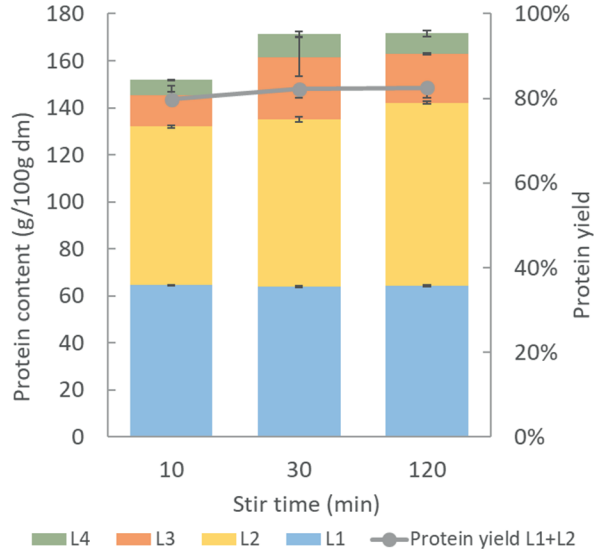

Figure S2.2 *Protein content and yield of 2500 rpm mung bean fine fraction after aqueous phase separation with stirring 10, 30, 120 min.*

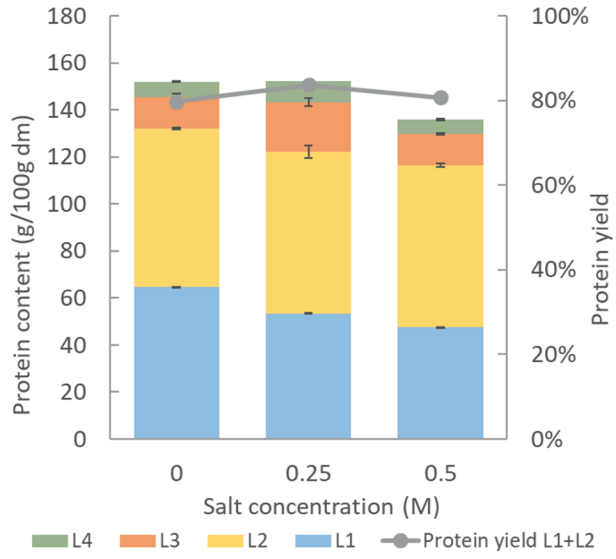

Figure S2.3 *Protein content and yield of 2500 rpm mung bean fine fraction without, with 0.25M and 0.5M NaCl addition in aqueous phase separation with 10 min stirring*

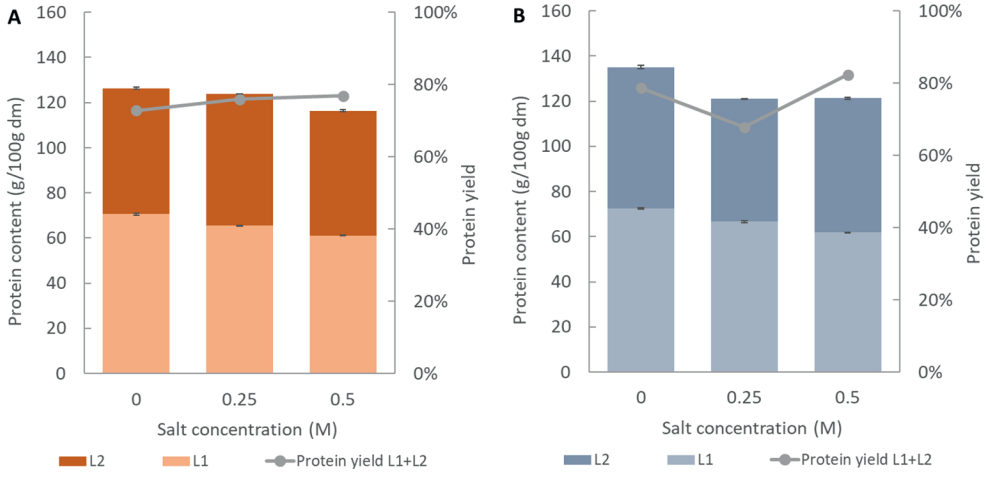

Figure S2.4 *Protein content and yield of dehulled mung bean fine fraction at A) pH 6 (neutral) and B) pH 8 with 0M, 0.25M and 0.5M NaCl addition in aqueous phase separation with 10 min stirring.*

Figure S3.1 *MBPSC solution ultracentrifuged at 10,000 g for 30 min.*

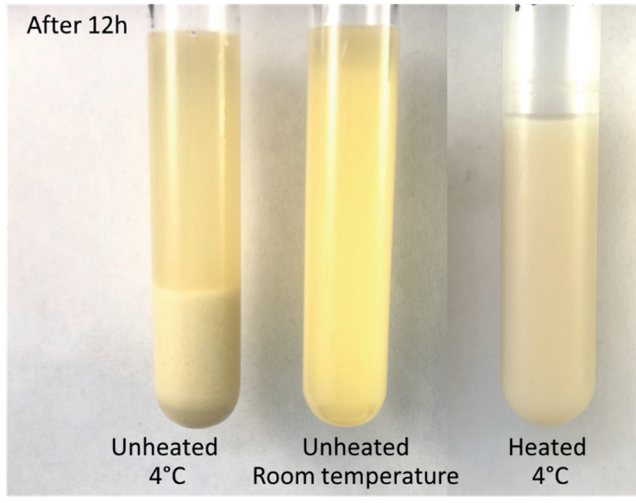

Figure S3.2 *Phase separation extent of unheated MBPC solutions stored at 4 ˚C (left) and room temperature (right) overnight.*

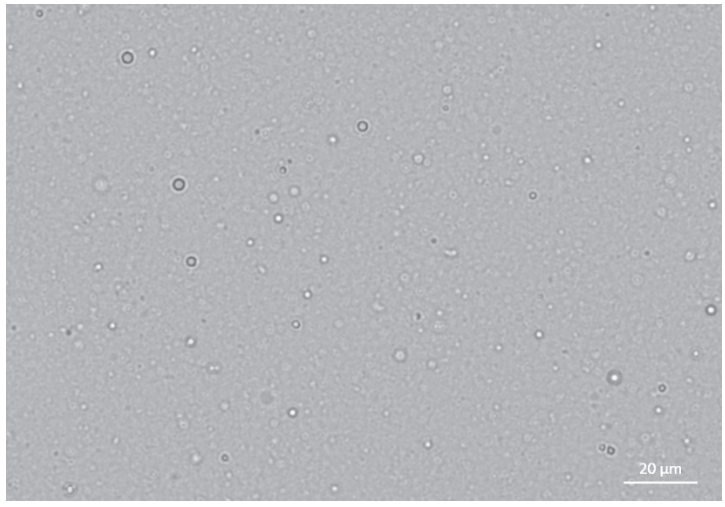

Figure S3.3 *Images of Pellet obtained from 4 ˚C phase separation. The scale bar corresponding to 20 µm.*

Figure S3.4 *Images of supernatant obtained from 4 °C phase separation. The scale bar corresponding to 20 µm.*

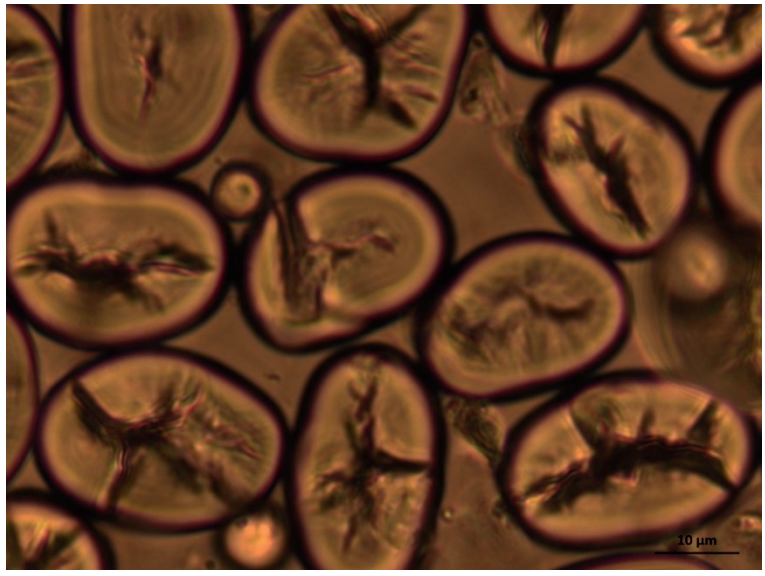

Figure S4.1 *Light microscopy image of FF (fine fraction) suspended in 20 mM PO4 buffer.*

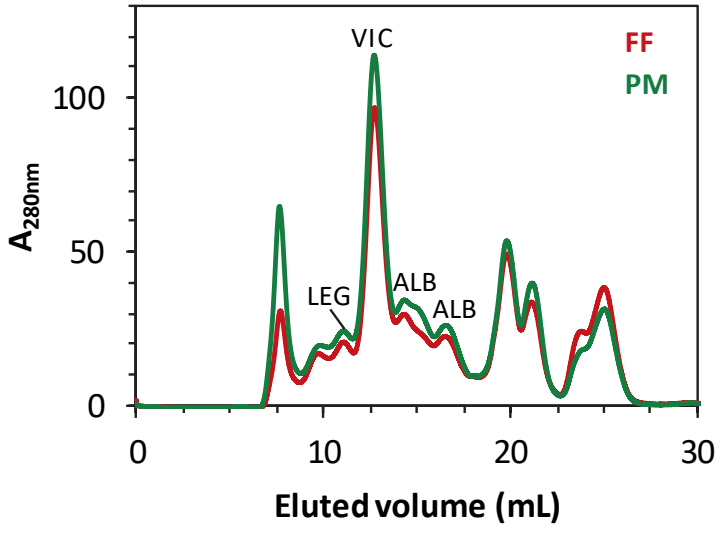

Figure S4.2 *SEC chromatogram with the 280 nm absorbance over eluted volume of FF (fine fraction) and PM (protein mixture).*

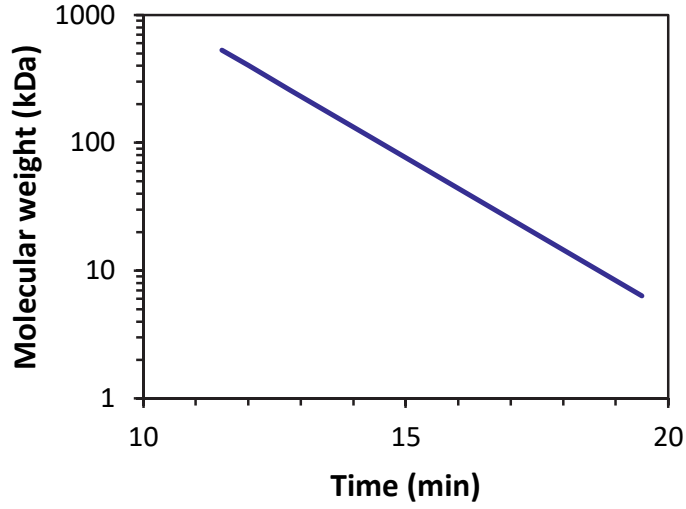

Figure S4.3 *SEC calibration curve with molecular weight over time at 280 nm absorbance.*

Table S4.1 *All fitting parameters of the step-dilatation experiments*

Extension	a (-)	b (-)	c (-)	β (-)	τ1 (s)	τ2 (s)
FF	2.9 ± 0.5	1.6 ± 0.5	49.8 ± 3.4	0.60 ± 0.03	32.4 ± 6.9	649 ± 89
PM	3.6 ± 0.4	2.6 ± 0.4	54.4 ± 3.0	0.60 ± 0.02	30.8 ± 8.4	526 ± 53
GLOB	4.2 ± 0.8	1.8 ± 0.4	52.9 ± 1.8	0.54 ± 0.05	22.2 ± 3.7	617 ± 64
ALB	3.0 ± 0.2	2.1 ± 0.2	49.1 ± 1.5	0.53 ± 0.03	19.2 ± 8.0	622 ± 37
COL	3.7 ± 1.3	2.3 ± 0.6	54.0 ± 5.9	0.57 ± 0.04	25.2 ± 5.1	624 ± 101

Compression	a (-)	b (-)	c (-)	β (-)	τ1 (s)	τ2 (s)
FF	-2.5 ± 0.4	-1.8 ± 0.3	47.0 ± 3.4	0.58 ± 0.00	27.9 ± 7.1	584 ± 96
PM	-4.7 ± 0.4	-3.3 ± 0.5	51.1 ± 3.5	0.59 ± 0.03	23.8 ± 4.0	510 ± 34
GLOB	-5.3 ± 1.4	-2.5 ± 0.4	50.9 ± 3.7	0.60 ± 0.05	17.3 ± 5.3	490 ± 204
ALB	-3.4 ± 0.9	-1.8 ± 0.4	48.5 ± 2.4	0.60 ± 0.06	18.1 ± 3.5	418 ± 98
COL	-3.6 ± 1.0	-4.2 ± 2.1	51.8 ± 6.4	0.63 ± 0.04	34.1 ± 8.2	590 ± 170

Determination of viscosity

The kinematic viscosity of the samples was determined using a viscometer (Ubberlohde, SI Analytics, Weilheim, Germany) placed in a water bath at 25 ˚C. The kinematic viscosity $v(\mathrm{m2/s})$ was calculated from:

$$v = Kt \tag{S1}$$

Here, *t* is the measured flow time (s), *K* (mm^2/s^2) is the capillary constant at 25˚C (*K*=0.01078 mm^2/s^2 for the present study). Subsequently, the densities of protein solutions were measured using an oscillating U-tube density meter (Anton Paar DMA 5000, Graz, Austria). The dynamic viscosity *η (Pa s)* was calculated from:

$$\eta = v\rho \tag{S2}$$

where ρ is the density (kg/m^3). All measurements were performed in triplicate.

Table S4.2 *The viscosity of protein solutions at 1% protein concentration*

	FF	NPC	GLOB	ALB	COL
Viscosity η (Pa.s)	1.06E-03	9.93E-04	1.02E-03	1.00E-03	1.13E-03

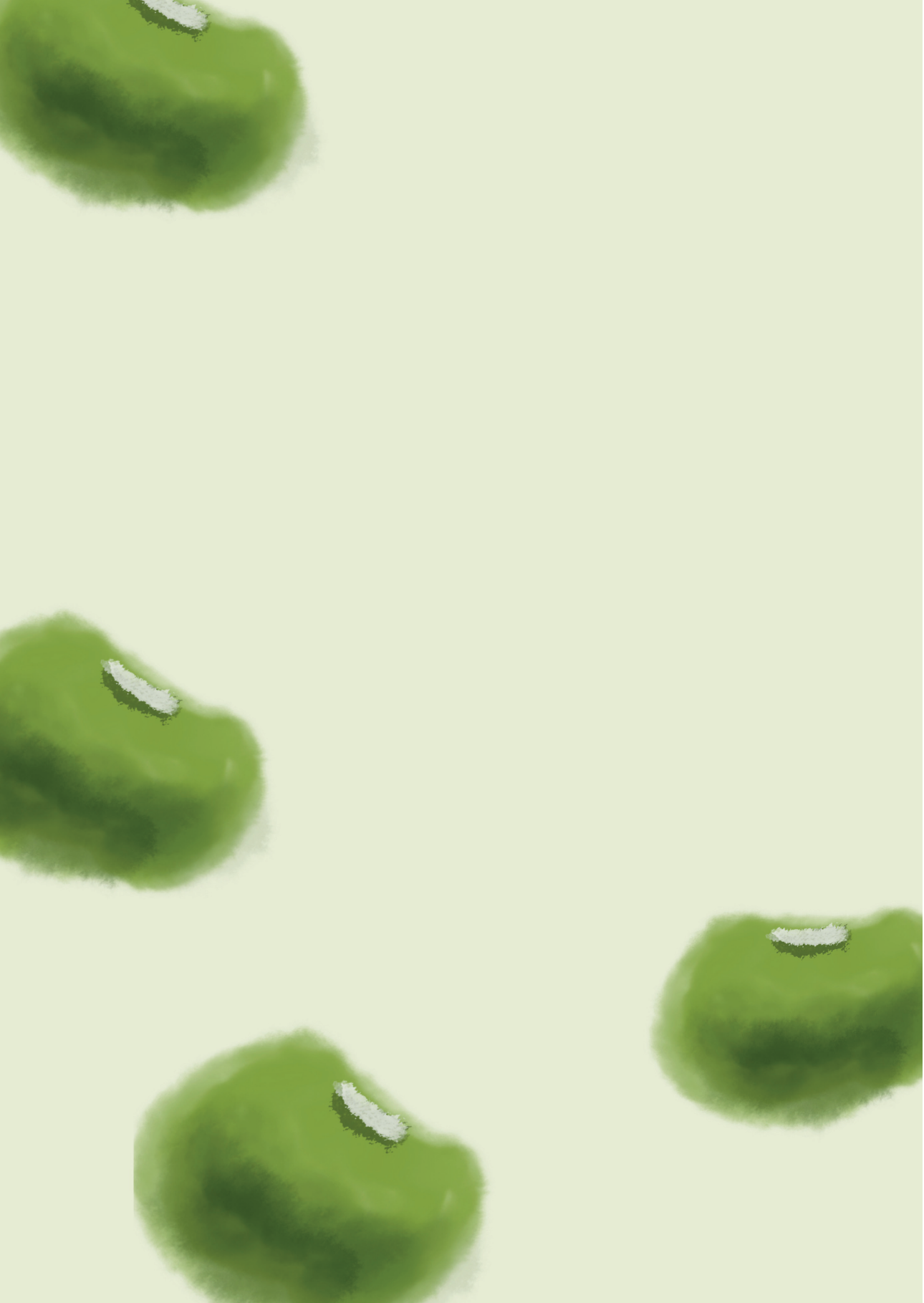

Acknowledgements

Thanks to everyone who has ever supported and helped me along the way,
I wouldn't be here without you.

Special thanks to my Papa and Miamia,
I wouldn't be me without you.

About the author

Qiuhuizi (Evelen) Yang was born on 16 September 1992 in Zhangye, China. She completed her undergraduate studies in Food Technology and Engineering at Nanjing Agricultural University in China in 2015. Afterwards, she enrolled for the master's programme Food Technology in Wageningen University & Research. During her master's she specialized in Ingredient Functionality and got the chance to do a thesis at the R&D facility of Danone Nutricia (The Netherlands). She completed her Master programme with an internship at the Food Science department of Copenhagen University (Denmark). In the meantime Qiuhuizi focused on the functionalities of rapeseed proteins, which resulted in a publication in 2019.

After obtaining her MSc degree in 2017, Qiuhuizi received a China Scholarship Council (CSC) scholarship to pursue a doctoral degree. She continued her study and research as a PhD candidate at the chair groups of Physics and Physical Chemistry of Foods & Physical Chemistry and Soft matter of Wageningen University in 2018. Her PhD project explored the potential of Mung bean proteins as a novel and highly functional food protein ingredient.

Email: evelen6612@hotmail.com

LinkedIn:

List of publications

This thesis

- **Yang, Q.**, Eikelboom, E., van der Linden, E., de Vries, R., & Venema, P. (2022). A mild hybrid liquid separation to obtain functional mung bean protein. *Lwt*, 154.

- **Yang, Q.,** Venema, P., van der Linden, E., & de Vries, R. (2023). Soluble protein particles produced directly from mung bean flour by simple coacervation. *Food Hydrocolloids*, 108541.

- Yang, J.*, **Yang, Q**.*, Waterink, B., Venema, P., de Vries, R., & Sagis, L. M. C., Physical, interfacial and foaming properties of different mung bean protein fractions. ***Submitted.***

- **Yang, Q**.*, Yang, J.*, Waterink, B., Sagis, L. M. C., de Vries, R. & Venema, P., Mung bean protein colloids mixtures and their fractions - a novel and excellent foam stabilizer. ***Submitted.***

Other research

- Yang, J., Kornet, R., Diedericks, C. F., **Yang, Q.**, Berton-Carabin, C. C., Nikiforidis, C. V., Venema, P., van der Linden, E., & Sagis, L. M. C. (2022). Rethinking plant protein extraction: albumin — from side stream to an excellent foaming ingredient. *Food Structure*, *31*, 100254.

- **Yang, Q**.*, Xia, W.*, Zhang, M., Sagis, L. M. C., de Vries, R., & Venema, P., Heat-induced gels from mildly extracted mung bean fractions: Rheology and microstructure. ***Manuscript in preparation.***

** Shared first authorship*

Overview of completed training activities

Discipline specific courses

Microscopy and Spectroscopy in Food and Plant Sciences	Wageningen, NL	2019
Electron Microscopy course	Wageningen & Amsterdam, NL	2019
Rheology: The do's and don'ts	Online	2020
Modelling of habitual dietary intake	Wageningen, NL	2021
Sensory Perception & Food Preference: into the Future!	Wageningen, NL	2021
2nd Edible soft matter workshop	Wageningen, NL	2022

Conferences and symposia

Wageningen Food Science Symposium	Wageningen, NL	2020
NIZO Plant Protein Functionality Conference	Online	2020
Research Conference Plant-Based Foods & Proteins Europe	Online	2021
4th Food Structure & Functionality symposium	Online	2021
35th EFFoST International Conference [2]	Lausanne, CH	2021
18th Food Colloids Conference: Structure, dynamics and function [2]	Online	2022
BGR-NRV joint rheology symposium	Leuven, BE	2022
2nd Edible soft matter conference [1]	Wageningen, NL	2022
6th International soft matter conference [1]	Poznań, PL	2022

[1] Oral presentation, [2] Poster presentation

General courses

VLAG PhD week	Baarlo, NL	2019
Philosophy and Ethics of Food Science & Technology	Wageningen, NL	2019
Searching and Organising Literature	Wageningen, NL	2018
Project and time management	Wageningen, NL	2020
Communication with the Media & the General Public	Wageningen, NL	2021
Reviewing a Scientific Manuscript	Wageningen, NL	2022
Career orientation	Wageningen, NL	2022
Introduction to R	Wageningen, NL	2022
Applied statistics	Wageningen, NL	2022

Other activities

Preparation of research proposal	Wageningen, NL	2018
Weekly science meetings within chair group - FPH	Wageningen, NL	2018-2022
Weekly science meetings within chair group - PCC	Wageningen, NL	2018-2022

Teaching and Supervision

Supervision of 2 BSc thesis	FPH	2018-2020
Supervision of 5 MSc thesis	FPH	2019-2022
Teaching assistant for *NTU-Food Physics* (CH9202)	FPH	2020
Practical supervisor for *Food Ingredient Functionality* (FCH30306)	FCH & FPH	2020-2021

Colophon

The research described in this thesis was financially supported by China Scholarship Council (CSC).

Additional financial support from Physics and Physical Chemistry of Foods, Physical Chemistry and Soft Matter, and the VLAG Graduate School of Wageningen University for completing the final stage of the thesis as well as for printing this thesis is gratefully acknowledged.

Cover design: Jingjing Zhao, Qiuhuizi Yang

Thesis layout: Qiuhuizi Yang

Printed by ProefschriftMaken